Model Predictive Control for Smart Energy Systems

Rasmus Halvgaard

Kongens Lyngby 2014
PHD-2014-327

Technical University of Denmark
Department of Applied Mathematics and Computer Science
Building 303B, Matematiktorvet, DK-2800 Kongens Lyngby, Denmark
Phone +45 45253031
compute@compute.dtu.dk
www.compute.dtu.dk

PHD-2014-327, ISSN 0909-3192

Preface

This thesis was prepared at the Department of Applied Mathematics and Computer Science (DTU Compute, formerly known as DTU Informatics) at the Technical University of Denmark in partial fulfillment of the requirements for acquiring the PhD degree in engineering. The project was funded by the DTU Informatics Graduate School ITMAN that started up in 2005 with a grant from the Danish Agency for Science Technology and Innovation. ITMAN is a co-operation between DTU Informatics and public as well as private companies: Danish Research Centre for Magnetic Resonance, Dong Energy, Danish Technological Institute, National Environmental Research Institute, DHI - Water and Environment, and Danish Meat Association.

The thesis deals with modeling and control of the future power system often referred to as the Smart Grid. In particular Model Predictive Control (MPC) is applied as a control and optimization method for intelligently enabling flexible energy resources. In Denmark, some of these resources are expected to be residential heat pumps, solar power, and batteries in electric vehicles. All these consumers use electricity potentially produced by green suppliers, e.g. wind turbines or solar power.

The thesis consists of a summary report and a collection of six research papers written during the period November 2010 to February 2014. Two were published in international peer-reviewed scientific journals and four were published at peer-reviewed scientific conferences.

Kgs. Lyngby, February 2014

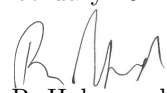

R. Halvgaard

Acknowledgments

I gratefully acknowledge DTU Compute for the financial support of the scholarship that made this project a reality.

First and foremost, I would like to thank my three supervisors. John B. Jørgensen, for opening my eyes to MPC and process control and for teaching me to write great scientific papers. Niels K. Poulsen, for always keeping his door open and having a good control-theory-angle-of-attack on my problems. Henrik Madsen, for his insight in energy systems and great skills within predictive control and forecasting. I'm looking very much forward to future collaboration.

I would also like to thank Prof. Lieven Vandenberghe for taking good care of me during my very fruitful research stay at UCLA. Thank you for patiently teaching me optimization methods important to this thesis and for co-authoring a few papers.

Thanks also go to my fellow Ph.D. student, friend, and collaborator, Tobias G. Hovgaard, for joint work and countless Smart Grid discussions. Thanks to Anders Thavlov and Anders B. Pedersen, Preben Nyeng (and Tobias) for helping me found the Danish Smart Grid Research Network that has led to inspiring workshops and networking between many cross-disciplinary Smart Grid researchers. I would also like to acknowledge Peder Bacher for providing excellent forecasts. Daniel Esteban M. Bondy for choosing me as co-supervisor on his project and Francesco Marra for his EV knowledge and paper contributions. Thanks to Anders Skajaa, Emil Sokoler, Laura Standardi, and Lars Petersen for being great colleagues and for joint work.

Finally, I would like to thank my wife Christina for her constant support the past three years.

Summary (in English)

In this thesis, we consider control strategies for flexible distributed energy resources in the future intelligent energy system – the Smart Grid. The energy system is a large-scale complex network with many actors and objectives in different hierarchical layers. Specifically the power system must supply electricity reliably to both residential and industrial consumers around the clock. More and more fluctuating renewable energy sources, like wind and solar, are integrated in the power system. Consequently, uncertainty in production starts to affect an otherwise controllable power production significantly. A Smart Grid calls for flexible consumers that can adjust their consumption based on the amount of green energy in the grid. This requires coordination through new large-scale control and optimization algorithms. Trading of flexibility is key to drive power consumption in a sustainable direction. In Denmark, we expect that distributed energy resources such as heat pumps, and batteries in electric vehicles will mobilize part of the needed flexibility.

Our primary objectives in the thesis were threefold:

1. Simulate the components in the power system based on simple models from literature (e.g. heat pumps, heat tanks, electrical vehicle battery charging/discharging, wind farms, power plants).
2. Embed forecasting methodologies for the weather (e.g. temperature, solar radiation), the electricity consumption, and the electricity price in a predictive control system.
3. Develop optimization algorithms for large-scale dynamic systems. This includes decentralized optimization and simulation on realistic large-scale dynamic systems.

Chapter 1 introduces the power system, the markets, and the main actors. The objectives and control hierarchy is outlined while Aggregators are introduced as new actors.

Chapter 2 provides linear dynamical models of Smart Grid units: Electric Vehicles, buildings with heat pumps, refrigeration systems, solar collectors, heat storage tanks, power plants, and wind farms. The models can be realized as discrete time state space models that fit into a predictive control system.

Chapter 3 introduces Model Predictive Control (MPC) including state estimation, filtering and prediction for linear models.

Chapter 4 simulates the models from Chapter 2 with the certainty equivalent MPC from Chapter 3. An economic MPC minimizes the costs of consumption based on real electricity prices that determined the flexibility of the units. A predictive control system easily handles constraints, e.g. limitations in power consumption, and predicts the future behavior of a unit by integrating predictions of electricity prices, consumption, and weather variables. The simulations demonstrate the expected load shifting capabilities of the units that adapts to the given price predictions. We furthermore evaluated control performance in terms of economic savings for different control strategies and forecasts.

Chapter 5 describes and compares the proposed large-scale Aggregator control strategies. Aggregators are assumed to play an important role in the future Smart Grid and coordinate a large portfolio of units. The developed economic MPC controllers interfaces each unit directly to an Aggregator. We developed several MPC-based aggregation strategies that coordinates the global behavior of a portfolio of units by solving a large-scale optimization and control problem. We applied decomposition methods based on convex optimization, such as dual decomposition and operator splitting, and developed price-based aggregator strategies.

Chapter 6 provides conclusions, contributions and future work.

The main scientific contributions can be summarized to:

- Linear dynamical models of flexible Smart Grid units: heat pumps in buildings, heat storage tanks, and electric vehicle batteries.
- Economic MPC that integrates forecasts in the control of these flexible units.
- Large-scale distributed control strategies based on economic MPC, convex optimization, and decomposition methods.
- A Matlab toolbox including the modeled units for simulating a Smart Energy System with MPC.

Resumé (in Danish)

I denne afhandling beskriver vi styringsstrategier til fleksible distribuerede energi ressourcer i fremtidens intelligente energisystem – Smart Grid. Energisystemet er et stort komplekst netværk med mange aktører og modstridende mål på forskellige hierarkiske niveauer. En effektiv måde at transportere energi over lange afstande er med elektricitet. El-nettet skal pålideligt forsyne både private og industrielle forbrugere med strøm døgnet rundt. Men i takt med udrulningen af flere vedvarende energikilder, som vind og sol, mindskes forsyningssikkerheden betydeligt på en ellers kontrollerbar el-produktion. Et Smart Grid har derfor brug for fleksible forbrugere, der kan ændre deres forbrug i en bæredygtig retning, hvor der anvendes større andele af grøn energi. Det kræver koordination på stor skala med nye styrings- og optimerings-algoritmer. Et Smart Grid skal derfor sørge for, at der er nok fleksibilitet til rådighed. Særligt i Danmark forventer vi, at en del af den nødvendige fleksibilitet skal komme fra varmepumper og el-biler.

Vores tre primære forskningsmål med denne afhandling var at:

1. Simulere enhedernes dynamiske forbrug og produktion i el-systemet baseret på simple dynamiske modeller (fx varmepumper, varmeakkumuleringstanke, elbillers batterier, vindmøller, kraftværker).

2. Integrere forudsigelser af vejret (fx udetemperatur og solindstråling), elforbruget, og elpriser i et modelprædiktivt kontrolsystem.

3. Udvikle optimeringsalgoritmer til dynamiske storskala systemer. Herunder decentral optimering og simulering af realistiske systemer.

Kapitel 1 introducerer energi systemet, markederne og hovedaktørerne. Deres mål og rolle i kontrolhierarkiet opsummeres, mens Aggregatorer introduceres som ny aktør.

Kapitel 2 formulerer lineære dynamiske modeller af følgende Smart Grid enheder: el-biler, varmepumper i bygninger, kølesystemer, solvarme, varmeakkumuleringstanke, kraftværker og vindmølleparker. Modellerne realiseres som tilstandsmodeller i diskret tid, der passer ind i et prædiktivt reguleringssystem.

Kapitel 3 introducerer modelprædiktiv regulering (MPC). Herudover estimering af tilstande, og prædiktion af lineære modeller.

Kapitel 4 simulerer modellerne fra Kapitel 2 med certainty-equivalent MPC'en fra Kapitel 3. En økonomisk MPC minimerer omkostningerne til forbrug baseret på rigtige elpriser. Prædiktionerne af prisen bestemmer derved styresignalerne og fleksibiliteten af enheden. Samtidig overholder den prædiktive regulering systemets begrænsninger, fx den øvre grænse for effekt-forbruget i en varmepumpe, ved at udnytte viden fra modellerede forudsigelser af fx elpriser, forbrug og vejret. Simuleringer viser tydeligt, at den økonomiske MPC minimerer omkostningerne ved at tidsforskyde forbruget afhængigt af priserne. Endvidere undersøgte vi de økonomiske besparelser for forskellige styringsstrategier og forudsigelser.

Kapitel 5 beskriver og sammenligner de foreslåede Aggregator styringsstrategier for storskala systemer. Aggregatorer forventes at spille en stor rolle i fremtidens Smart Grid ved at koordinere store porteføljer af enheder. Den udviklede økonomiske MPC kan interface til en Aggregator enten gennem priser eller direkte styresignaler. Vi har udviklet MPC-baserede styrestrategier, der kan koordinere globale mål for hele porteføljen af enheder ved at løse stor-skala optimerings- og kontrol-problemer. Vi brugte konvekse dekomponeringsmetoder, såsom dual dekomponering og operator splitting.

Kapitel 6 opsummerer afhandlingens konklusioner, bidrag og beskriver fremtidigt arbejde.

De videnskabelige hovedbidrag kan opsummeres til:

- Lineære dynamiske modeller af fleksible Smart Grid enheder: varmepumper i bygninger, varmeakkumuleringstanke, el-biler, kølesystemer, kraftværker, vindmøller.
- Økonomisk MPC til styring af enhedernes forbrug og integrere relevante forudsigelser, der påvirker styringsstrategien.
- Stor-skala distribuerede styringsstrategier baseret på MPC, konveks optimering, og dekomponeringsmetoder.

- En Matlab toolbox til simuleringer af de modellerede enheder med MPC.

List of publications

Peer-reviewed papers

The following papers were published or submitted for publication in international journals or in conference proceedings during the project period. They constitute the main contributions of the Ph.D. project and we advice the reader to pick up on the specific details in the papers after reading the summary report.

[A] R. Halvgaard, N. K. Poulsen, H. Madsen, and J. B. Jørgensen Economic Model Predictive Control for Building Climate Control in a Smart Grid *Proceedings of 2012 IEEE PES Innovative Smart Grid Technologies (ISGT), 2012*

[B] R. Halvgaard, D. E. M. Bondy, F. Marra, N. K. Poulsen, H. Madsen, and J. B. Jørgensen Electric Vehicle charge planning using Economic Model Predictive Control *Proceedings of 2012 IEEE International Electric Vehicle Conference (IEVC), 2012*

[C] R. Halvgaard, P. Bacher, B. Perers, E. Andersen, J. B. Jørgensen, N. K. Poulsen, and H. Madsen Model Predictive Control for a Smart Solar Tank based on Weather and Consumption Forecasts *Energy Procedia, Vol. 30, pp. 270-278, 2012*

[D] R. Halvgaard, N. K. Poulsen, H. Madsen, and J. B. Jørgensen Thermal Storage Power Balancing with Model Predictive Control *Proceedings of 2013 European Control Conference (ECC), pp. 2567-2572, 2013*

[E] R. Halvgaard, L. Vandenberghe, N. K. Poulsen, H. Madsen, and J. B. Jørgensen Distributed Model Predictive Control for Smart Energy Systems *Submitted to IEEE Transactions on Smart Grid, 2014*

[F] R. Halvgaard, J. B. Jørgensen, and L. Vandenberghe Dual Decomposition for Large-scale Power Balancing *Proceedings of 18th Nordic Process Control Workshop (NPCW), 2013*

Contents

Part I

Summary Report

Chapter 1

Introduction

In this chapter we motivate the need for Model Predictive Control (MPC) in Smart Energy Systems starting from the huge climate change challenge that the world is currently facing. This green challenge currently drives the current power system into unexplored territory that calls for flexible control strategies.

1.1 Transition to a Fossil-Free Energy System

The Danish energy policy stipulates that by 2020 more than 35% of the energy consumed in Denmark should come from renewable energy sources [MHMV13]. 50% of electricity consumption should be supplied by wind power. By 2050 Denmark should be independent of fossil fuels. From a Danish political point of view the interest in this transformation of the energy system is to

- Reduce the emission of greenhouse gases and global warming
- Increase energy efficiency
- Maintain a high security of energy supply
- Ensure macroeconomic cost-effectiveness by using market-based solutions

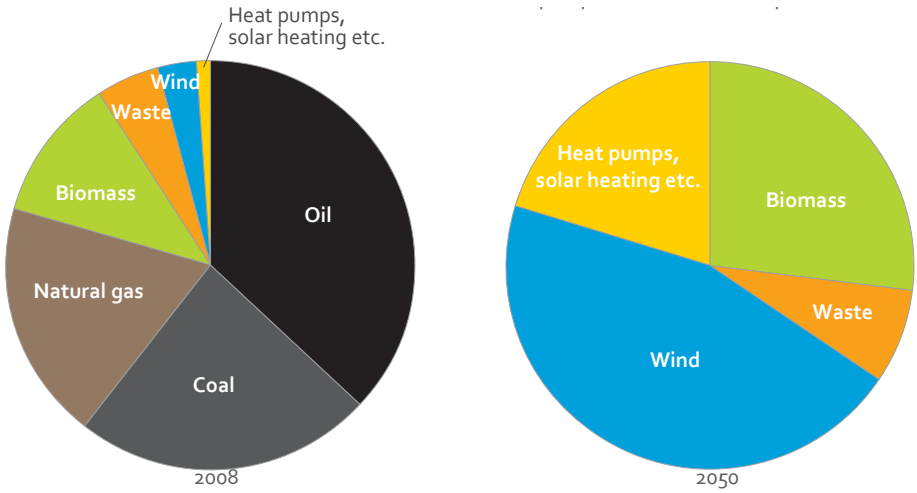

Figure 1.1: *Distribution of energy sources in 2008 and in 2050 as foreseen by the Danish Climate Commission [Dan10].*

- Continue a high level of economic growth
- Ensure positive business development and promote international competitiveness of business in Denmark
- Ensure an environmentally sustainable development

All of these seven criteria are included in the fossil fuel independent future scenario developed by the Danish Climate Commission [Dan10].

Not only Denmark but the entire world is facing this grand challenge. Reducing the fossil fuel consumption from 80% of the energy consumption to a clean 0% in 40 years, requires significant amount of production from renewable energy sources and an efficient utilization of energy in buildings, in the process industries, and the transportation sector. In Denmark, the major part of this energy will be produced by offshore wind turbines as depicted in Fig. 1.1. On the consumption side, residential and commercial buildings will use heat pumps for heating and electrical vehicles will replace vehicles based on combustion engines. Accordingly, electricity will be the main energy carrier in such an energy system independent of fossil fuels. Depending on the rate of adoption of electrified vehicles, 40-70% of the energy consumption will originate from electricity in 2050. Today, 20% of the energy consumption is electricity. In Denmark, the production of wind energy must increase from 3.15 GW in 2008 to 10-18.5 GW in 2050. As it is much more difficult to store electricity than fossil fuels, such a large share of stochastic electricity production requires an intelligent power

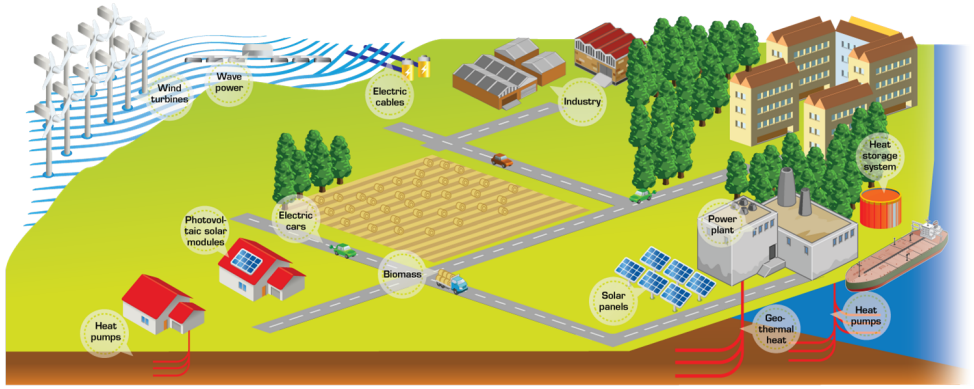

Figure 1.2: *Danish Climate Commission future scenario.*

system – a so-called *Smart Grid* – that continuously balances the power consumption and the power production [BKP11].

A Smart Grid calls for flexible energy producers and consumers that can actively help the grid. There will also be an economic incentive to exploit decentralized resources in Denmark [ED10]. Heat tanks in residential homes as well as in district heating plants must be established such that heat pumps can store electricity as heat in periods of cheap electricity. This requires that the power consumption by heat pumps, and similarly the charging and discharging of the batteries in electrical vehicles, can be adjusted to some extent such that surplus of cheap wind energy is utilized efficiently. The power consumption by the process and retail industries (refrigeration in supermarkets and large cooling houses) must also be made flexible. Future grids are expected to increasingly deploy Smart Grid technologies, such as digital communication and control technologies, to co-ordinate the needs and capabilities of electricity generators, end-users and grid operators. Additional benefits include greater system reliability, a lower cost of electricity supply (through fuel savings and delayed investment in additional generation capacity) and reduced environmental impact [OEC13].

1.2 The Energy System

Industrial, commercial, and residential consumers require various forms of energy services provided by different infrastructures. In Denmark we typically use, coal, petroleum products, biomass, and grid-bound energy carriers such as electricity, natural gas, and district heating. Fig. 1.3 illustrates an example of this infrastructure. So far, the different infrastructures are considered and operated almost independently. In a Smart Energy System these systems should be combined to achieve synergies

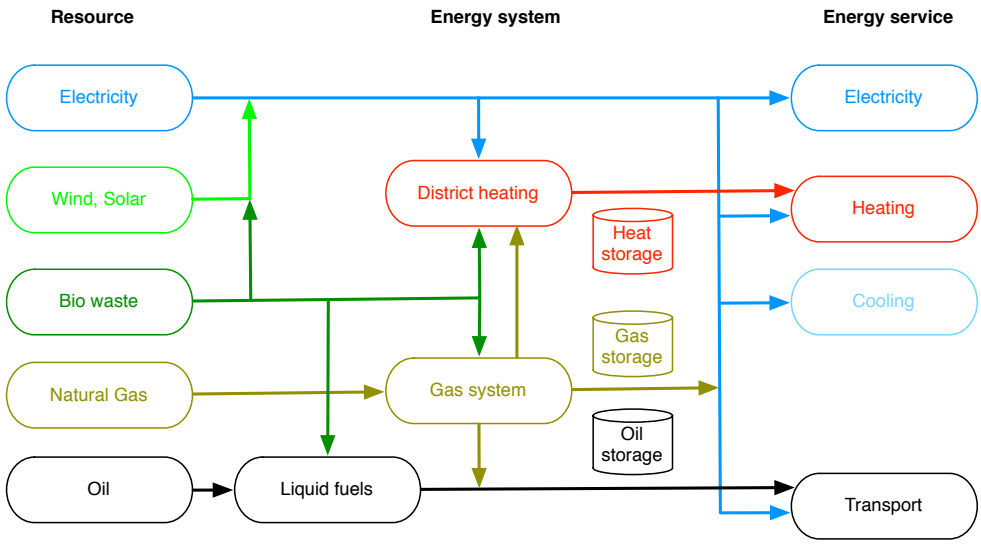

Figure 1.3: *Energy system from resource to service.*

between transformation, conversion, and storage of various forms of energy [GA07]. Electricity can be transmitted over long distances with comparably low losses. Chemical energy carriers such as natural gas can be stored employing relatively simple and cheap technologies. Coupling the infrastructures enables power exchange between them. Couplings are established by converter devices that transform power into other forms. When energy sources with intermittent primary energy like wind, solar are considered, energy storage is important. Storage provides redundancy in supply, stronger reliability, and a larger degree of freedom for optimization.

1.3 The Power System

This section briefly summarizes the markets and actors of todays power system. [Sve06] provide a detailed description of power system infrastructure. Electricity is regarded as an absolute necessity in modern society and is consumed at the same moment as it is generated. It cannot be stored in significant quantities in an economic manner. [HM11] describes characteristics and storage costs of large-scale electricity storage technologies, e.g. batteries, liquid flow batteries, electrolysis, fuel cells, Compressed Air Energy Storage (CAES), pumped hydro, hydrogen storage. These technologies are able to store energy at different time scales. Without storage, electricity must be delivered instantaneously [Wan07]. Therefore, the power system consists of an electrical grid that transports electricity between producers and consumers. The

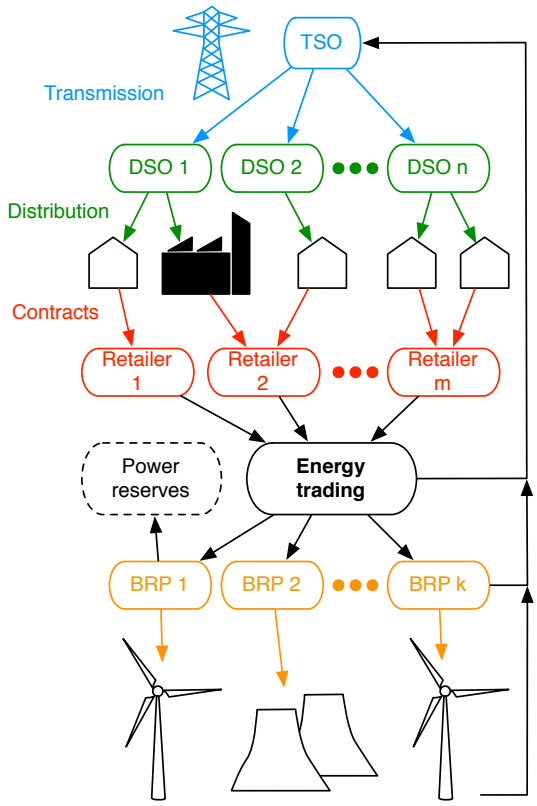

Figure 1.4: *The power grid and actors.*

grid is split in several layers as shown in Fig. 1.4. The upper most layer is a high voltage transmission system where conventional producers like power plants and wind turbines are connected. Their generated power is transported to the end consumers through low voltage distribution grids. Consumers ensure their supply of electricity through a contract with a retailer. The retailer also has a contract with a wholesaler that buys electricity either at a power exchange market, from a producer, or from a third party trader. In principle the wholesaler and the retailer could be the same entity, and they are combined in the figure. The consumer can freely change from one electricity supplier to another through the retail market. Most electricity markets in Europe are liberalized like this and share common features.

The electricity market is usually split in several parts: transmission, distribution, retail activities, and generation. Markets promote competition in generation and retail, while transmission remains a monopoly managed by noncommercial organizations called System Operators (SO).

The Distribution System Operator (DSO) operates the distribution network and logs the production and consumption by metering individual producers or consumers. The metered data is a basis for the following imbalance financial settlements. There are multiple DSOs in Denmark, acting as monopolies in each region. Besides a stable local voltage control, the main challenge for the DSO is to prevent bottlenecks in the distribution grid. Such bottlenecks may be caused by the changing demand from end consumers. Traditionally, congestion problems are overcome by physically expanding the grid capacity.

The Transmission System Operator (TSO) is responsible for the daily operation of the transmission grid, its maintenance and expansion. In Denmark the TSO is represented by the state-owned monopoly Energinet.dk. They own the high voltage transmission lines that connect the power producers to the distribution network and to neighboring countries. It is their responsibility to secure and stabilize the transmission system, where production and consumption must balance at all time scales, and where the power quality must also be maintained by a stable voltage control. Finally, the TSO develops market rules and regulations that in the long run provide a reliable framework for the energy market. In general, a TSO does not own production units and relies on *ancillary services* from suppliers to balance the production and consumption in the transmission grid. Imbalances could destabilize the grid and lead to outages for a large number of end-consumers with subsequent financial losses.

Balance Responsible Parties (BRP) enter agreements with the TSO to produce or consume energy. The BRPs sells or submit bids for purchase of energy into the energy markets ahead of time. The bids are based on the anticipated demand within each hour from the group of electricity wholesalers they represent. A BRP is financially responsible for any consumer-caused imbalances, i.e. any deviations between the amount of energy purchased on the market, and imbalances are settled on the balancing market.

1.3.1 Markets

Electricity is transported in a continuous flow at the speed of light. A unit of electricity (a kWh) delivered to a consumer cannot be traced back to the producer that actually generated it. This feature puts special requirements on the metering and billing system for electricity and motivates the need for markets. Production and consumption must balance at any given moment, minute-by-minute, day and night throughout the whole year. Traditional price mechanisms cannot handle the fast dynamics in real time. Electricity pricing always has to be either ahead of real time or after real time.

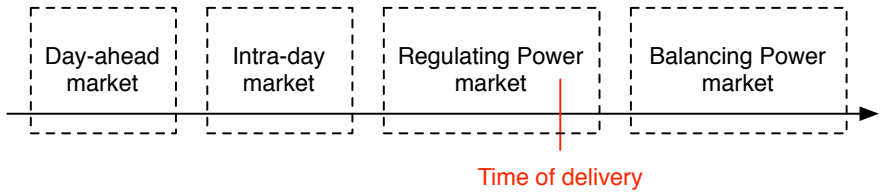

Figure 1.5: *Market time scale [PHB+13].*

Today, trading of electricity is organized in pools or exchanges, where producers and consumers submit bids for energy delivery – both from and to the grid. The Nordic power exchange is called NordPool. NordPool is completely owned by the Nordic TSOs, that together with the DSOs are regulated monopolies, and are subject to strict regulation. One company can take on multiple roles, e.g. the Danish power company DONG Energy who represents both a BRP, retailer, and producer. The electricity consumption is variable with a well predictable characteristic pattern during day/night, the week, and on seasonal and annual time scales as well. Several markets are available depending on the time scale of operation. Daily transactions are made on a day-ahead market often referred to as a forward market in the US and spot market in Europe. Adjustments in energy needs are made in intra-day markets and in a real-time or regulation market [Zug13]. Fig. 1.5 shows a broad time scale of these energy markets. Precise timings can be found in [PHB+13].

1.3.1.1 Energy Markets

NordPool includes a day-ahead market named Elspot. Producers, retailers and large consumers submit bids for delivery and withdrawal of electricity throughout the following day. Market participants must submit 24 bids in total, one for each hour of the following day. The deadline for submitting bids is at noon the day before delivery. In the coming hour the market is cleared and the prices are published and communicated to each participant along with their production and consumption schedules. NordPool establishes system prices by matching supply and demand curves. Fig. 1.6 illustrates this matching. If grid bottlenecks (congestion) arise as a result of the accepted production and consumption plan, then the prices are adjusted based on the geographical area of the grid [Nor]. The intra-day market Elbas, allows trading up to one hour before delivery and allows participants to adjust plan according to any changes. Today, this market is rather illiquid as it accounts for only 1% of the total electricity consumption in Scandinavia. Balance responsible parties (BRP) can submit bids on a balancing market until 45 min before delivery. On TSO request bids must be activated within 15 minutes, to restore the balance between production and consumption whenever other participants deviate from the schedule resulting from

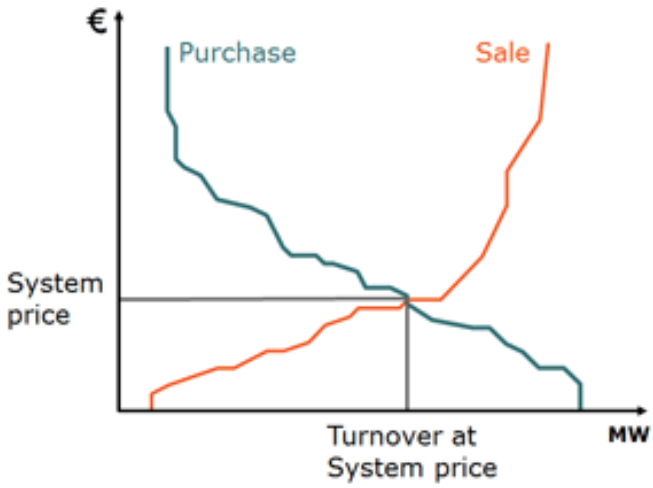

Figure 1.6: *Matching supply and demand curves.*

their trade in the day-ahead and intra-day markets. These unwanted deviations constitute balancing power and are settled ex-post according to the metered production and consumption of the market participant.

All power imbalances are settled at the balancing market price, i.e. at the marginal price of regulating power for the hour. This implies that any unwanted deviation is actually rewarded by a price that is more attractive than the day-ahead price as long as the deviation is in the opposite direction compared to the system imbalance. If the system is in deficit power (up regulation), then producers with negative deviations (underproduction) must pay a balancing price (higher than the day-ahead price), while it receives day-head price for positive unwanted deviation (overproduction). In case of power surplus (down regulation) a producer pays the day-ahead price for unwanted deviation (underproduction). This settlement is referred to as a one-price model. On the contrary, in a two-price system the balancing market price applies only to deviations in the same direction as the system's [Zug13].

1.3.1.2 Capacity Market

Day-ahead, intra-day, and balancing markets are energy markets. Capacity markets ensure availability of sufficient regulating power in the market. When deviations from the scheduled production and consumption result in system imbalances that no market can cover, the TSOs have emergency reserves that can be used to restore

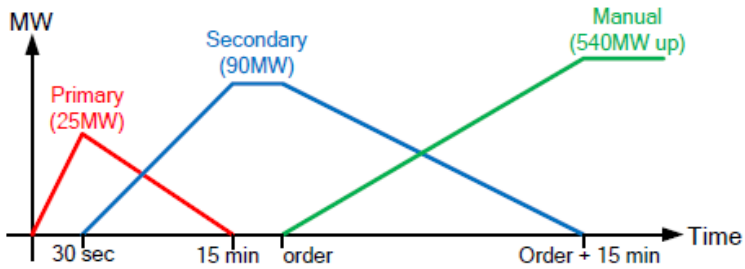

Figure 1.7: *Frequency reserves.*

balance, for instance in the case of a major breakdown. Fig. 1.7 illustrates the timing of the reserves.

Primary Frequency Reserve The primary frequency reserve is an automatic frequency control that stabilize the frequency usually around 50 or 60 Hz. Primary frequency reserves must be activated within 10-30 seconds and must be based on a local control loop at the unit including local grid frequency measurements. The primary control reserve must be active until secondary control takes over.

Secondary Frequency Reserve The secondary frequency reserve is activated by a TSO reference signal. Its main objective is to restore power balance in a control area and to take part in stabilizing the frequency. The secondary reserve restores the primary reserve. The time scale for activation of secondary reserve is around 15 minutes.

Tertiary Frequency Reserve Tertiary control is a reserve that can be activated manually by a TSO. Activation of tertiary reserves will make the suppliers of the tertiary reserves change their planned operation such that the necessary up- or down-regulation is achieved. The purpose of the tertiary reserve is to resolve persistent balance or congestion problems and in this way restore the secondary and primary frequency reserve. The time scale of activating tertiary reserve is also in the magnitude of 15 minutes. In the Nordic market the bids accepted in this market will get a reservation payment. Once the operational day is entered, the accepted bids will be transferred to the Nordic Operation Information System (NOIS) list. The TSO then starts activating bids from the NOIS list according to needs.

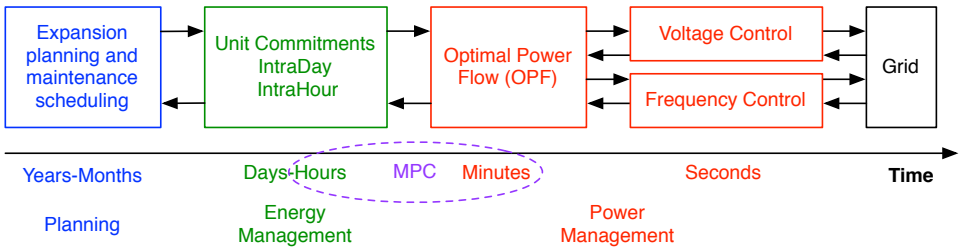

Figure 1.8: *Control hierarchy.*

Manual Power Regulation Manual power regulation is essentially the same as tertiary frequency reserve. However, bids can be placed during the operational day and these bids are transferred directly to the NOIS list, where all bids are put in a merit order. The TSOs can then choose to activate the best offers according to their demand.

From a control point of view all these ancillary services require a tight power regulation in real-time. Consumers and producers are expected to participate in similar markets in the future and must be able to control their power in a flexible way.

1.3.2 Control Hierarchy

Due to economic, political and social constraints of the power system, some hierarchical decomposition to achieve reliable decentralized control is almost mandatory [SM72]. Most complex systems consist of many interacting subsystems with conflicting objectives. The power system is no exception [Ara78]. The power system hierarchy is split in several levels. Basically, it is decomposed geographically in transmission and distribution networks. Also the market dynamics are decomposed in a sequential structure as shown in Fig. 1.5. There is a wide range of response times in electric power systems that depends on the natural response characteristics of the system. Fig. 1.8 shows the control hierarchy of the current power system.

Control functions at a higher level often apply to slower time scale than at the lower level. At the very left we find power system planning and expansion of equipment with the longest time horizon. Also maintenance scheduling can included at this level. In Denmark the long term planning involves closing down coal-fired power plants and putting up wind farms. A flexible demand is a way of delaying expensive grid capacity expansions.

At the next level energy management ensures that power is available on a daily and hourly basis. This level integrates predictions of the future power demand day-ahead

or hour-ahead. The predictions identifies commitments from the generating units. As more renewables emerge, the prediction uncertainty at this level rises significantly and calls for more regulating power reserves [MCM+14]. If all units are operated by a single entity, then the Unit Commitment Problem (UCP) is rather straightforward to construct. The Unit Commitment is focused on economics and includes unit start-up and shut-down decisions (integer variables) as well as ramp rate constraints. The computational complexity is high for these Mixed Integer Linear Programs (MILP) and therefore runs at slower time scales [AHJS97].

In contrast to energy management we have power management at the bottom with the objective of regulating instantaneous power. In general, power management occurs at two timescales [SC12]. At fast time-scales (on the order of seconds) the voltage and frequency must be stabilized [DT78, KO13, SN12]. Specifically, there is a strong coupling between real power and voltage angle as well as between reactive power and voltage magnitude. Power generators sense this change by a small decrease in voltage angle, and compensate by slightly increasing mechanical power to the generator. Similarly, a drop in voltage magnitude can be compensated by increasing reactive power. At larger time-scales (on the order of minutes) the load flow relations are used to define an Optimal Power Flow (OPF) problem. The OPF seeks to optimize the operation of electric power generation, transmission, and distribution networks subject to system constraints and control limits. This nonlinear optimization problem is widely studied in literature [SIS12, AHV13, KCLB14].

In this thesis, we assume sufficient capacity and disregard both frequency and voltage control. Also the investigated control strategies work on a hour-minute scale and applies to active power and energy scheduling.

1.4 The *Future* Power System

In the wake of introducing fluctuating power generation from renewables such as wind and solar power, the future grid needs flexible consumers and producers. In today's power system, the electricity load is rather predictable and primarily large power production units provide the needed regulating power to absorb fast imbalances. A Smart Grid introduces a major paradigm shift in the power system from producing according to demand to letting demand follow production [BKP11, HHM11]. Hence, it is obvious and even economically efficient [ED10] to include the rising electrification of the demand side as a flexible and controllable actuator. The future Smart Grid calls for new control strategies that integrates flexible demand and efficiently balances production and consumption of energy. Research advances within predictive control and forecasting opens up for a control-based demand response as a vital option to increase the power system flexibility [ARB13]. The control challenges for

implementing demand response successfully are to identify reliable control strategies, interface these strategies to the markets, and manipulate the power balance of all flexible units. In the remaining part of the thesis, we focus on methods for control of the future electricity loads.

1.4.1 Distributed Energy Resources

The future Smart Grid units are often referred to as *Distributed Energy Resources* (DERs) [CC09, ZT11] and constitute: consumers, distributed power generation units, and energy storage systems. A DER is defined as smaller production units such as heat pumps, heat storage tanks, electric vehicles, refrigeration systems, district heating units, etc.. We formulate dynamic models of these units in Chapter 2. DERs are distributed in the power system and have local controllers that should be able to communicate with the rest of the system. Communication enables flexibility support to the grid, e.g. an Electric Vehicle is able to charge its battery autonomously, but could offer a flexible active power consumption.

1.4.2 Different Objectives for Multiple Actors

The introduction of flexible DERs in the system rises two major challenges for the current power system. First, new market actors will most likely be introduced to represent the flexible part of the load towards the system operators, either as a BRP itself or through an existing BRP. Secondly, as more demand is put on the distribution grid, a future balancing market operated by the DSO in each distribution network could potentially emerge. The principle behind the DSO balancing market will be almost identical to the current TSO-operated market, but the motivation is quite different. *The TSO currently operates a balancing problem whereas the DSO operates a capacity problem.* The different objectives of the different actors are briefly listed here

- The TSO is responsible for the security of supply and to balance production and consumption, with minimum reserves available. Currently the TSO has no direct control over production or consumption, only indirectly through the regulating power market, where electricity prices stabilize the exchange of power. Therefore, the TSO has interest in extending the power markets to end-consumers and potential DERs.
- The DSO is responsible for the distribution of electricity. Distribution networks were formerly designed for a predominantly passive operation because their task was mainly to distribute electricity with unidirectional power flow from

the transmission level down to the consumer. The future distribution system should be more actively controlled to utilize both the network and the DERs more efficiently, e.g. to avoid congestion.

- The BRP, the electricity supplier, or a retailer all buy or sell electricity. Their objective is to maximize profits. Accurate control and timing is thus crucial to their operation. Furthermore, a BRP must pay penalties for causing imbalances, i.e. deviating from its planned consumption or production. Controlling the consumption minimizes the penalties and adjusts consumption to follow a plan on shorter time scales.
- The generating companies represent a broad range of actors, from a single wind turbine to large companies with a portfolio of power producing units. Their main objective is to maximize profit with little interest in controlling the consumption.
- Industrial consumers mainly wish to maximize profits without sacrificing product quality.
- Consumers have very different control objectives. Some might be very interested in reducing costs, others in reducing environmental impact or even improving comfort [WdG10].

Naturally conflicting objectives arise in interconnected systems. However, for power systems the common single goal of all subsystems is to satisfy customer demands at the lowest cost subject to the system being sufficiently reliable. Smart Grid research points in the direction of a comprehensive hierarchical and distributed control framework to push the power grid development towards a unified large-scale control framework that simultaneously optimizes operation across markets, balancing, operational and transactive customer levels [Taf12]. Modern optimization methods should be incorporated such as layered optimization and decomposition methods to solve the large-scale control problems. This will allow for multiple competing objectives, multiple constraints, and breaks down the hierarchy so that each utility and energy service has the ability to solve its local grid management problems, but within an overall framework that ensures grid stability. New market players, *aggregators*, are expected play an important role in the future hierarchy and connect the rising number of flexible consumers in the future Smart Grid.

1.4.3 Aggregators

The total power consumption of each DER is typically too small to reach the current markets and affect the power balance. Currently, it requires a large volume to place actual bids in the markets. But if a large number of controllable DERs are pooled

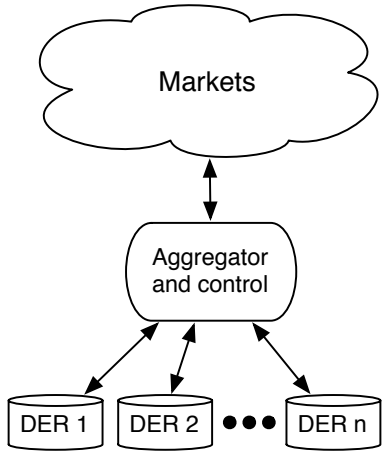

Figure 1.9: *Aggregator role.*

together their aggregated power could be valuable in the markets. Therefore new BRP market players, referred to as *aggregators* are expected to control the future portfolio of flexible DERs [GKS13, BS08]. There can be many aggregators that each control a specific group of DERs, e.g. split geographically in the grid [VPM+11] or by unit type [DSE+12, RSR13]. Figure 1.9 illustrates the role of an aggregator. A local controller at each DER controls the unit according to its local objectives and constraints, while the aggregator coordinates the system-wide flexibility of a large number of DERs in the portfolio [ADD+11]. The DERs are expected to cooperate and respond to control signals communicated by the aggregator. The control signals should coordinate the response according to the aggregator objective. This concept is often referred to as demand response [OPMO13]. The choice of control strategy changes how the DERs respond and the communication requirements [FM10]. Some type of agreement or contract with the aggregator must be in place to ensure an actual response and settlement. The aggregator can exploit the flexibility of its portfolio to operate it in the most profitable way. Depending on the characteristics of the DERs, the aggregator can provide different services for the day-ahead markets or the ancillary service markets. Examples of services could be to keep the consumption below a certain threshold to avoid congestion or to increase consumption during non-peak hours. Different time scales are important to take into account when considering the whole system [PBM+12, UACA11, JL11]. How the market connection should be established by the aggregator is still an open research question [AES08, RRG11, Zug13]. Based on the market today it is realistic to assume that the aggregator bids into the day-ahead market depended on the available portfolio flexibility [ZMPM12, RRG11]. If accepted, the resulting bid must be followed while markets at shorter time scales can be used to maximize profit [TNM+12]. Model predictions and communication with the DERs is crucial to estimate the total flexibility and apply them intelligently.

The requirements to communication will vary depending on the control strategy. It is easier to predict the aggregated behavior of a large number of DERs than predicting their individual behavior [COMP12, TLW13, Cal11]. Forecast of the consumption relies on historical data and actual forecasts of outdoor temperature, wind, etc.

The aggregator's key ability is to control the power consumption or production of its portfolio. And the best control strategy for doing so is not trivial at all. Optimal decisions on individual energy consumption and production requires knowledge of future production and consumption by all other units in the system. In this thesis we investigate different aggregator control strategies [LSD+11] ranging from centralized [PSS+13, HEJ10] to decentralized [WLJ12, JL11] Model Predictive Control [Jør05, MSPM12] using various hierarchical levels and levels of information exchange between the individual controllers. We also investigate decomposition techniques based on price signals [Sca09].

Chapter 2

Models

In this chapter, we formulate linear dynamic models of some of the common energy units in the future Danish energy system:

- Electric Vehicles
- Buildings with heat pumps
- Refrigeration systems
- Solar collectors and heat storage tanks
- Power plants
- Wind farms

The models originate from Paper A, Paper B, and Paper C, and the rest from [HHLJ11, EMB09, Hov13, Sok12].

2.1 Dynamical Systems

We characterize the state of a dynamical system by its state variables. The state variables are stacked in a time-varying state vector $x(t)$ referred to as the system

state. The state variables are changed from its initial state $x(t_0) = x_0$ by underlying dynamical processes. The development of the states depend on several inputs: control signals $u(t)$, disturbances $d(t)$, and unmeasured stochastic process disturbances $w(t)$. For many dynamical systems it is possible to describe the state development with a process on the form

$$\frac{d}{dt}x(t) = \dot{x} = f(x, u, d, w, t) \quad x(t_0) = x_0 \tag{2.1}$$

i.e. n_x coupled nonlinear differential equations. n_x is also the number of variables in x. The process noise is distributed as $w_k \sim N_{iid}(0, R_{ww}(t))$, and we assume that u, d, and w are piecewise linear. The output variables $z(t)$ and measurements $y(t)$ from the system are related to the states and inputs

$$y(t) = g(x, u, v, t) \tag{2.2a}$$
$$z(t) = h(x, u, d, t) \tag{2.2b}$$

with measurement noise $v(t) \sim N_{iid}(0, R_{vv}(t))$. In this thesis, we only consider linear systems of finite dimension, i.e. linear f, g, and h, and we start our energy systems modeling with one of three different model formulations. A state space model based on differential equations of the modeled physical system, a Stochastic Differential Equation (SDE) with parameters estimated from data, or a transfer function model defining the input and output relations with simple parameters. As illustrated in Fig. 2.1 all these model formulations can be converted in to discrete time state space models that readily fit the control framework presented later in Chapter 3. In Chapter 5 we model a portfolio of units using ARX and ARMAX models. The impulse response model is explained in detail in Section 2.2.2.

2.1.1 Continuous Time State Space Model

A continuous time stochastic state space representation is

$$\dot{x}(t) = A_c(t)x(t) + B_c(t)u(t) + E_c(t)d(t) + G_c(t)w(t) \tag{2.3a}$$
$$y(t) = C(t)x(t) + v(t) \tag{2.3b}$$
$$z(t) = C_z(t)x(t) + D_z(t)u(t) + F_z(t)d(t) \tag{2.3c}$$

The state space matrices $(A_c, B_c, E_c, G_c, C, C_z, D_z, F_z)$ can be time-varying.

2.1.2 Stochastic State Space Model

A stochastic differential equation is formulated as

$$\mathrm{d}x(t) = (A_c(t)x(t) + B_c(t)u(t) + E_c(t)d(t))\,\mathrm{dt} + G_c(t)\mathrm{d}w(t) \tag{2.4}$$

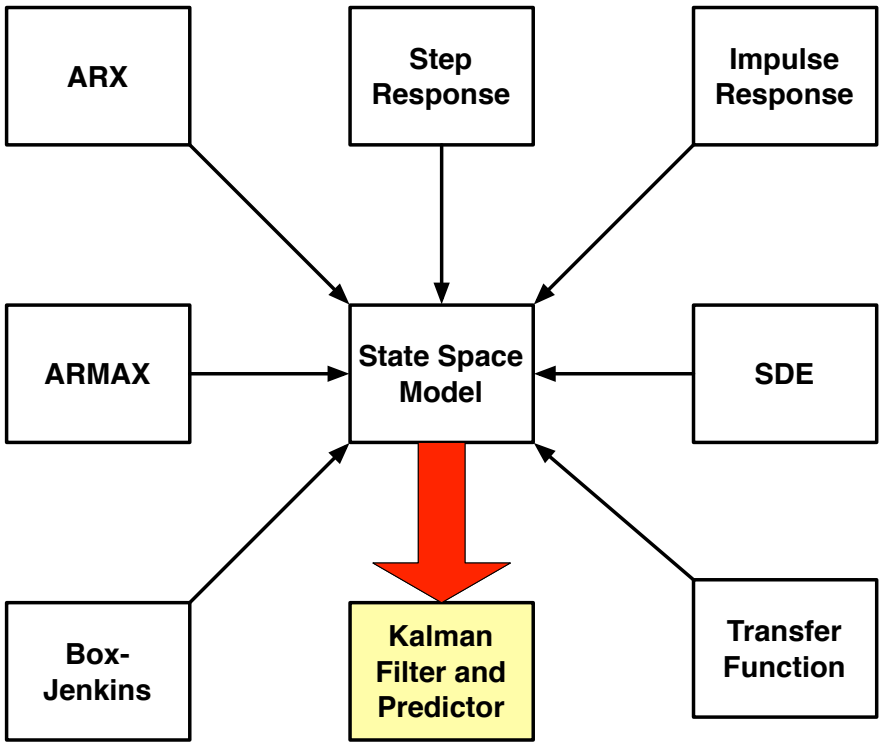

Figure 2.1: *State space model realization.*

The model includes a diffusion term to account for random effects, but otherwise it is structurally similar to ordinary differential equations.

2.1.3 Transfer functions

A transfer function $g(s)$ describes the relation between input and output via the coefficients of two polynomials $a(s)$ and $b(s)$

$$g(s) = \frac{b(s)}{a(s)} = \frac{b_0 s^n + b_1 s^{n-1} + \cdots + b_{n-1} s + b_n}{s^m + a_1 s^{m-1} + \cdots + a_{m-1} s + a_m} \tag{2.5}$$

We can describe multiple input and multiple output (MIMO) systems with sets of transfer functions in a matrix $G(s)$. Examples of transfer functions described with

simple parameters are

$$G_1(s) = \frac{K}{\tau s + 1} \tag{2.6}$$

$$G_2(s) = \frac{K(\beta s + 1)}{(\tau s + 1)^2} \tag{2.7}$$

A transfer function $G(s)$ for $Y(s) = G(s)U(s)$ is related to a state space model through

$$G(s) = C(sI - A)^{-1}B + D$$

where I is the identity matrix.

2.2 Discrete Time State Space Model

Once the model is described as either a transfer function or a state space model we can discretize the system into a discrete-time state space model. We assume a zero-order-hold discrete sampling describes the system well. The matrix exponential discretizes the state space system with sampling period T_s as

$$\begin{bmatrix} A & B & E \\ 0 & I & 0 \\ 0 & 0 & I \end{bmatrix} = \exp\left(\begin{bmatrix} A_c & B_c & E_c \\ 0 & 0 & 0 \\ 0 & 0 & 0 \end{bmatrix} T_s \right)$$

Hence, with discrete time step subscripted k we obtain

$$x^+ = x_{k+1} = Ax_k + Bu_k + Ed_k + Gw_k \tag{2.8a}$$

$$y_k = Cx_k + v_k \tag{2.8b}$$

$$z_k = C_z x_k + D_z u_k + F_z d_k \tag{2.8c}$$

Assume that the model and the true system are identical. Then uncertainties in the state prediction originate from the stochastic nature of the initial state, the process noise, and the measurement noise. In this case, the optimal filter and predictor is the Kalman filter and predictor. Under the same assumptions the optimal controller for the system can be split into an estimator and a certainty equivalence regulator.

2.2.1 Filtering and Prediction

We can use a state estimator to estimate the current state and predict its future evolution. The filtered state estimate, $\hat{x}_{k|k} = E\{x_k\}$, of a system governed by (2.8)

is computed using the Kalman filter [KSH00, JHR11]. The innovation is computed as

$$e_k = y_k - \hat{y}_{k|k-1} = y_k - C\hat{x}_{k|k-1} \tag{2.9}$$

The innovation covariance, $R_{e,k}$, the filter gain, $K_{fx,k}$, and the filtered state covariance, $P_{k|k}$, are computed as

$$R_{e,k} = R_{vv} + CP_{k|k-1}C^T \tag{2.10a}$$
$$K_{fx,k} = P_{k|k-1}C^T R_{e,k}^{-1} \tag{2.10b}$$
$$P_{k|k} = P_{k|k-1} - K_{fx,k}R_{e,k}K_{fx,k}^T \tag{2.10c}$$

such that the filtered state can be computed by

$$\hat{x}_{k|k} = \hat{x}_{k|k-1} + K_{fx,k}e_k \tag{2.11}$$

Equations (2.9)-(2.11) are standard Kalman filter operations for the measurement update. Given the conditional predictions of the external disturbances, $\hat{d}_{k+i|k}$, and the manipulated variables, $\hat{u}_{k+i|k}$, the conditional predictions of the states and the outputs are

$$\hat{x}_{k+1+i|k} = A\hat{x}_{k+i|k} + B\hat{u}_{k+i|k} + E\hat{d}_{k+i|k} \tag{2.12a}$$
$$\hat{y}_{k+i+1|k} = C\hat{x}_{k+1+i|k} \tag{2.12b}$$

for $i = 0, 1, \ldots, N-1$ and all $k \geq 0$. The expected value of the stochastic normal distributed process noise is $\mathbb{E}(w_{k+i|k}) = 0$, and the term disappears from (2.12a). The corresponding covariances of the predicted states are

$$P_{k+i+1|k} = AP_{k+i|k}A^T + GR_{ww,k+i}G^T + ER_{dd,k+i|k}E^T \tag{2.13}$$

This Kalman filter minimizes the errors from measurement noise, process noise, and model mismatch [Åst70].

2.2.2 FIR

When the current state estimate is calculated we can predict the expected future state evolution with a Finite Impulse Response (FIR) model [WÅÅ02]. We can construct

a FIR predictor of an output by eliminating the states using (2.12) such that

$$x_k = A^k x_0 + \sum_{j=0}^{k-1} A^{k-1-j} B u_j + E d_j \tag{2.14a}$$

$$y_k = C x_k = C A^k x_0 + \sum_{j=0}^{k-1} C A^{k-1-j} B u_j + C A^{k-1-j} E d_j \tag{2.14b}$$

$$z_k = C_z x_k + D_z u_k + F_z d_k = C_z A^k x_0 + \sum_{j=0}^{k-1} C_z A^{k-1-j} D_z u_j + F_z d_j \tag{2.14c}$$

The dynamic relation (2.14) can be written in matrix terms as [ESJ09]

$$Y = \Gamma_{yu} U + \Gamma_{yd} D + \Phi x_0 \qquad\qquad Z = \Gamma_{zu} U + \Gamma_{zd} D + \Phi_z x_0$$

where

$$\Gamma_{yu} = \begin{bmatrix} 0 & 0 & \cdots & 0 \\ H_1^{yu} & 0 & \cdots & 0 \\ H_2^{yu} & H_1^{yu} & \cdots & 0 \\ \vdots & \vdots & & \vdots \\ H_N^{yu} & H_{N-1}^{yu} & \cdots & H_1^{yu} \end{bmatrix} \qquad \Gamma_{yd} = \begin{bmatrix} 0 & 0 & \cdots & 0 \\ H_1^{yd} & 0 & \cdots & 0 \\ H_2^{yd} & H_1^{yd} & \cdots & 0 \\ \vdots & \vdots & & \vdots \\ H_N^{yd} & H_{N-1}^{yd} & \cdots & H_1^{yd} \end{bmatrix}$$

$$\Gamma_{zu} = \begin{bmatrix} D_z & 0 & \cdots & 0 \\ H_1^{zu} & 0 & \cdots & 0 \\ H_2^{zu} & H_1^{zu} & \cdots & 0 \\ \vdots & \vdots & & \vdots \\ H_N^{zu} & H_{N-1}^{zu} & \cdots & H_1^{zu} \end{bmatrix} \qquad \Gamma_{zd} = \begin{bmatrix} F_z & 0 & \cdots & 0 \\ H_1^{zd} & 0 & \cdots & 0 \\ H_2^{zd} & H_1^{zd} & \cdots & 0 \\ \vdots & \vdots & & \vdots \\ H_N^{zd} & H_{N-1}^{zd} & \cdots & H_1^{zd} \end{bmatrix}$$

$$\Phi = \begin{bmatrix} C \\ CA \\ CA^2 \\ \vdots \\ CA^N \end{bmatrix} \qquad \Phi_z = \begin{bmatrix} C_z \\ C_z A \\ C_z A^2 \\ \vdots \\ C_z A^N \end{bmatrix}$$

and

$$Z = \begin{bmatrix} z_k \\ z_{k+1} \\ \vdots \\ z_{k+N} \end{bmatrix} \qquad Y = \begin{bmatrix} y_k \\ y_{k+1} \\ \vdots \\ y_{k+N} \end{bmatrix} \qquad U = \begin{bmatrix} u_k \\ u_{k+1} \\ \vdots \\ u_{k+N-1} \end{bmatrix} \qquad D = \begin{bmatrix} d_k \\ d_{k+1} \\ \vdots \\ d_{k+N-1} \end{bmatrix}$$

N is the number of approximate time steps needed to represent the impulse response. The impulse response coefficients (Markov parameters) are used to build the matrices

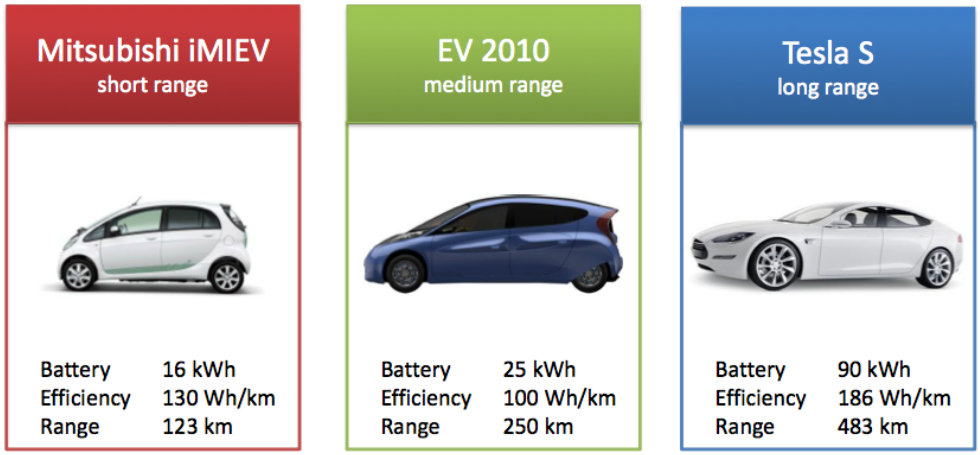

Figure 2.2: *Three types of EVs [HF].*

Γ and Γ_d

$$H_i^{yu} = CA^{i-1}B \qquad H_i^{yd} = CA^{i-1}E \qquad i = 1, 2, \ldots, N$$
$$H_i^{zu} = C_zA^{i-1}B \qquad H_i^{zd} = C_zA^{i-1}E \qquad i = 1, 2, \ldots, N$$

In the case when $D_z = 0$ and $F_z = 0$ the output at $k = 0$, z_0, is removed. The process disturbance d_k can be predicted by a prognosis system and is predicted independently of the measurements y. In many situations in smart energy systems, d involves variables such as temperature and solar radiation. Accordingly, the forecast D is the result of a weather prognosis.

2.3 Smart Grid Units

To control flexible units in a Smart Grid, we need dynamic models of the units in the form just described in Section 2.1.

2.3.1 Batteries in Electrical Vehicles

Electrical Vehicles (EVs) are expected to replace traditional combustion engine cars in the future transport sector. Electric Vehicles contain batteries that must be charged to drive the vehicle. The state-of-charge, $\zeta \in [0; 1]$, of a battery indicates the charge

level and is limited by the constraints

$$\zeta_{\min} \leq \zeta(t) \leq \zeta_{\max} \tag{2.15}$$

When fully discharging or charging the battery, the efficiency decreases. So to stay within a linear operating range typically: $\zeta_{\min} = 0.2$ and $\zeta_{\max} = 0.9$. The state-of-charge may then be modeled as

$$Q_n \dot{\zeta} = \eta^+ P^+ - \eta^- P^- \tag{2.16}$$

$Q_n \in [16; 90]$ kWh is the nominal capacity of the battery. $P^+ = u^+$ is the power transferred from the grid to the battery, and P^- is the power used for driving or the power transferred back to the grid. $P^-(t) = d(t) + u^-(t)$ where $d(t) > 0$ is the power used for driving and $u^-(t)$ is the power transferred from the battery to the grid. The ability to transfer power back to the grid is called Vehicle-to-Grid (V2G) and was first proposed in [KL97]. This is not yet a standard technology for EVs. η^+ is the efficiency of the charger when charging the battery and η^- is the efficiency when discharging the battery. Note that $\eta^+ \leq \eta^-$. Power can only be transferred to or from the battery when the vehicle is plugged in, i.e. when it is not driving. We therefore add the indicator function

$$\bar{d}(t) = \begin{cases} 1 & \text{for } d(t) = 0 \\ 0 & \text{otherwise} \end{cases}$$

to the charging constraints

$$0 \leq u^+(t) \leq \bar{d}(t)\, P^+_{\max} \tag{2.17a}$$

$$0 \leq u^-(t) \leq \bar{d}(t)\, P^-_{\max} \tag{2.17b}$$

Typical commuter driving patterns suggest that the vehicles will be plugged in most of the time. The range of charging powers for current Li-ion EV batteries are $P^+_{\max} \leq \{3.3, 9.6, 16.8\}$ kW (residential charging, three-phase charging, fast-charging). A typical battery with capacity $Q_n = 24$ kWh can thus be fully charged at home in approximately 7 hours at $P^+_{\max} = 3.3$ kW.

The manipulated variables for the battery is the charging and discharging, $u_j = [u^+; u^-]$. Consequently, the contribution of the battery operation to the power balance is: $\bar{z}_j(t) = [-1 \;\; 1] u_j(t) = -u^+(t) + u^-(t)$.

2.3.2 Residential Heating based on Heat Tanks and Solar Collectors

A method for residential heating illustrates the use of solar heated roof-top collectors and electrical heating in combination with a storage tank for heating residential

Figure 2.3: *Heat storage tank connected to solar thermal collector on building roof.*

buildings. An energy balance for the storage tank

$$C_w \dot{T_w} = Q_s + Q_e - Q_c - Q_{loss} \tag{2.18}$$

provides the water temperature, T_w, of the tank. Q_s is the heat from the solar collectors. $Q_{loss} = UA(T - T_a)$ is the heat loss to the ambient air in the room where the heat tank is placed. Q_c is the consumption used for space heating or hot water e.g. showering or dishwashers. $Q_e = \eta_e W_e$, is the heat provided to the tank by conversion of electrical power, W_e, to heat with efficiency η_e. The electrical heating is limited by the hard constraint

$$0 \leq W_e \leq W_{e,\max} \tag{2.19}$$

The temperature in the heat tank is limited by the constraints

$$T_{\min} \leq T \leq T_{\max} \tag{2.20}$$

The manipulated variable for the heat tank system is, $u_j(t) = W_e(t)$, such that the contribution of this system to the overall power balance is $\bar{z}_j(t) = -u_j(t) = -W_e(t)$.

2.3.3 Heat Pumps for Residential Heating

Buildings account for up to 40% of the total energy use in Europe [PLOP08]. Therefore, intelligent control of the energy use in buildings is essential. One of the main

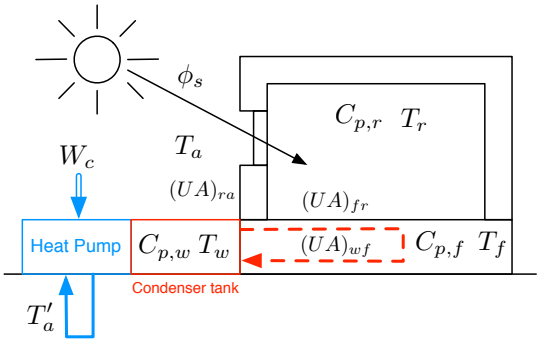

(a) Building and heat pump floor heating system and its thermal properties. The dashed line represents the floor heating pipes.

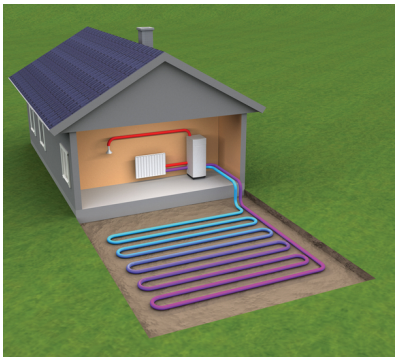

(b) Ground source heat pump.

sources for heating of buildings in Denmark will be heat pumps combined with water based floor heating systems. Heat pumps are very energy efficient as their coefficient of performance (COP) is typically 3 or larger, i.e. for each kWh electricity supplied, they deliver more than 3 kWh heat. As heat pumps are driven by electricity and supply heat to buildings with large thermal capacities, they are able to shift the electricity consumption and provide a flexible consumption.

Residential heating using a heat pump and a water based floor heating system may be modeled by the energy balances

$$C_r\dot{T}_r = Q_{fr} - Q_{ra} + \phi_s \tag{2.21a}$$
$$C_f\dot{T}_f = Q_{wf} - Q_{fr} \tag{2.21b}$$
$$C_w\dot{T}_w = Q_c - Q_{wf} \tag{2.21c}$$

where T_r is the room temperature, T_f is the floor temperature, T_w is the temperature of the water in the floor pipes, and ϕ_s is the solar radiation on the building. The heat transfer rates are

$$Q_{ra} = (UA)_{ra}(T_r - T_a) \tag{2.22a}$$
$$Q_{fr} = (UA)_{fr}(T_f - T_r) \tag{2.22b}$$
$$Q_{wf} = (UA)_{wf}(T_w - T_f) \tag{2.22c}$$

and the effective heat added by the compressor to the water in the pipes is given by

$$Q_c = \eta W_c \tag{2.23}$$

where W_c is the compressor work. The compressor work is constrained by the hard constraints

$$0 \leq W_c \leq W_{c,max} \tag{2.24}$$

Table 2.1: Description of variables

Variable	Unit	Description
T_r	°C	Room air temperature
T_e	°C	Building envelope temperature
T_f	°C	Floor temperature
T_w	°C	Water temperature in floor heating pipes
T_a	°C	Ambient temperature
T'_a	°C	Ground temperature
W_c	W	Heat pump compressor input power
ϕ_s	W	Effective solar radiation power
P_s	W/m^2	Solar radiation power

and the temperatures must obey the following soft constraints

$$T_{r,\min} \leq T_r \leq T_{r,\max} \tag{2.25a}$$
$$T_{w,\min} \leq T_w \leq T_{w,\max} \tag{2.25b}$$

The room temperature limits are time varying set-points specified by the residential inhabitants. Table 2.2 reports parameters for a low energy building represented by this residential heating model using a heat pump. Table 2.3 provides parameters estimated from a modern 198 m^2 residential house [AJRM13]. In that case the model was

$$\begin{aligned}
C_r\dot{T}_r &= 2(UA)_{ra}(T_e - T_r) + (UA)_{fr}(T_f - T_r) + A_s P_s \\
C_e\dot{T}_e &= 2(UA)_{ra}(T_a - T_e) + (UA)_{ra}(T_r - T_e) \\
C_f\dot{T}_f &= (UA)_{wf}(T_w - T_f) + (UA)_{fr}(T_r - T_f) \\
C_w\dot{T}_w &= \eta W_c - (UA)_{wf}(T_w - T_f)
\end{aligned}$$

The compressor power is the manipulated variable, $u_j(t) = W_c(t)$, such that the heat pumps contribution to the overall power balance is $\tilde{z}_j(t) = -u_j(t) = -W_c(t)$.

2.3.4 Supermarket Refrigeration System

The cooling capacity of goods in super market systems may be used in balancing supply and demand of power in electrical systems [HEJ10]. Energy balances for the cold rooms in supermarket refrigeration systems yield

$$C_{p,food}\dot{T}_{food} = Q_{food-air} \tag{2.26a}$$
$$C_{p,air}\dot{T}_{air} = Q_{load} - Q_{food-air} - Q_e \tag{2.26b}$$

Table 2.2: Estimated model parameters for low energy building

	Value	Unit	Description
C_r	810	kJ/°C	Heat capacity of room air
C_f	3315	kJ/°C	Heat capacity of floor
C_w	836	kJ/°C	Heat capacity of water in floor heating pipes
$(UA)_{ra}$	28	kJ/(°C h)	Heat transfer coefficient between room air and ambient
$(UA)_{fr}$	624	kJ/(°C h)	Heat transfer coefficient between floor and room air
$(UA)_{wf}$	28	kJ/(°C h)	Heat transfer coefficient between water and floor
c_w	4.181	kJ/(°C kg)	Specific heat capacity of water
m_w	200	kg	Mass of water in floor heating system
η	3		Compressor coefficient of performance (COP)

Table 2.3: Estimated model parameters for modern residential house

	Value	Unit	Description
C_r	3631	kJ/°C	Heat capacity of room air
C_f	10030	kJ/°C	Heat capacity of floor
C_e	1171	kJ/°C	Heat capacity of building envelope
$(UA)_{ra}$	243.7	kJ/(°C h)	Heat transfer coefficient between room air and ambient
$(UA)_{fr}$	1840	kJ/(°C h)	Heat transfer coefficient between floor and room air
$(UA)_{wf}$	243.7	kJ/(°C h)	Heat transfer coefficient between water and floor
A_s	4.641	m^2	Building area

where T_{food} is the temperature of the stored food and T_{air} is the temperature of the air in the cold room. The heat conduction from food to air in the cold room and from the cold room to the supermarket are

$$Q_{food-air} = (UA)_{food-air}(T_{air} - T_{food}) \tag{2.27a}$$

$$Q_{load} = (UA)_{a-cr}(T_a - T_{air}) + Q_{dist} \tag{2.27b}$$

T_a is the temperature in the supermarket and Q_{dist} represents injection of heat into the bold room (e.g. in connection with opening the cold room). The heat transferred from the cold room to the evaporator of the refrigeration system is in this paper approximated by

$$Q_e = \eta W_c \tag{2.28}$$

where η is the efficiency. In more rigorous models, $\eta = \eta(T_e, T_{out})$ is a function of the evaporator temperature, T_e, as well as the outdoor temperature, T_{out}.

The evaporator duty is constrained by the hard constraint

$$0 \leq Q_e \leq Q_{e,\max,k} \tag{2.29}$$

in which

$$Q_{e,\max} = (UA)_{evap,max}(T_{air} - T_{e,\min}) \tag{2.30}$$

where $T_{e,\min}$ is the minimum allowable evaporator temperature. The food temperature in the cold room is constrained by the soft constraints

$$T_{food,\min} \leq T_{food} \leq T_{food,\max} \tag{2.31}$$

The compressor power, $u_j = W_c$, is the manipulated variable. Its contribution to the overall power balance is given by $\bar{z}_j(t) = -u_j(t) = -W_c(t)$.

2.3.5 Power Plant

The production of power by a thermal power plant consisting of a boiler and turbine circuit may be modeled as [Sok12]

$$Z_j(s) = G_j(s)U_j(s) \qquad G_j(s) = \frac{1}{(\tau_j s + 1)^3} \tag{2.32}$$

$z_j(t)$ is the produced power, while $u_j(t)$ is the corresponding reference signal. Consequently, $\bar{z}_j(t) = z_j(t)$. The cost of producing one unit of power at time k is c_j. For most thermal power plants, τ_j is approximately 60 seconds [EMB09].

The discrete-time input signal is constrained by limits and rate-of-movement constraints

$$u_{\min,j} \leq u_j(t) \leq u_{\max,j} \tag{2.33a}$$
$$\Delta u_{\min,j} \leq \Delta u_j(t) \leq \Delta u_{\max,j} \tag{2.33b}$$

2.3.6 Wind Turbine

The production of power by individual wind turbines or wind farms may be described by the model [EMB09, Sok12]

$$Z_{w,j}(s) = H_j(s)(U_{w,j}(s) + D_{w,j}(s))$$
$$H_j(s) = \frac{K_{w,j}}{\tau_{w,j}s + 1}$$

$z_{w,j}(t)$ is the produced power by the wind turbine(s), $d_{w,j}(t)$ is the available power in the wind, and $u_{w,j}(t)$ is a reference signal to the wind turbine specifying how much

power to extract from the wind. In discrete-time, this command signal is constrained by the hard constraints

$$-d_{w,j}(t) \leq u_{w,j}(t) \leq 0 \tag{2.34a}$$
$$\Delta u_{w,\min,j} \leq \Delta u_{w,j}(t) \leq \Delta u_{w,\max,j} \tag{2.34b}$$

Similarly, wind turbine design and grid-code specifications constrains the produced power by the following soft constraints

$$0 \leq z_{w,j}(t) \leq z_{w,\max,i} \tag{2.35a}$$
$$\Delta z_{w,\min,j} \leq \Delta z_{w,j}(t) \leq \Delta z_{w,\max,j} \tag{2.35b}$$

The produced power to the net by wind turbine is $\bar{z}_{w,i}(t) = z_{w,i}(t)$. The time constant $\tau_{w,j}$ is approximately 5 seconds (or smaller).

2.4 Energy balance

For the considered consumption units the control variable u is always the consumed power and equal to the output z. The controlled output y could be a measured temperature state x of a thermal storage unit. For production units the control variable could for instance be a fuel or simply a reference signal changing the production, while the output z is the production. We can formulate a balance constraint connecting the produced and consumed power from all n units indexed j as

$$\bar{z}_k = \sum_{j=1}^{n} \bar{z}_{k,j} = \sum_{j=1}^{n} C_{z,j} x_{k,j} + D_{z,j} u_{k,j} \tag{2.36}$$

Later in Chapter 5 we deal with consumption units exclusively such that

$$\bar{z} = \bar{C}_z \bar{x} + \bar{D}_z \bar{u} \tag{2.37}$$

where $D_z \in \mathbf{R}^{N \times N n n_u}$ simply sums all contributions to the total power consumption

$$\bar{D}_z = \begin{bmatrix} I & I & \cdots & I \end{bmatrix} \tag{2.38}$$

Here $I \in \mathbf{R}^{N \times N}$ is the identity matrix and n_u is the number of control inputs per unit.

We describe all models as state space models so they fit in the Model Predictive Control framework described in the following chapter.

Chapter 3

Model Predictive Control

This chapter introduces Model Predictive Control (MPC) and how it is applied to the systems described in Chapter 2. In particular, we formulate an economic MPC that leads to a linear optimization problem.

3.1 Introduction

Model Predictive Control (MPC) is a control methodology that computes an optimal control action based on a model of a dynamical system and its predicted future evolution [Mac02, RBJ+08, CB07, CMT87, MH99, GPM89, KH05]. The control objective and the mathematical model is formulated as a real-time optimization problem that repeatedly computes the control inputs. The objective may be related to maximizing profit, minimizing operational costs, or forcing the system to follow a pre-computed set point trajectory. Only the computed inputs associated with the current time step is actuated on the physical system. A new current model state is estimated regularly when new measurements are available and the real-time optimization procedure is repeated. This principle is illustrated in Figure 3.1 and is also often referred to as Receding Horizon Control (RHC). As illustrated in Figure 3.1, the estimation part uses historical data to estimate the current state. A Kalman filter does exactly this for linear models subject to process noise and measurement noise. The regulation

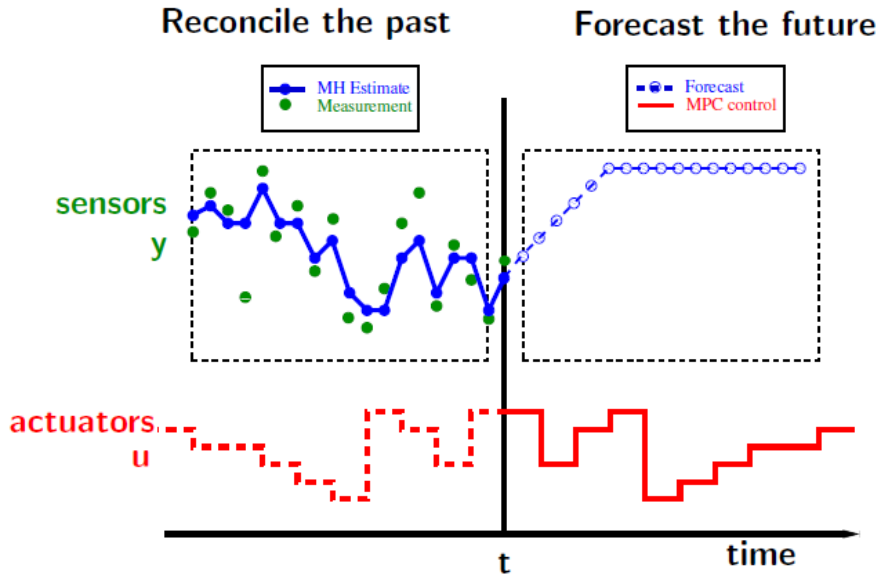

Figure 3.1: *Moving horizon estimation and control principle.*

part, computes a trajectory of the manipulated variables (u) such that the predicted output (z) follows the target as well as possible. The first part of u is implemented and the procedure is repeated at the next sampling time by moving the estimation and regulation window as illustrated in Figure 3.1. The procedure is computational intensive as large-scale optimal control problems must be solved numerically in real-time. It is important to realize that this repeated optimization procedure provides closed-loop feedback and enables the MPC to counteract model uncertainties and external disturbances. The idea of moving horizon control is not new as illustrated by:

> One technique for obtaining a feedback controller synthesis from knowledge of open-loop controllers is to measure the current control process state and then compute very rapidly for the open-loop control function. The first portion of this function is then used during a short time interval, after which a new measurement of the process state is made and a new open-loop control function is computed for this new measurement. The procedure is then repeated. [LM67]

Advances in computer science radically changed the notion of *very rapidly* from 1960 to 1985. Both the increasing computational speed of the hardware and important research advances in optimization algorithms allowed MPC to be implemented in

industrial practice [QB03]. For more than 30 years, MPC has been used routinely in the oil refining industry as well as in the process industries. The reason for the early adoption of MPC by these industries is the slow time constant of the processes involved and the availability of ample computer power. These two characteristics enabled real-time solution of the optimization problem representing the MPC within one sample period. The early implementations of MPC was based on linear convolution models such as impulse and step response models. Even today, the majority of MPC applications are based on linear models [KH05, RBJ+08, CB07]. Discrete-time convolution models (impulse- and step-response models), input-output models (ARX, ARMAX), and state space models are used for the filtering and predictions in MPC. However, the computations in these implementations are based on a state space representation of the system even if the system is parameterized using a convolution model or an input-output model [HPJJ10, JHR11]. For MPC based on linear prediction models the resulting optimization problem is either a linear program (LP) or a convex quadratic program (QP). Fast optimization algorithms for solving these problems have been developed in the past decades [Bix12]. Specifically, the LPs and QPs stemming from an MPC have a special structure that may be utilized by tailor made algorithms for the efficient solution of such problems [Jør05]. The advances in optimization algorithms for linear MPC have enabled this control strategy for new classes of systems, e.g. very large scale systems and systems with fast dynamics. One advantage of MPC is its ability to approximate and solve most optimal control problems numerically with much lower computational effort than classical approaches like dynamic programming [Ber00]. Dynamic programming finds the optimal control solution but suffers from the curse of dimensionality. MPC can handle much bigger problems. Furthermore, MPC also has a unique ability to handle system limitations simply by adding them as constraints in the optimization problem. Examples of these limitations could be the battery capacity or the maximum charge power available in an Electric Vehicle. MPC also handles multivariate (MIMO) systems very well and in general allows operation closer to the system constraints. This ability and greater coordination frequently lead to greater profits or better performance.

3.2 Economic MPC

Large-scale feedback control systems are typically dominated by economic performance goals like profitability, efficiency of operation, cost cutting, lean operation, etc [RAB12]. The current paradigm for achieving overall economic objectives for a given plant is to split the decision making and control system into several layers [Sca09, Sko02]. Fig. 3.2 shows how MPC fits in this traditional control hierarchy. The uppermost layer operates on the slowest time scale and constitutes maintenance and expansion planning of the plant or system to be controlled. The second layer, Real Time Optimization (RTO), optimizes the static steady-state plant variables

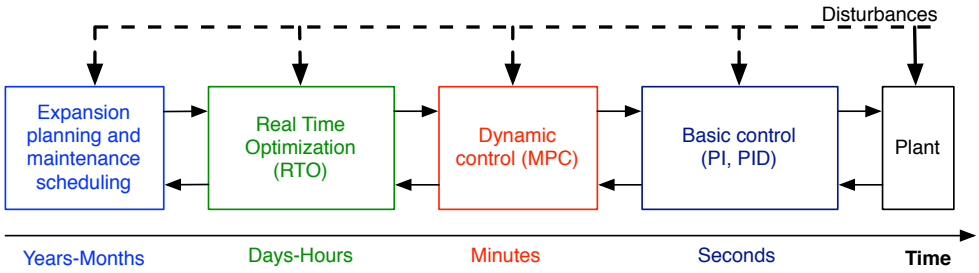

Figure 3.2: *Control hierarchy.*

hourly or daily without considering plant dynamics. The resulting setpoints from the RTO are passed to the third layer controlling the dynamics. MPC is often chosen as control strategy at this level because of its flexibility, performance, robustness, and the ability to directly handle hard constraints on both inputs and states. The MPC tracks the steady-state setpoints and rejects any dynamic disturbances. The disturbances enter at all layers but vary in signal form and frequency depending on the time scale. This control hierarchy can be compared to the power system hierarchy in Fig. 1.8. The hierarchical partitioning of layers has significant effects whenever the process deviates from its setpoint. The objective function used by the controller is usually shaped to achieve fast asymptotic tracking to setpoint changes and low output variance in the face of disturbances, and is usually unrelated to the economic costs of operating the system. There are several proposals to improve the effective use of dynamic and economic information throughout the hierarchy. One is to move dynamic information into the RTO layer. Another approach is to move economic information into the control layer. When the control problem is posed as an optimization problem, such as in MPC, this approach involves modifying the traditional tracking objective function.

In traditional tracking control, the objective is to minimize the unconstrained error between a given reference r and the measured output. In that case we can use a quadratic least squares objective

$$\phi_{reg}(u, y) = \frac{1}{2} \sum_{k=0}^{N-1} ||y_k - \bar{y}_k||_Q^2 + ||u_k - \bar{u}_k||_R^2 \tag{3.1}$$

The weights Q and R are tunable and $(\bar{y}, \bar{u})$ are the steady-state set points (outputs, inputs). Control action is penalized through R as a regularization term. The regularization term must be included to obtain well behaved control action. We apply this objective in some of the control strategies presented in Chapter 5.

In economic MPC, the objective function contains an additional term ϕ_{eco}

$$\phi_{eco}(u, s) = \sum_{k=0}^{N-1} c_k^T u_k + \rho_k^T s_k \tag{3.2}$$

This economic term represents both the cost of operating the subsystems, c, and the cost of violating soft output constraints, ρ. We can combine (3.1) and (3.2) to approximate a Mean-Variance-based objective function [Cap14]

$$\phi = \alpha\phi_{eco} + (1 - \alpha)\phi_{reg}, \qquad \alpha \in [0; 1] \tag{3.3}$$

The economic term is a certainty-equivalent approximation to the mean of the cost function, and the regularization term approximates the variance. The parameter, α, adjusts the trade-off between the two terms, i.e. between expected cost and risk aversion. Solutions in between constitute the efficient frontier [Mar52]. In Section 3.6, we show an example of this trade-off in an example with the objective (3.3) applied to an economic MPC controlling a simple first order model. Other measures of risk than the mean-variance formulation that can be used to regularize the solution are Value-at-Risk (VaR) and Conditional Value-at-Risk (CVaR) [MCM+14]. These methods also take skewed probability distributions into account as the variance alone only provides a good risk measure when considering a symmetric distribution.

The key advantage of using a deterministic formulation (with only expected values of the uncertainty in the objective function) is that the computational load is significantly reduced compared to a mean-variance approach based on Monte Carlo simulations. In this thesis we use the certainty equivalent and insert the mean values of the costs and predictions of states, disturbances etc. An alternative approach to handling uncertainty is via probabilistic constraints [OPJ+10].

3.3 Time Scales

The dynamics involved in power production in power plants and in wind power generators have very fast dynamics compared to the slower thermal storage systems exemplified by residential heating with heat pumps in buildings. When combining multi rate systems in one model the fast sampling rates might result in frequent turning on and off of a heat pump that in practice results in low energy efficiencies. In that case, the control action must be regularized properly, but the MPC problem size is still large. When considering dynamical systems at different time scales in one model, the fastest system dictates the sampling period and thereby the MPC problem size. To reduce the computational burden for controlling linear multi-timescale systems we could augment the models by applying short sampling periods at the first steps and longer sampling periods further into the future. In MPC the predicted control

actions are not implemented anyway, only the first part. When using a time-varying sample period, e.g. exponentially increasing with prediction horizon, $T_s(k) \in \mathbf{R}^N$ we obtain the following state response analogue to (2.14a)

$$x_k = \left(\prod_{i=k}^{0} A_i\right) x_0 + \sum_{j=0}^{k-1} \left(\prod_{i=j}^{1} A_i B_j u_j\right) + E_j d_j$$

Here we set $A_0 = I$. The measurement matrix C stays fixed regardless of the sampling period and can be multiplied to get the output.

[Sca09, PBM+12, JL11, UACA11] deal with this time scale problem by separating the control into a fast and a slow part. As explained in Chapter 1 these different time scales are treated in the current power market structure where markets exist for different time scales. Components that operate at different time scales should therefore operate in different markets and solve different problems.

3.4 Certainty Equivalent Economic MPC

In Section 2.2.1 we defined a stochastic state space system that nicely represents the models in Section 2.2. We also established the optimal filtering and prediction for this system. Next we show how to apply MPC to this problem, i.e. computing the manipulated variables, u_k. We use a certainty equivalence assumption such that the regulator uses mean value predictions for all variables. Consequently, at time k, the predicted operating cost looking N time steps ahead is

$$\phi_{eco} = \sum_{i=0}^{N-1} \hat{c}_{k+i|k}^T \hat{u}_{k+i|k} + \sum_{i=0}^{N-1} \rho_{k+i+1|k}^T s_{k+i+1|k} \tag{3.4}$$

This cost function is linear in $\hat{u}$ and s. For some scenarios or disturbances, it may be very expensive or even impossible to keep the outputs z_k within their constraints. This leads to infeasible optimization problems with no solution. Robust MPC methods exist that specifically deals with uncertainties have been studied widely in literature [BM99, GOJ10]. For our certainty equivalent MPC we simply soften the hard output constraints

$$r_{k+i+1|k}^{\min} \leq \hat{z}_{k+i+1|k} \leq r_{k+i+1|k}^{\max} \tag{3.5}$$

with the additional slack variable, s [ZJM10]. This variable is minimized and penalized heavily to always force solutions towards the feasible set of constraints. So s will only be non-zero if the output is outside the reference interval. In energy systems, the reference interval $\mathcal{R}_k \in [r_k^{\min},\ r_k^{\max}]$ can be related to the power consumption, indoor temperature in a building, temperatures in a refrigeration system or some desired state-of-charge of a battery.

To optimize over future events we need forecasts of the costs and disturbances, $\mathcal{C}_k$ and $\mathcal{D}_k$, respectively. We denote the mean of the forecasts as

$$\mathcal{C}_k = \left\{\hat{c}_{k+j|k}, \rho_{k+j+1|k}\right\}_{j=0}^{N-1} \qquad \mathcal{D}_k = \left\{\hat{d}_{k+j|k}\right\}_{j=0}^{N-1} \tag{3.6}$$

In many situations related to energy systems, d involves variables such as wind speed, temperature and solar radiation. Accordingly, the forecast $\boldsymbol{d}_{k+j|k}$ is the result of a weather prognosis.

The optimal trajectory of the predicted manipulated variables and slack variables, $\left\{\hat{u}_{k+i|k}, s_{k+i+1|k}\right\}_{i=0}^{N-1}$ may be computed by solution of the linear program

$$\begin{aligned}
\underset{\hat{u},s}{\text{minimize}} \quad & \phi\left(\hat{u}, s\right) && \text{(3.7a)}\\
\text{subject to} \quad & \hat{x}_{k+1+i|k} = A\hat{x}_{k+i|k} + B\hat{u}_{k+i|k} + E\hat{d}_{k+i|k} && \text{(3.7b)}\\
& \hat{y}_{k+i+1|k} = C\hat{x}_{k+1+i|k} && \text{(3.7c)}\\
& \hat{z}_{k+i+1|k} = C_z\hat{x}_{k+1+i|k} + D_z\hat{u}_{k+1+i|k} + F_z\hat{u}_{k+1+i|k} && \text{(3.7d)}\\
& u^{\min}_{k+i+1|k} \leq \hat{u}_{k+i|k} \leq u^{\max}_{k+i+1|k} && \text{(3.7e)}\\
& \Delta u^{\min}_{k+i+1|k} \leq \Delta\hat{u}_{k+i|k} \leq \Delta u^{\max}_{k+i+1|k} && \text{(3.7f)}\\
& y^{\min}_{k+i+1|k} \leq \hat{y}_{k+i+1|k} \leq y^{\max}_{k+i+1|k} && \text{(3.7g)}\\
& \hat{z}_{k+i+1|k} + s_{k+i+1|k} \geq r^{\min}_{k+i+1|k} && \text{(3.7h)}\\
& \hat{z}_{k+i+1|k} - s_{k+i+1|k} \leq r^{\max}_{k+i+1|k} && \text{(3.7i)}\\
& s_{k+i+1|k} \geq 0 && \text{(3.7j)}
\end{aligned}$$

At every time step k the goal is to compute $\{u_{k|k}\}_{k=0}^{N-1}$ such that the predicted output trajectory $\{y_k\}_{k=0}^{N-1}$ lies within the specified output trajectory $\{r^{\min}_{k|k}, r^{\max}_{k|k}\}_{k=0}^{N-1}$. N is the prediction horizon, which is normally chosen quite large in order to avoid discrepancies between open loop and closed loop profiles. N must also be large enough to capture the dominating dynamics of the system. We then apply the first control input to the system, i.e. only the first input, $\hat{u}_{k|k}$, of this sequence is implemented. As new information becomes available at the next sampling time, we redo the process of solving the linear program using a moving horizon and keep applying the first control input of the solution to the system. The input and output constraints are inherently taken into consideration and handled by this optimal controller.

The function involving solution of (3.7) and selecting $\hat{u}_{k|k}$ is denoted as

$$u_k = \hat{u}_{k|k} = \mu(\hat{x}_{k|k}, u_{k-1}, \mathcal{D}_k, \mathcal{R}_k, \mathcal{C}_k) \tag{3.8}$$

and requires a number of inputs: the mean value of the forecasts, i.e. $\mathcal{D}_k$, $\mathcal{R}_k$, and $\mathcal{C}_k$, the filtered state, $\hat{x}_{k|k}$, from (2.11), the previous input, u_{k-1}, the predictions (2.12)

and the objective function (3.4). If the process noise and measurement is correlated an additional term must be added to the state estimate (3.10a) [JHR11].

In the economic MPC (3.7) the external cost, c, is the only driver of the control variables. The problem does not track the outputs as long as they stay within certain ranges. The certainty equivalent economic MPC (3.7) is listed in Algorithm 1. It computes the manipulated variable, u_k, based on the current measurement, y_k, the previous input, u_{k-1}, the forecasts $(\mathcal{D}_k, \mathcal{R}_k, \mathcal{C}_k)$, and the smoothed mean-covariance estimate $(\hat{d}_{k-1|k}, R_{dd,k-1|k})$. The main computational load in Algorithm 1 is solution of the linear program (3.7).

3.4.1 Stability

Stability and performance of MPC control schemes has lately been studied extensively. MPC of constrained systems is nonlinear and requires the use of Lyaponov stability theory. This has lead to the addition of a terminal constraint in the cost function to provide stability [AAR12, DAR11, RBJ+08, RM93]. [MAA13] finds update rules for the terminal weight penalty that results in good robust performance. Recently, stability has been investigated without terminal constraints [Grü12a, Grü12b, GPSW12, BGW13]. Hence, it is possible to guarantee asymptotic stability or a desired performance for nonlinear systems without terminal constraints by choosing a minimum prediction horizon length. With some assumptions on controllability the system can be asymptotically stabilized for sufficiently large horizon. From this analysis, the computational burden of MPC can then be reduced as the prediction horizon is decreased. In this thesis, we apply MPC to linear stable energy systems and use long horizons compared to the system dynamics to ensure stability. This is a practical approach but under these assumption we achieve *stability properties associated with an infinite horizon* [MRRS00].

3.5 Solving the MPC problem

Predictive control problems with a quadratic objective function and linear constraints are efficiently solved with algorithms such as Active Set methods [FBD08, BB06, JRJ96], interior-point methods [SFS+14, RWR98, SKC10, JFGND12] and first-order methods [Nes07, BT09, CSZ+12].

Interior point methods (IPMs) solve a linear system of equations in each iteration of the IPM algorithm. A structured interior-point method efficiently solves the optimal control problem arising in traditional MPC via the discrete-time Riccati recursion

[RWR98, FJ13]. The computational cost of this approach is linear in the horizon length, compared with cubic growth for a naive approach. A nonlinear version of the problem can also be solved using an IPM [ARB13]. In Chapter 4, we provide MPC simulation results using a warm started IPM.

An Active Set method for QPs updates the working set of the active constraints. The QP solver can exploit application-specific structure in a computationally efficient and fairly robust manner [BB06]. Later in this chapter we show computational speeds from an Active Set method solving an MPC problem.

Gradient methods are reliable, easy to implement, and guarantees convergence for well behaved functions. Unfortunately, they have slow convergence rates compared to higher order methods. [RJM12, Gis12] investigate fast gradient methods for the solution of linear quadratic MPC problems with input constraints. In particular, the first order methods scale very well for large-scale systems and has been applied widely in Distributed MPC strategies [MN14], that is considered essential within Smart Grid control [KA12]. In Chapter 5 we implement two first order methods on the same MPC problem. The methods are dual decomposition and Douglas-Rachford splitting.

Two ways of speeding up MPC is warm starting, i.e. re-using the solution from previous problems, or early termination, i.e. stopping the optimization algorithm at the required solution tolerance and letting closed loop feedback eliminate errors [SFS+14, WB10].

3.5.1 Economic MPC

One way of solving the linear economic MPC (3.7) is to eliminate the states by condensing the state space model to a finite impulse response (FIR) model [PJ08], see Section 2.2. The output variable is $Z = \Gamma_u U + \Phi x_0 + \Gamma_d D$. The individual economic MPC open loop problems are expressed as Linear Programs (LPs) in the form

$$\begin{aligned} \underset{U,S}{\text{minimize}} \quad & c^T U + \rho^T S \\ \text{subject to} \quad & U_{\min} \leq U \leq U_{\max} \\ & \Delta U_{\min} \leq \Delta U \leq \Delta U_{\max} \\ & Y_{\min} \leq Y \leq Y_{\max} \\ & R_{\min} \leq Z + S \\ & R_{\max} \geq Z - S \\ & S \geq 0 \end{aligned}$$

We re-used the state space models and vector notation from Section 2.2 and additionally define the MPC-related vectors

$$S = \begin{bmatrix} s_i \\ s_{i+1} \\ \vdots \\ s_{i+N} \end{bmatrix} \qquad R_{\min} = \begin{bmatrix} r_i^{\min} \\ r_{i+1}^{\min} \\ \vdots \\ r_{i+N}^{\min} \end{bmatrix} \qquad R_{\max} = \begin{bmatrix} r_i^{\max} \\ r_{i+1}^{\max} \\ \vdots \\ r_{i+N}^{\max} \end{bmatrix} \tag{3.14}$$

$$\Delta U = \begin{bmatrix} \Delta u_i \\ \Delta u_{i+1} \\ \vdots \\ \Delta u_{i+N-1} \end{bmatrix} \quad \Delta U_{\min} = \begin{bmatrix} \Delta u_i^{\min} \\ \Delta u_{i+1}^{\min} \\ \vdots \\ \Delta u_{i+N-1}^{\min} \end{bmatrix} \quad \Delta U_{\max} = \begin{bmatrix} \Delta u_i^{\max} \\ \Delta u_{i+1}^{\max} \\ \vdots \\ \Delta u_{i+N-1}^{\max} \end{bmatrix} \tag{3.15}$$

Note that $\Delta u_i = u_i - u_{i-1}$ such that $\Delta U = \Lambda U - I_0 u_{-1}$

$$\Lambda = \begin{bmatrix} I_0^T \\ \Lambda_d \end{bmatrix} \qquad I_0 = \begin{bmatrix} I \\ 0 \\ \vdots \\ 0 \end{bmatrix} \qquad \Lambda_d = \mathtt{diag}\left(\begin{bmatrix} I_d & I_d & \dots & I_d \end{bmatrix}\right) \qquad I_d = \begin{bmatrix} -I & I \end{bmatrix}$$

In short standard matrix notation required by most numerical solvers the LP is simply

$$\begin{aligned} &\text{minimize} && g^T x \\ &\text{subject to} && Ax \geq b \end{aligned} \tag{3.16}$$

with

$$x = \begin{bmatrix} U \\ S \end{bmatrix} \qquad g = \begin{bmatrix} c \\ \rho \end{bmatrix} \qquad A = \begin{bmatrix} I & 0 \\ -I & 0 \\ \Lambda & 0 \\ -\Lambda & 0 \\ \Gamma_{yu} & 0 \\ -\Gamma_{yu} & 0 \\ \Gamma_{zu} & I \\ -\Gamma_{zu} & I \\ 0 & I \end{bmatrix} \qquad b = \begin{bmatrix} U_{\min} \\ -U_{\max} \\ \Delta\bar{U}_{\min} \\ -\Delta\bar{U}_{\max} \\ Y_{\min} \\ -Y_{\max} \\ \bar{R}_{\min} \\ -\bar{R}_{\max} \\ 0 \end{bmatrix}$$

and

$$\Delta\bar{U}_{\max} = \Delta U_{\max} + I_0 u_{-1} \qquad \bar{R}_{\max} = R_{\max} - \Phi x_0 - \Gamma_d D$$
$$\Delta\bar{U}_{\min} = \Delta U_{\min} + I_0 u_{-1} \qquad \bar{R}_{\min} = R_{\min} - \Phi x_0 - \Gamma_d D$$

In the case when $\phi = \frac{1}{2}||Z - R||_Q^2$ is a quadratic tracking objective we can formulate the problem as a Quadratic Program (QP)

$$\begin{aligned} &\text{minimize} && \frac{1}{2} x^T H x + g^T x \\ &\text{subject to} && Ax \geq b \end{aligned} \tag{3.17}$$

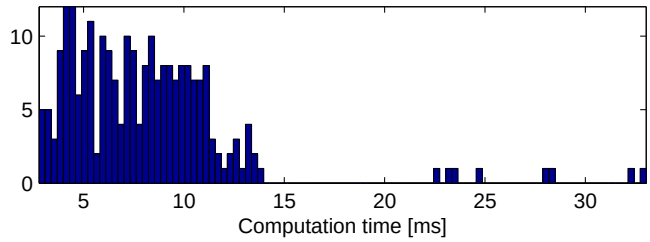

Figure 3.3: *Computation time distribution for all open loop profiles calculated in the five days closed loop simulation with prediction horizon 48 hours.*

If $\Gamma = \Gamma_{zu}$, $\Gamma_d = \Gamma_{zd}$, and $\bar{R} = R - \Gamma_d D - \Phi x_0$, then

$$\begin{aligned}\frac{1}{2}||\Gamma U - \bar{R}||_Q^2 &= \frac{1}{2}(\Gamma U - \bar{R})^T \bar{Q}(\Gamma U - \bar{R}) \\ &= \frac{1}{2}U^T\Gamma^T\bar{Q}\Gamma U - (\Gamma^T\bar{Q}\bar{R})^T U + \frac{1}{2}\bar{R}^T\bar{Q}\bar{R} \\ &= \frac{1}{2}U^T H U + g^T U + h\end{aligned}$$

and

$$\bar{Q} = \texttt{diag}\left(\left[Q, Q, \ldots, Q\right]\right) \quad \Gamma_Q = \Gamma^T\bar{Q} \quad H = \Gamma_Q\Gamma \quad g = -\Gamma_Q\bar{R} \quad h = \frac{1}{2}\bar{R}^T\bar{Q}b$$

3.5.2 Solvers

There are many methods and tools for solving the QPs and LPs arising from the MPC problem. The choice of solver depends highly on the application. In Smart Grids each unit might need embedded real-time solvers, e.g. CVXGEN [MB12], FORCES [DZZ+12], qpOASES [FBD08], that execute fast, reliable and with small code size. The computational demands of MPC also lead research towards offline control law solutions, known as explicit MPC [AB09, BMDP02]. Fast FPGA and GPU implementations are found in [LYM06, KF12].

In this thesis, we mainly used solvers that interface intuitively with Matlab, i.e. MOSEK [AA99] and CVX [CVX12]. But we also used a custom made Active Set solver written in FORTRAN. Figure 3.3 shows the computation times of this Active Set solver when solving the open loop optimization problems from Paper A using an Intel Core i7 2.67 GHz laptop. The average computation time is seen to be around 8 ms. Using hard constraints the average computation time reduces to 1 ms. Note that this is for small LPs.

3.6 Mean-Variance Economic MPC

In this section we provide an example of applying the Mean-Variance-objective (3.3) to an economic MPC controlling a simple first order model. We assume known prices, c, but uncertain disturbances, d, given as n_ω different forecasted disturbance scenarios with increasing variance a long the prediction horizon. The economic MPC problem is

$$\begin{aligned}
\underset{u}{\text{minimize}} \quad & \phi_{MV} = \alpha\mathbb{E}(c^T u) + (1-\alpha)\mathbb{V}ar(c^T u) && \text{(3.18a)}\\
\text{subject to} \quad & x^\omega_{k+1+i|k} = Ax^\omega_{k+i|k} + Bu^\omega_{k+i|k} + E\hat{d}^\omega_{k+i|k} && \text{(3.18b)}\\
& y^\omega_{k+i+1|k} = Cx^\omega_{k+1+i|k} && \text{(3.18c)}\\
& u^{\min}_{k+i+1|k} \le u^\omega_{k+i|k} \le u^{\max}_{k+i+1|k} && \text{(3.18d)}\\
& y^{\min}_{k+i+1|k} \le y^\omega_{k+i+1|k} \le y^{\max}_{k+i+1|k} && \text{(3.18e)}
\end{aligned}$$

The expected value and the variance can re reduced to matrix notation such that

$$\mathbb{E}(c^T u) = \hat{\phi} = \frac{1}{n_\omega}\sum_{\omega}^{n_\omega} c^T u^\omega = \Omega u \tag{3.19}$$

$$\mathbb{V}ar(c^T u) = \frac{1}{\bar{n}_\omega}\sum_{\omega}^{n_\omega}(\phi^\omega - \hat{\phi})^2 = \frac{1}{\bar{n}_\omega}\sum_{\omega}^{n_\omega}(c^T S^\omega u - \Omega u)^2 = u^T \Lambda u \tag{3.20}$$

The economic MPC problem is clearly a QP with objective

$$\phi_{MV} = \alpha\Omega u + (1-\alpha)u^T\Lambda u$$

Figure 3.5 shows an open-loop simulation of a first order system with $\tau = 12$ h. The expected value of the control input keeps the expected value of the output above the dashed constraint. Just below we plotted the $n_\omega = 30$ disturbance forecast scenarios used in the simulation. Figure 3.4 shows the efficient frontier, i.e. the expected cost (negative profit) as a function of the trade-off parameters α. The value $\alpha \simeq 0.4$ maximizes the ratio of expected cost to risk.

3.7 Summary

In this chapter, we presented linear Model Predictive Control, its principle and place in the control hierarchy. We formulated an economic MPC and defined its objectives, including a stochastic formulation based on a Mean-Variance objective. We briefly reviewed the literature on stability for MPC. We described the algorithm for a certainty equivalent economic MPC mainly used in this thesis, and showed how to solve the underlying optimization problem including state estimation.

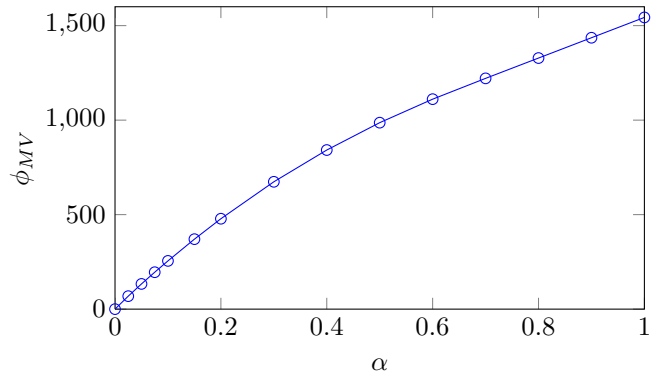

Figure 3.4: *Efficient frontier of Mean-Variance economic MPC simulation.*

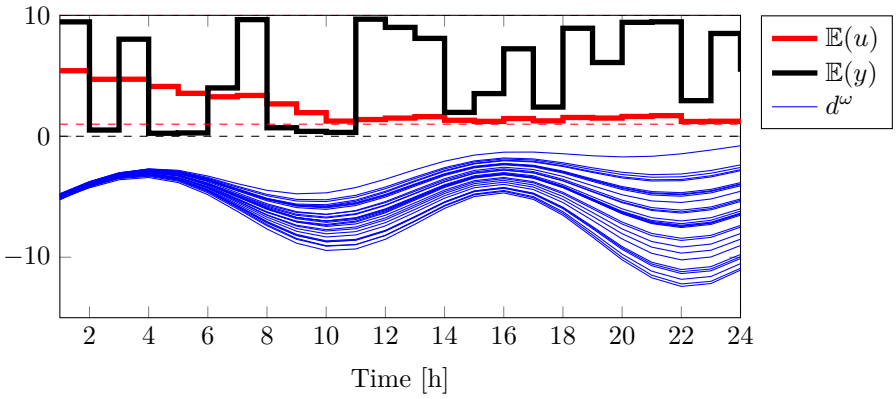

Figure 3.5: *Mean-Variance economic MPC simulation of a first order system with unity gain and* $\tau = 12$ *h.* $n_{\omega} = 30$ *disturbance scenarios.* $\alpha = 0.4$.

Algorithm 1 Certainty equivalent economic MPC with external forecasts

Require:
Input: y_k, u_{k-1}
Memory: $\hat{x}_{k-1|k-1}$, $P_{k-1|k-1}$.
Forecasts:

$$\mathcal{D}_k = \left\{\hat{d}_{k+i|k}\right\}_{i=0}^{N-1}, \ (\hat{d}_{k-1|k}, R_{dd,k-1|k}) \tag{3.9a}$$

$$\mathcal{R}_k = \left\{r^{\min}_{k+i+1|k}, r^{\max}_{k+i+1|k}\right\}_{i=0}^{N-1} \tag{3.9b}$$

$$\mathcal{C}_k = \left\{\hat{c}_{k+i|k}, \rho_{k+i+1|k}\right\}_{i=0}^{N-1} \tag{3.9c}$$

One-step predictor and filter:
Compute the one-step prediction

$$\hat{x}_{k|k-1} = A\hat{x}_{k-1|k-1} + Bu_{k-1} + E\hat{d}_{k-1|k} \tag{3.10a}$$

$$\hat{y}_{k|k-1} = C\hat{x}_{k|k-1} \tag{3.10b}$$

Compute the innovation

$$e_k = y_k - \hat{y}_{k|k-1} \tag{3.11}$$

Compute

$$\begin{aligned} P_{k|k-1} = {} & AP_{k-1|k-1}A^T \\ & + GR_{ww,k-1}G^T + ER_{dd,k-1|k}E^T \end{aligned} \tag{3.12a}$$

$$R_{e,k} = R_{vv} + CP_{k|k-1}C^T \tag{3.12b}$$

$$K_{fx,k} = P_{k|k-1}C^T R_{e,k}^{-1} \tag{3.12c}$$

$$P_{k|k} = P_{k|k-1} - K_{fx,k}R_{e,k}K_{fx,k}^T \tag{3.12d}$$

Compute the filtered state

$$\hat{x}_{k|k} = \hat{x}_{k|k-1} + K_{fx,k}e_k \tag{3.13}$$

Regulator:
Compute $u_k = \mu(\hat{x}_{k|k}, u_{k-1}, \mathcal{D}_k, \mathcal{R}_k, \mathcal{C}_k)$ by solution of the linear program (3.7).
Return:
Manipulated variable: u_k
Update the memory with: $\hat{x}_{k|k}$, $P_{k|k}$

Chapter 4

Economic MPC Simulations

In this chapter, we provide simulations of the units modeled in Chapter 2 with the certainty equivalence linear economic MPC (3.7) presented in Chapter 3. These simulation results are the main contributions from Paper A, B and C, that investigated three different and important Smart Grid consumer units: a building with a heat pump, an Electric Vehicle (EV), and a heat storage tank connected to solar thermal collector.

4.1 Introduction

Each unit uses an economic MPC to minimize its consumption costs given the predicted price vector. Meanwhile, the controller tries to keep the outputs within their flexible operating ranges. So instead of tracking a set point, e.g. a desired indoor temperature, the economic MPC respects a set of user defined constraints (comfort bounds) and let the price drive the output. This economic MPC has been extensively investigated for refrigeration systems in [Hov13] that includes detailed non-linear models, predictors, and some handling of uncertainty. We deal with uncertainty in a practical way by simply assuming a constraint back-off strategy and by using soft output constraints.

The economic MPC repeatedly requires price predictions from external forecasts. In

our simulations we used the actual day-ahead prices from the Nordic electricity market, Elspot, as described in Section 1.3.1. These prices are settled in the day-ahead market and are based on pre-negotiated energy delivery schedules. So broadcasting this day-ahead price to all consumers will cause energy imbalances. However, we still use this price signal in our simulations for a number of reasons: 1) to illustrate the economic MPC concept 2) these prices reflect the amount of wind power in the system 3) we expect a similar price signal in the future Smart Grid, and 4) later in Section 5.5 we replace the price signal with our own and reuse the controller. The resulting cost savings of using economic MPC are also calculated as part of the results. These savings are *best case* upper bounds as no uncertainty nor unknown disturbances were taken into account.

4.2 Building with Heat Pump

In Paper A, we simulated an economic MPC controlling the indoor temperature of a low-energy residential building with a floor heating system and a heat pump. Fig. 4.1 illustrates the optimal heat pump compressor schedule and the indoor temperature for five days. Also the two disturbances are shown: the outdoor temperature, T_a, and the solar radiation, ϕ_s. The outdoor temperature reflects a cold climate, i.e. the outdoor temperature is lower than the indoor temperature. The solar radiation also contributes to heating the building. The constraints indicate that during night time the temperature is allowed to be lower than at day time. Clearly, the heat pump power consumption is moved to periods with cheap electricity and the thermal capacity of the building floor is able to store enough energy such that the heat pump can be left off during day time while maintaining an acceptable indoor temperature. In the beginning the comfort level is compromised very little due to the initial conditions. However, the economic MPC problem stays feasible. The simulations show cost savings up to 35 %.

4.3 Electric Vehicle battery

As in the previous Section 4.2 Paper B reports the same approach applied as a charging strategy for an EV battery. Fig. 4.2 shows the simulation results. Real commuter driving patterns defined the disturbance scenarios while the day-ahead electricity prices influenced the charging pattern. Comparing different charging strategies clearly showed the potential of using economic MPC to shift the load in a cost efficient way. The simulations showed annual savings up to 50%.

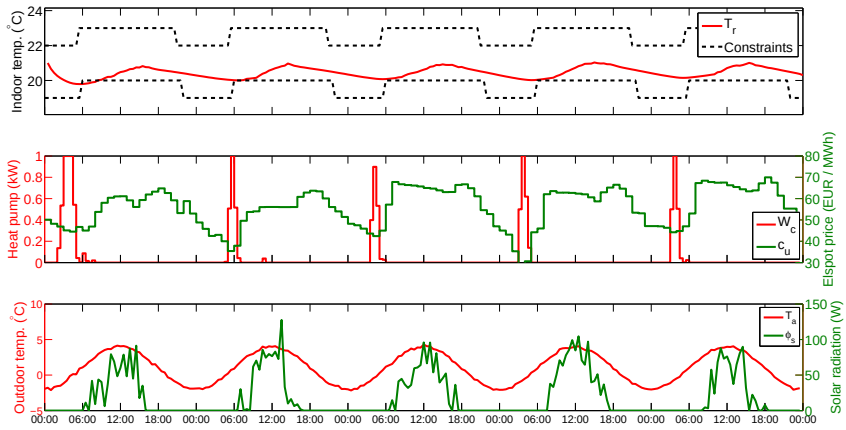

Figure 4.1: *The simulation shows the indoor temperature in a building for five days starting midnight 20 JAN 2011. The middle figure shows the electricity price and the optimal schedule for the heat pump. The lower figure contains the outdoor temperature and solar radiation. The heat pump is on when the electricity price is low.*

4.4 Solar thermal collector and heat storage tank

Paper C investigated the potential of applying economic MPC to a heat storage tank connected to a solar thermal collector. But this time the controller integrated state-of-the-art forecasts of the solar radiation and consumption. The forecasts were based on measurements and models of actual residential buildings based. The solar thermal power was forecast with the method described in [BMP11]. This forecast was based on a conditional parametric model and applied for forecasting the hourly solar thermal power up to 36 hours ahead. Several important modeling factors were taken into account: numerical weather predictions of the global radiation, the collector thermal performance, the orientation of the collector, and shading from objects in the surroundings. Again an economic MPC controlled the power consumption of the auxiliary heating elements in the heat storage tank. The electrical heating elements were turned on in periods when the incoming solar energy alone could not meet the heat demand, e.g. hot water usage and space heating in a residential household. Figure 4.3 shows the simulation results of an entire year. The controller performance showed electricity cost savings of 25-30% compared to current thermostat control strategy for six different households.

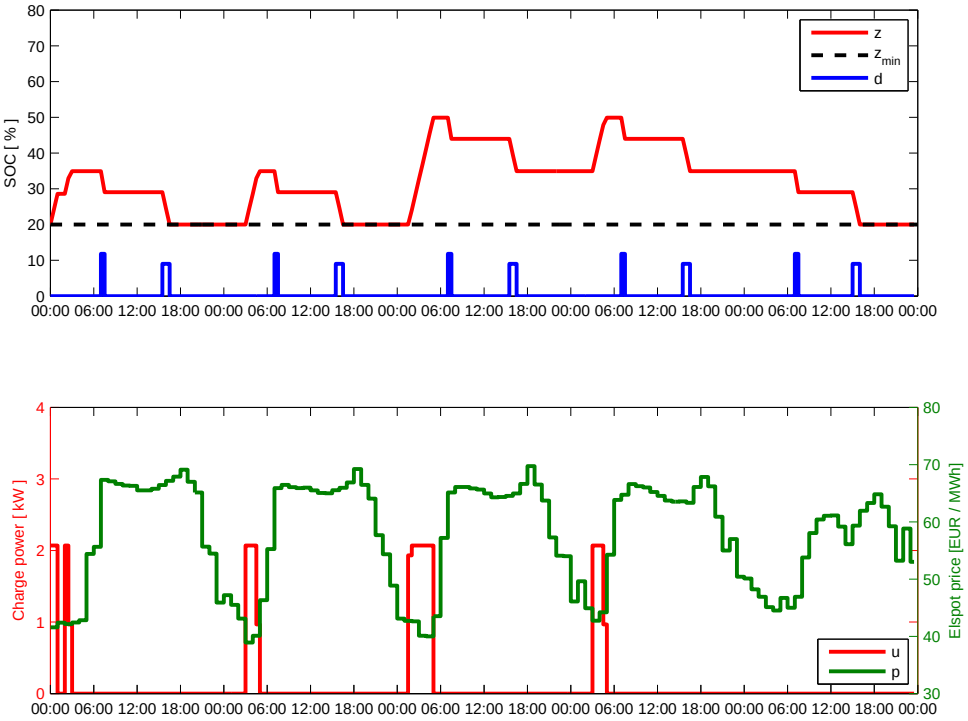

Figure 4.2: *Optimal charging of EV for five days using economic MPC with prediction horizon $N = 48$ h. The upper plot shows the state-of-charge ζ and the driving pattern (demand) d_k. The lower plot shows the electricity price and the controlled charge power.*

4.4.1 Estimating Model Parameters

The heat dynamics of the storage tank in Section 2.3.2 was modeled as a grey-box model based on real data sets and maximum likelihood methods. A modeling tool, CTSM [KMJ04], estimated the unknown parameters of an Extended Kalman Filter (EKF) bases on the SDE from (2.4). CTSM assumes the model to be a set of stochastic differential equations describing the dynamics of a system in continuous time and a set of algebraic equations describing how measurements are obtained at discrete time instants. Given a grey-box model structure, any unknown model parameters can be estimated from data suing this tool, including the parameters of the diffusion term. The parameter estimation method in CTSM is based on a maximum likelihood (ML) method and a maximum a posteriori (MAP) method from [KMJ04].

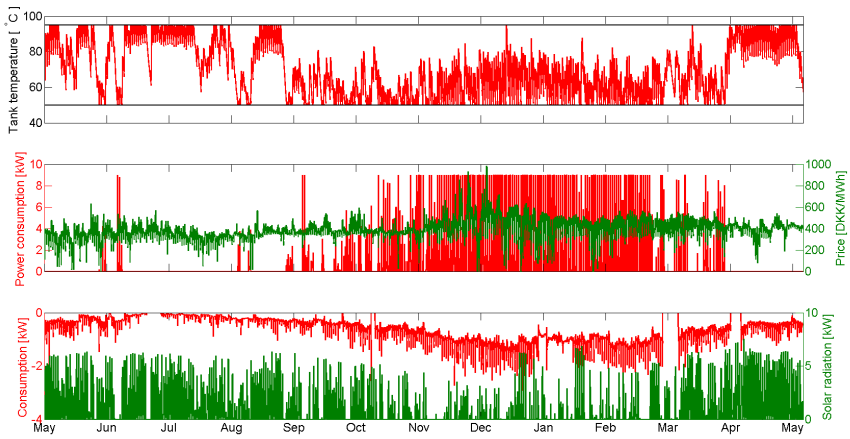

Figure 4.3: *A one-year simulation starting May 17 2010 with 24 h prediction horizon using uncertain forecasts. The upper plot shows the tank temperature, the middle plot contains the electricity price and the optimal power consumption for the heating element, and the lower plot contains the solar heat input and the consumption demand from space heating or hot water. The heating element is turned on when the electricity price is low.*

4.5 Economic MPC Savings

We also conducted simulations with constant electricity prices. In that case the economic MPC objective is equivalent to minimizing the power consumption without considering prices, i.e. the objective function is $\phi(u) = \mathbf{1}^T u$. Consequently no load shifting is performed. Compared to an economic MPC that took the day-ahead prices into account we observed annual economic savings up to 50% for the EV case study and around 25% for both the solar collector heat tank and the building with a heat pump. In Denmark these savings are only on the day-ahead price that constitutes approximately 20% of the total end-user bill after adding taxes.

4.5.1 Prediction Horizon

In the solar tank case study we also compared the economic MPC to thermostat control and evaluated the performance. For a one year simulation we calculated the annual power consumption and electricity costs from closed loop simulations for four

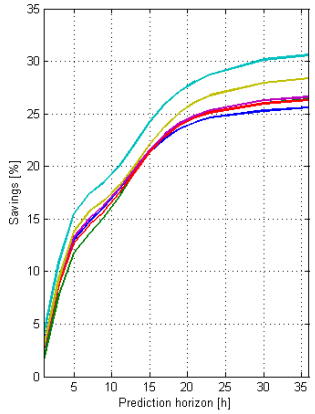

(a) Annual savings in percent compared to conventional thermostat control for six different buildings.

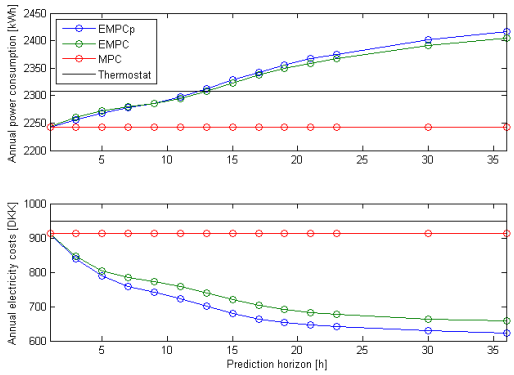

(b) Annual power consumption (upper) and electricity costs (lower) for a building as a function of the prediction horizon N for four different control strategies. Closed loop economic MPC with known inputs (EMPCp), with forecasts subject to uncertainty (EMPC), a constant electricity price (MPC) and a thermostat control.

Figure 4.4: Economic MPC performance for the solar collector heat storage tank.

different control strategies. The results as a function of prediction horizon are shown in Fig. 4.4.

As the prediction horizon grows larger than 24 hours, the cost savings do not increase much. This is shown in Fig. 4.4(b) and is due to the dynamics of the tank and its constraints. Predictions about the solar energy and the consumption next week do not change the optimal consumption pattern because both the maximum input power and the storage capacity of the tank is limited. Furthermore, using perfect forecasts, i.e. knowing the future inputs and disturbances exactly, does not increase the savings significantly compared to forecast based on historical data.

Fig. 4.4(a) shows that the power consumption for the economic MPC grows larger than for the ordinary thermostat control as the prediction horizon increases. However the costs go down. Consequently, to save more money, more power must be used for boosting control actuation in the cheap periods. The increased power consumption can be justified by the electricity price that should reflect the amount of available renewable energy and power system needs.

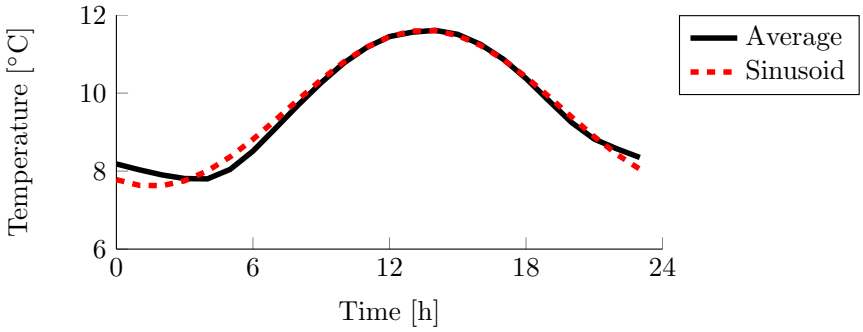

Figure 4.5: *Hourly temperature averages for 2011 in Eastern Denmark. On average a simple sinusoid models the trend quite well.*

4.5.2 Outdoor Temperature Prediction

On average the outdoor temperature trend matches a simple sinusoid quite well as seen in Fig. 4.5. A linear transfer function of a sinusoid with frequency $\omega = 2\pi/T$, period T, amplitude a and offset b is

$$y(t) = a\sin(\omega t) + b \qquad Y(s) = \frac{a\omega}{s^2 + \omega^2} + b$$

The equivalent state space model is

$$\begin{aligned} \dot{x} &= \begin{bmatrix} 0 & -\omega^2 & 0 \\ 1 & 0 & 0 \\ 0 & 0 & 0 \end{bmatrix} x + w \\ y &= \begin{bmatrix} 0 & 1 & 1 \end{bmatrix} x + v \end{aligned}$$

$x_3 = b$ is the estimated offset, i.e. the current mean temperature. We assume the period to be diurnal and known $T \simeq 24$ h. We apply a Kalman filter to estimate the states and model parameters in order to provide outdoor temperature predictions to an economic MPC. We validated this simple predictor analogue to [HBLJ13] by evaluating the economic savings for the heat pump and building modeled in Section 2.3.3. We used two data sets from West Denmark 1) the 2011 day-ahead market prices and 2) the 2011 average outdoor temperature from the Danish Meteorological Institute. The annual savings improvement of using known inputs compared to this simple predictor were below 3.6% even for prediction horizons up to 48 hours.

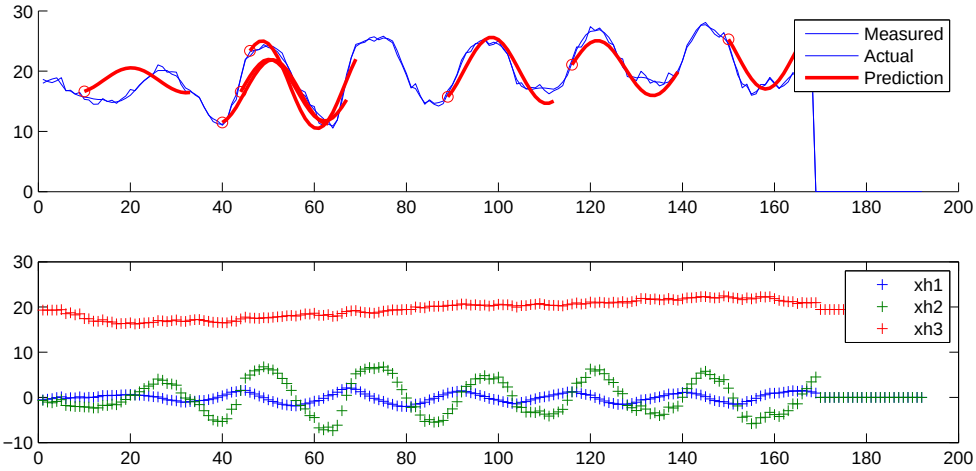

Figure 4.6: *Forecast of outdoor temperature from a sinusoidal model and state estimation.*

4.6 Smart Energy System

In this section, we present a case study simulation with a portfolio of units: two power plants, a wind farm, and a fleet of 10,000 EVs. Section 2.2 describes the dynamics of the individual units. The fleet of EVs are aggregated and used as flexible storage to help balance the load. The charging and discharging constraints should be quite conservative since they depend on the availability of the EVs, i.e. it is assumed that an EV is not connected to the grid and able to charge while driving. However, based on driving pattern analysis the availability has been reported to be more than 90% assuming that the EV is able to charge whenever it is parked [WNØ+10]. The EV batteries have a finite battery capacity Q_c that limits the size of the EV storage such that

$$0 \leq y_v \leq Q_n n_{ev} \tag{4.1}$$

where $n_{ev} = 10^4$ is the number of EVs in the fleet and y_v is the EV fleet state of charge. We use $Q_n = 24$ kWh as EV battery capacity. The power balance (2.36) must be nonnegative, $\bar{z}_t \geq 0$, in order to meet the demand. Also a base load d_b is added as a disturbance, i.e. the reference load from all other unmodeled power consumers that must be supplied. We apply an economic MPC (3.7) with sampling period $T_s = 5$ s to the problem that minimizes the electricity costs of operating a number of power plants, a fleet of EVs, the wind farm and consumers based on predictions of the demand, production and operating costs over the prediction horizon. Power demands must be met at all times and any imbalances would be economically penalized in a

	Value	Unit	Description
K	$[1, 1]$		Power plant gain
K_w	1	MW/(m/s)	Wind farm gain
τ	$[1, 1]$	s	Power plant time constant
τ_w	0.7	s	Wind farm time constant
η^+	0.9		EV charge efficiency
η^-	0.9		EV discharge efficiency
u_{min}	[0,0,0,0]	MW	Minimum control input
u_{max}	[5,7,3,3]	MW	Maximum control input
Δu_{min}	[-2,-0.2,-0.6,-0.6]	MW/s	Minimum control ramp input
Δu_{max}	[2,0.2,0.6,0.6]	MW/s	Maximum control ramp input
y_{min}	[0,0,0,0]		Minimum output
y_{max}	[5,7,240,∞]		Maximum output
c	[10,5,0,5]	MW^{-1}	Production costs

Table 4.1: Case study parameters

real power market where external spinning reserves otherwise must be activated to restore the balance. Consequently, in our case the slack variable penalty in (3.7h)-(3.7i) could also be an actual cost or penalty for not providing enough power.

The optimal power production within the prediction horizon is the solution to (3.7). This control action is calculated at every time step k and represents a decision plan, stating when to produce and with how much power. The EV storage charge and discharge is also part of the decision plan. The control action is optimal in terms of economy and is the cheapest based on the predictions and model assumptions available at time $k = 0$.

Fig. 4.7 illustrates a closed loop simulation of this system. We used the parameters from Table 4.1 and a prediction horizon of $N = 6$ min. The upper plots show the power plant production and set points. The expensive but fast power plant is used to balance the load while the slower but cheaper power plant ramps up production. The second plot shows how the aggregated EV fleet is controlled and the resulting charge and discharge power. In the beginning of the simulation the EV fleet discharges to the grid to boost production. Consequently, the EV batteries are depleted and the state of charge decreases. The charge demand d_v from the EVs was modeled as a sinusoid. The third plot shows overall power balance including a base load disturbance and the wind power production. Also the power balance $\bar{z}_k$ is shown. It expresses the imbalances from the positive production and negative consumption. Since we have no uncertainty on the load forecasts this imbalance is mostly zero.

4.7 Matlab MPC toolbox for Smart Energy Systems

We gathered the models in a MATLAB toolbox available for download[1]. The toolbox also contains the economic MPC from (3.7) that balances production and consumption of the units. Figure 4.8 shows a flowchart of the toolbox code. The main script, `empctoolbox.m`, currently consists of a single script with all sub-functions included. Per default, the script runs a sample scenario similar to the one in Section 4.6. This scenario can easily be modified. The number of units, their type, the prediction horizon, the simulation time, and sampling periods can be chosen initially. It is possible to simulate model mismatch by setting up different models used by the controller. `SetupSystem` and `SetupScenario` generates the model parameters, constraints and disturbance forecasts used in the simulation. Given these variables `computeModel` builds all unit models from their discrete-time state space and impulse response models.`designMPC` prepares all fixed constraint matrices for the solver. The soft output constraints penalties are set here, and the controller model is built. During the closed loop simulation two functions update and compute the individual open loop MPC problems at every simulation time step. `updateMPC` basically packs the current open loop MPC problem into matrices ready to be fed to a standard LP solver. It updates measured outputs, estimates states using a Kalman filter, updates disturbance forecasts and other time-varying constraints. `computeMPC` concatenates the fixed matrices with updated information. We also re-build the constraints from all models again here. We assume that the models are allowed to be time-varying and potentially need a re-discretization and update. In the default scenario the models are not time-varying. The actual solver is called from `computeMPC`. We use MATLABs linprog and quadprog interface, but recommend to install MOSEKs faster solvers that replaces these functions. Finally, the simulated system is actuated, the states are updated, and the results are plotted.

4.8 Summary

In this chapter we:

- Simulated different Smart Grid units: A building heat pump, EV, a heat storage tank connected to a solar collector simulations and scenarios
- Integrated forecasts based on real data in the predictive control system
- We used system identification tools to model the parameters

[1] www.compute.dtu.dk/~rhal/code

- Compared the control performance for different control strategies
- Investigated the effect of the prediction horizon
- Calculated electricity cost savings of taking prices into consideration
- Formulated a simple predictor for the outdoor temperature and evaluated the performance to perfect forecasts, i.e. known inputs
- Integrated the forecasts using a Kalman filter
- Simple predictors of outdoor temperatures in combination with a Kalman filter do not decrease economic savings significantly
- Simulated a smart energy systems with a portfolio of units
- Presented the developed MATLAB toolbox for simulating economic MPC and linear models including a library of Smart Grid units

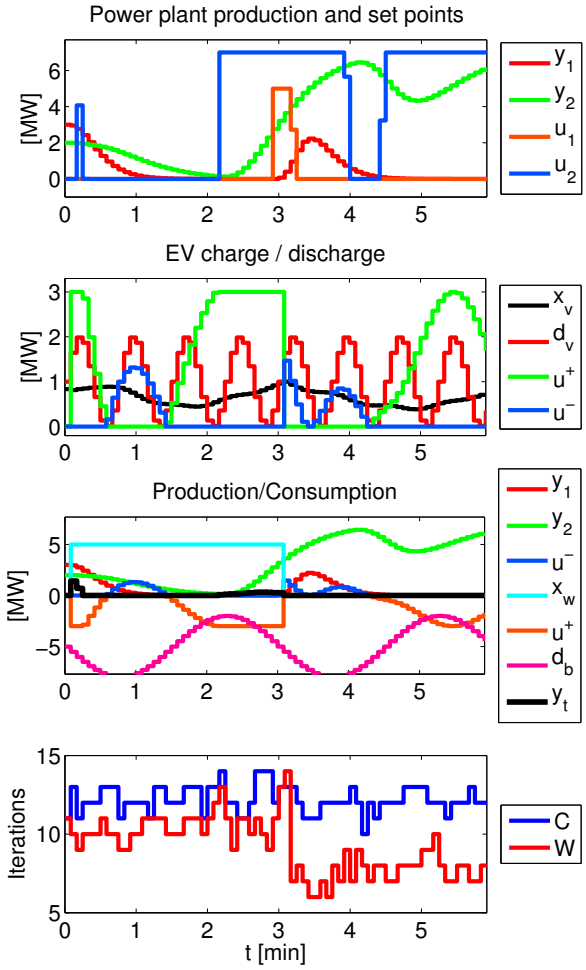

Figure 4.7: Case study simulation with two power plants, a wind farm, a large EV fleet and a base load consumption. $\{y_1, y_2\}$ are the power plant output powers, x_w the wind farm production Shows the resulting closed loop economic MPC decisions of production and consumption over 6 minutes. Performance when warm-starting our algorithm (W) is compared to standard cold-starting (C) at the bottom.

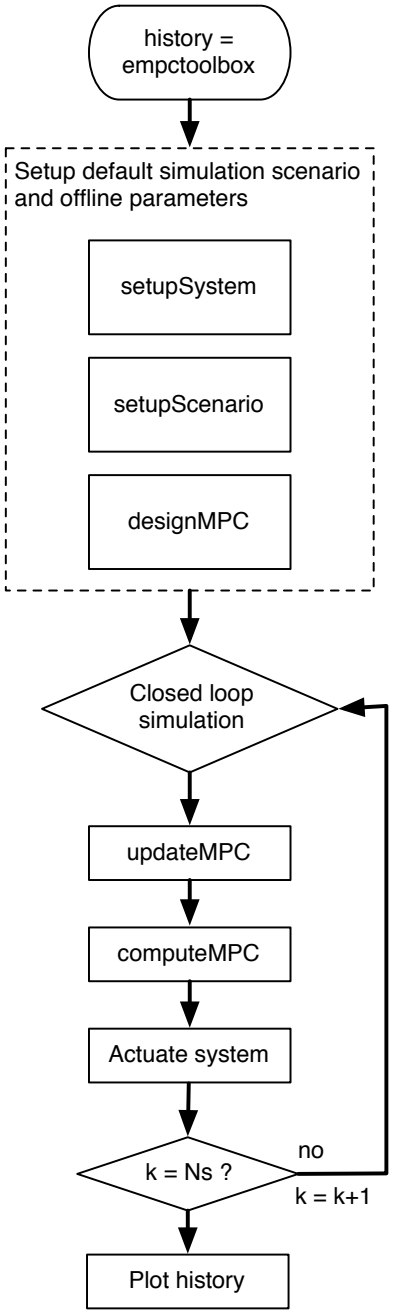

Figure 4.8: *Flowchart of* `empctoolbox.m`.

Chapter 5

Aggregator Control Strategies

The simulations in this chapter show the different ways of aggregating the units with the economic MPC presented in Section 3.4. We summarize different MPC-based aggregator control strategies described in Paper D, E and F. In the first Section 5.2 we formulate the common aggregator problem to be solved. To solve this large-scale control problem and make it computational tractable we apply two decomposition methods in Section 5.3, Douglas-Rachford splitting and dual decomposition. In Section 5.5 we investigate dual decomposition using a low-order aggregated model inspired by Paper F. A decentralized control strategy is presented in Section 5.4 based on Paper D. Section 5.6 shows results from warm-starting an interior point method using the methods described in [SFS+14, SAY12]. Finally, Section 5.7 compares the different aggregator methods and provides a good overview.

5.1 Introduction

In the future Smart Grid a hierarchical structure of controllers, including aggregators, will most likely exist to reduce the complexity [GKS13]. The aggregator strategies for controlling DERs in a Smart Grid broadly categorizes into: direct control and indirect control [BS08, ANAS10, LSD+11].

A direct control strategy assumes direct access to the control inputs of each DER,

and feedback through two-way communication. The direct controller must calculate and communicate a consumption plan to each DER. This leads to large-scale control problems with high complexity and fast communication requirements. An agreement between the DERs and the aggregator about the available flexibility and control maneuverability is also mandatory. An indirect control strategy relies on a unidirectional signal, such as prices, to incentivize DER control action [HYB+12]. The aggregator either measures the response through aggregated grid measurements or through markets.

Different MPC strategies can be applied in these strategies and are often referred to as Decentralized MPC (DMPC) [MN14, BB10]. The architecture of DMPC and the coordination between local controllers is defined by the following categories: decentralized, distributed, and hierarchical. A control system is *centralized* if there is a single controller that solves the plant-wide problem. The control is *decentralized* when there are local controllers in charge of the local subsystems of the plant that require no communication among them. When the local controllers communicate in order to find a cooperative solution for the overall control problem, the control system is *distributed*. Finally, the control system is *hierarchical* if there are different control layers that coordinate the process. In this case, upper layers manage the global objectives of the process and provide references for the lower layers that directly control the plant. An exchange of candidate control decisions may also happen during the decision making process, and iterated until an agreement is reached among the different local controllers.

Our strategies do not include the distribution grid, implicitly assuming that the underlying network has enough capacity to distribute the power demanded by the users without causing congestion. Furthermore, we only consider power balance in steady-state and ignore fast timescale dynamics such as frequency and voltage fluctuations due to random supply and demand. The aggregator strategies are also targeted consumption units.

The current work has several limitations based on assumptions often made in literature [CI12, TBS11]. First, our model does not include the distribution system, implicitly assuming that the underlying network has enough capacity to distribute the power demanded by the users without causing congestion. We do however limit the total aggregated active power when coordinating more units. Our results are mainly obtained for the case without uncertainty.

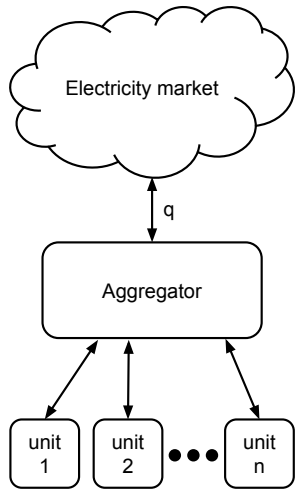

Figure 5.1: *Aggregator role and portfolio of units. The aggregator negotiates a consumption plan q to follow from the market.*

5.2 The Aggregator Balancing Problem

We wish to control the power consumption of a large number of flexible and controllable units. The motivation for controlling the units is to continuously adapt their consumption to the changing stochastic power production from wind and solar. In the future this power balancing might be done by solving large-scale control problems. We assume that an *aggregator* controls a large number of flexible consumption units as shown in Fig. 5.1. Based on predictions of the aggregated unit behavior, the aggregator bids into the day-ahead power market and buys a certain amount of energy for the coming day. The plan could be a result of solving a unit commitment problem [SB04], where stochastics and integer variables are taken into account. The resulting consumption plan must be followed to avoid imbalances and in turn economic penalties. So a real-time controller must regulate the power to minimize any imbalances caused by prediction errors. The MPC framework presented in Chapter 3 fits this problem very well. MPC and aggregators is the scope of the remaining part of this thesis.

5.2.1 Mathematical Formulation

The power consumption profile is a vector denoted $q \in \mathbf{R}^N$ and denotes the amount of power to be consumed at each time step k for the entire prediction horizon $k =$

$1, ..., N$. This profile must be followed by the aggregator, such that the combined power consumption from all units sum to this at every time instant. The centralized large-scale problem that includes all units and their variables (p, x_j, y_j, u_j) and constraints is

$$\underset{p_k, u_{j,k}}{\text{minimize}} \quad \sum_{k=0}^{N-1} g(p_k) + \sum_{j=1}^{n} \phi_j(u_{j,k}) \tag{5.1a}$$

$$\text{subject to} \quad p_k = \sum_{j=1}^{n} u_{j,k} \tag{5.1b}$$

$$x_{j,k+1} = A_j x_{j,k} + B_j u_{j,k} + E_j d_{j,k} \tag{5.1c}$$

$$y_{j,k} = C_j x_{j,k} \tag{5.1d}$$

$$y_{j,k}^{\min} \leq y_{j,k} \leq y_{j,k}^{\max} \tag{5.1e}$$

$$\Delta u_{j,k}^{\min} \leq \Delta u_{j,k} \leq \Delta u_{j,k}^{\max} \tag{5.1f}$$

$$u_{j,k}^{\min} \leq u_{j,k} \leq u_{j,k}^{\max} \tag{5.1g}$$

We model the $j = 1, 2, ..., n$ units with linear discrete-time state-space systems and define $\mathcal{U}_j$ as a closed convex set containing the model and constraints of the jth unit (5.1c)-(5.1g). $x_j \in \mathbf{R}^N$ is the time varying state vector in the discrete-time state-space system defined by the matrices (A_j, B_j, E_j, C_j). y_j is the output, of a linear system with controllable input u_j. d_j is the modeled and predictable disturbances (e.g. outdoor temperature). The time-varying input and output constraints are superscripted with max and min, and account for the available flexibility for each unit. For thermal storage units this is the power available and the accepted temperature interval, respectively. $\Delta u_{j,k} = u_{j,k} - u_{j,k-1}$ is the rate of movement, where k is the time step in the time varying input vector $u_j \in \mathbf{R}^N$. The total consumption $p \in \mathbf{R}^N$ is a sum of the predicted consumption profiles u_j. p can also be constrained to reflect capacity constraints in the power grid. g is the aggregator objective function. Examples of local objective functions are

$$\phi_j^{\text{eco}}(u_j) = c_j u_j \tag{5.2a}$$

$$\phi_j^{\text{soft}}(\nu_j) = \rho_j s_j \tag{5.2b}$$

$$\phi_j^{reg}(u_j) = ||\Delta u_j|| \tag{5.2c}$$

The functions ϕ_j and g may be indicator functions that represent constraints on the variables u_j or their sum. We exploit this later when decomposing the problem. The main aggregator objective, g is to track the given power consumption profile q by minimizing $e = p - q$.

5.3 Decomposition

Decomposition methods for convex MPC formulations includes dual decomposition [Ran09], Dantzig-Wolfe decomposition [DW61, CCMGB06], and Benders Decomposition [SY05, Ang04]. Splitting methods such as Douglas-Rachford splitting [EB92] handles more general convex functions, even non-linear, and converges under very mild conditions. A special case of Douglas-Rachford splitting leads to the ADMM formulation [BPC+11]. In the following section we briefly show how Douglas-Rachford splitting can be applied to the aggregator problem exemplified by simulations with thermal storage units e.g. heat pumps in buildings.

5.3.1 Problem Formulation

For the decomposition methods we mainly considered consumption units and we formulate a special case of the centralized problem (3.7). The power consumption profile is a vector denoted $r_{min} = q \in \mathbf{R}^N$ and denotes the amount of power to be consumed at each time step k for the entire prediction horizon $k = 1, ..., N$. This profile must be followed by the aggregator, such that the combined power consumption from all units sum to this at every time instant. We add an aggregator objective and formulate the centralized MPC problem (5.1) in shorthand notation as

$$\text{minimize} \quad \sum_{j=1}^{n} f_j(u_j) + g\left(\sum_{j=1}^{n} u_j\right) \tag{5.3}$$

The indicator functions $f_j : \mathbf{R}^N \to \mathbf{R}$ and $g : \mathbf{R}^N \to \mathbf{R}$ are closed and convex, and contain the constraints and objectives of the problem

$$f_j(u_j) = \begin{cases} \phi_j(u_j) & \text{if } u_j \in \mathcal{M}_j \\ +\infty & \text{otherwise} \end{cases} \tag{5.4}$$

where $\mathcal{M}_j$ is defined as a closed convex set containing the model and constraints of the jth unit, i.e. (3.7b)-(3.7g). On the standard matrix form we get

$$\begin{array}{ll} \text{minimize} & g(p) + f(u) \\ \text{subject to} & p = Su \end{array} \tag{5.5}$$

where $u = [u_1^T, u_2^T, \ldots, u_n^T]^T$ is a stacked vector of individual unit consumption profiles and $f(u)$ is a sum of the unit indicator functions from (5.4)

$$f(u) = \sum_{j=1}^{n} f_j(u_j)$$

The optimization problem (5.5) must be solved at every time instant by an MPC and for large-scale systems decomposition methods make it computational tractable. In Paper E and Paper F we limited the units to consumption units and defined the total consumption $p \in \mathbf{R}^N$ as a sum of the predicted consumption profiles u_j. Note that $S = \bar{D}_z$ from (2.37). p can be constrained to reflect capacity constraints in the power grid. We mainly considered power balancing objective where the residual $e = p - q$ is minimized as

$$g(e) = \frac{1}{2}||e||^2 = \frac{1}{2}||p - q||^2 \tag{5.6}$$

Applying MPC to the aggregator balancing problem requires the solution of a large-scale convex optimization problem in real-time. This motivates computational efficient optimization algorithms for the MPC that balances the power. The centralized problem can often be decomposed into smaller sub-problems that can be handled independently due to the inherent decoupled dynamics of the units. This is why decomposition methods are computationally attractive. The computation time grows polynomially in standard solvers as the number of units increase. By decomposing the problem and solving smaller subproblems in parallel, we can handle a much larger number of units. Compared to conventional centralized algorithms, decomposition methods requires less memory, and are much faster.

In the following sections we summarize the results from Paper E and Paper F that deal with first order decomposition methods based on convex optimization [BV04].

5.3.2 Douglas-Rachford Splitting

We apply the Douglas-Rachford splitting algorithm to (5.5) with the least squares objective (5.6) and get

$$u^+ = \text{prox}_{tf}(v) = \underset{u_j \in \mathcal{M}_j}{\text{argmin}} \left(\phi_j(u_j) + \frac{1}{2t}\|u_j - v_j\|_2^2 \right) \tag{5.7a}$$

$$z^+ = \text{prox}_{tg^*}(s) = \frac{1}{t+1}s - \frac{t}{t+1}q \tag{5.7b}$$

$$\begin{bmatrix} w^+ \\ m^+ \end{bmatrix} = \begin{bmatrix} I & tS^T \\ -tS & I \end{bmatrix}^{-1} \begin{bmatrix} 2u^+ - v \\ 2z^+ - s \end{bmatrix} \tag{5.7c}$$

$$v^+ = v + \rho(w^+ - u^+) \tag{5.7d}$$

$$s^+ = s + \rho(m^+ - z^+) \tag{5.7e}$$

The details and definitions can be found in Paper E. In our case the algorithm has the following interpretation:

1. The aggregator sends suggested consumption profiles v_j to the units

2. The units evaluate their subproblems, i.e. the prox-operator in (5.7a), by solving a QP with their local unit model, costs, constraints, and variables
3. The units respond in parallel with their updated consumption profiles u_j^+
4. The remaining steps (5.7b)-(5.7e) simply updates the other variables and are computed by the aggregator alone

It is important to note that the prox-operators don't have to be evaluated by the units. If the units upload their objective and constraints to the aggregator a large parallel computer could solve all the subproblems. This significantly reduces convergence speed and communication requirements in a practical system.

Note that ϕ_j contains slack variables and regularization. v_j can be interpreted as an individual linear coefficient for each unit. In our case, all of these quadratic subproblems reduce to finite horizon constrained LQR problems that can be solved efficiently by methods based on the Riccati recursion [Jør05, RWR98].

The (w, m)-update in (5.7c) gathers the unit consumption profiles and involves only multiplications with S and S^T. Due to the simple nature of S, defined in (2.38), we can simplify this update to simple sums

$$\begin{aligned} w_j &= \tilde{v}_j - \frac{1}{\tilde{n}} \left(t\tilde{s} + t^2 \sum_{j=1}^{n} \tilde{v}_j \right) \\ w^+ &= [w_1^T, w_2^T, \ldots, w_n^T]^T \\ m^+ &= \frac{1}{\tilde{n}} \left(\tilde{s} + t \sum_{j=1}^{n} \tilde{v}_j \right) \end{aligned}$$

where $\tilde{n} = 1 + nt^2$, $\tilde{v}_j = 2u_j^+ - v_j$, and $\tilde{s} = 2z^+ - s$.

The dual update of z must be evaluated through the prox-operator in (5.7b) and depends on the choice of aggregator objective $g(e)$.

The primal and dual optimality conditions provide a measure of convergence, i.e.

$$r_p = \frac{v - u^+}{t} + S^T z^+ \qquad\qquad r_d = \frac{s - z^+}{t} - Su^+. \tag{5.8}$$

The algorithm converges as the norm of these residuals decrease with a stopping criteria equal to a user-defined tolerance. [GTSJ13] provides more general convergence results. From theory, it is known that the step size t in the algorithm must remain constant. However, various heuristics provide adaptive strategies, see for instance the

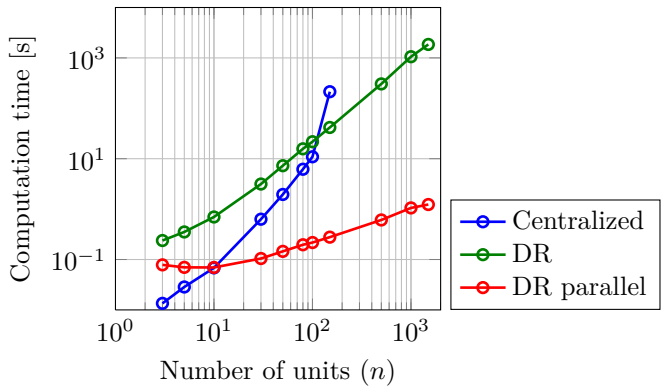

Figure 5.2: Convergence for open-loop problem with tuned step sizes t.

references in [BPC+11]. In practice t must be found experimentally. Also the scaling gain $\rho \in]0;2]$ must be selected and usually $\rho = 1.5$ is a good choice.

As the number of units increase the computation time also increases. This is shown in Fig. 5.2. We measured the computation of all the subproblems and took the average (labeled DR parallel) to illustrate the unit scaling behavior. The total computation time for the serial implementation is labeled DR. For a large number of units the Douglas-Rachford splitting algorithm is faster than just solving the original problem, even the serial implementation.

5.3.2.1 Simulation Example

We model a portfolio of different thermal storage systems as second order systems on the form

$$G_j(s) = \frac{y_j}{u_j} = \frac{K}{(\tau_j^a s + 1)(\tau_j^b s + 1)}$$

u_j is the consumption and y_j is the output temperature. One time constant is usually much bigger than the other. Realistic values for the dominating time constant in buildings with heat pumps or refrigeration systems is $\tau^a \in \{10; 120\}$ h [HPMJ12, Hov13]. In our simulations we also set $\tau^b = \tau^a/5$ and pick τ^a randomly. The same model works for disturbances d_j, e.g. ambient temperature, and is easily converted to the state space form (2.8). The constraints were selected equal for both units: $(y^{\min}, y^{\max}) = (15, 25)\ ^\circ C$, $(u^{\min}, u^{\max}) = (0, 50)\ W$, $(\Delta u^{\min}, \Delta u^{\max}) = (-50, 50)\ W$, and output slack variable penalty $\gamma = 10^4$.

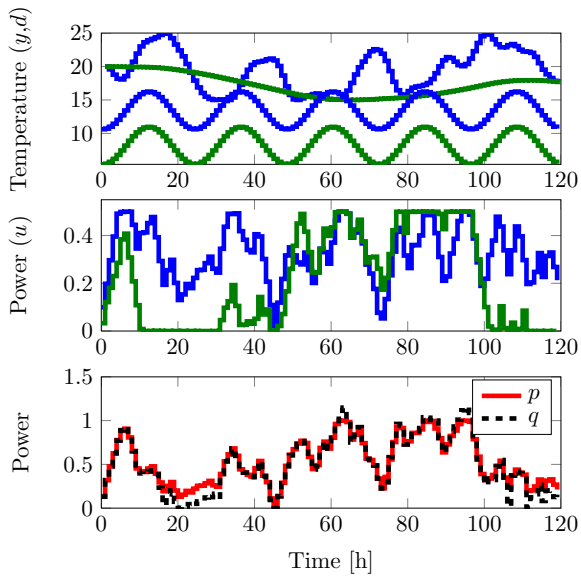

Figure 5.3: *Closed loop simulation of power balancing with $n = 2$ thermal storage units. Prediction horizon was $N = 24$ and we used a quadratic objective function. The first plot shows the output temperatures of the two units in blue and green respectively. The two sinusoids below are the disturbances. The second plot shows the input power consumption. Right below is the resulting total power p and tracking profile q. All powers are scaled, such that the total maximum power of p is equal to 1. Consequently for $n = 2$ units their maximum power is $1/n = 0.5$.*

We scale the gain K with $1/n$ such that the maximum possible power consumption automatically adds to $p_{\max} = 1$. The reference q is also scaled to always lie between 0 and 1. Better numerical performance and sensitivity to the step size t is obtained in this way.

5.3.2.2 Case Study ($n = 2$)

Fig. 5.3 shows the results for $t = 0.5$ after 25 iterations. Both the temperatures and the consumption are kept within their operating intervals. Their combined consumption p is seen to match the reference q very well. The plot illustrates two cases where it is not always possible to follow the plan q. Obviously in periods where q is larger than the maximum total power. And in periods where q is close to zero and the outputs are near the constraints, e.g. around 20 h. It is simply not possible to follow

the plan in that situation without violating the output constraints. However, around 45 h there is enough capacity to turn the units completely off for a short period of time. q could be any profile but was selected here as a scaled version of the difference between the wind power and the load from Paper E.

5.3.2.3 Case Study ($n = 100$)

To demonstrate that the algorithm works for a larger number of units, we chose $n = 100$ units with uniform randomly generated parameters as before. In Fig. 5.4 the same consumption profile q is tracked but we only plotted the first open-loop profile.

We solved the power balancing problem using a constrained model predictive controller with a least squares tracking error criterion. This is an example of a large-scale optimization problem that must be solved reliably and in real-time. We demonstrated how Douglas-Rachford splitting can be applied in solving this problem. By decomposing the original optimization problem thousands of units can be controlled in real-time by computing the problem in a distributed (parallel) manner. We considered a large-scale power balancing problem with flexible thermal storage units. A given power consumption profile can be followed by controlling the total power consumption of all flexible units through a negotiation procedure with the dual variables introduced in the method. An economic aggregator objective that takes the regulating power prices into account was derived. The solution obtained converges towards the original problem solution and requires two-way communication between units and the coordinating level. The resulting power balancing performance runs in closed loop while the local constraints and objectives for each unit are satisfied and aggregator operation costs are reduced.

5.3.3 Dual Decomposition

Another way to decompose and solve the same problem (5.5) iteratively is via the dual problem and the subgradient projection method. This method was explained and applied in Paper F. In this section we formulate the dual and show some simulation results form the paper.

The unconstrained dual problem of (5.3) is obtained from the Lagrangian L

$$L = \frac{1}{2}||e||^2 + \sum f_j(u_j) + z^T \left(e - \sum_j u_j + q \right)$$

where z is the dual variable associated with the power balance constraint.

The dual problem is

$$\text{maximize} \quad -\frac{1}{2}||z||^2 + q^T z - \sum_j S_j(z) \tag{5.9}$$

where $S_j(z)$ is the support function of $\mathcal{M}_j$

$$S_j(z) = \sup_{u_j \in \mathcal{M}_j} z^T u_j + \lambda ||\Delta u_j||_2^2$$

If $\mathcal{M}_j$ is a bounded polyhedron, we can evaluate S_j by solving the QP subproblem

$$u_j = \underset{u_j \in \mathcal{M}_j}{\operatorname{argmin}} \left(z^T u_j + \lambda ||\Delta u_j||_2^2 \right) \tag{5.10}$$

and the optimal u_j gives us a subgradient of S_j at z. Solving (5.9) with the subgradient projection method gives us the updates

$$z^+ = z + t^+ \left(\sum_j u_j^+ - (z + q) \right) . \tag{5.11}$$

The step size t^+ must be decreasing at each iteration j, i.e. $t^+ = \frac{t}{j} \to 0$, for $j \to \infty$. If t doesn't decrease the subgradient method will not converge to the minimum. The regularization term including Δu is required to make the problem converge and strictly convex. So

$$u_j^+ = \underset{u_j \in \mathcal{M}_j}{\operatorname{argmin}} \left(z^T u_j + \lambda ||\Delta u||_2^2 \right) \tag{5.12}$$

This problem formulation is equivalent to the ordinary optimal control problem with an added linear term, that can be solved efficiently by methods based on the Riccati recursion [Jør05, JFGND12]. Without the strictly convex regularization term the primal solution is not easily recoverable from the dual. Another strictly convex subproblem with a temperature set point reference is

$$u_j = \underset{u_j \in \mathcal{M}_j}{\operatorname{argmin}} \left(z^T u_j + \lambda ||y_j - r_j||_2^2 \right) \tag{5.13}$$

5.3.3.1 Simulation

We simulate an example with two different first order thermal storage systems and the objective (5.13). The models have unity gain, time constants 5 and 10, and both a temperature reference equal to $r_j = y_j^{\min}$. The results for step size $t = 0.3$ after 100

iterations is shown in Fig. 5.5. The power tracking profile is seen match most of the time, but it is not possible to control the consumption amplitude of each unit very accurate through the dual variables, since each unit has its own objective leaving the tracking at some compromise. However, shifting the load in time is quite accurate, since the sharp variations in the dual variables, that can be interpreted as prices, causes the consumption to be placed in this cheap period.

5.4 Indirect global set point control

Instead of assuming that each unit has a local model used in an Economic MPC, it is more realistic that units control their outputs with traditional set point based controllers like a Proportional-Integral (PI) controller or on/off hystereses control. With a set point controller that regulates the output, e.g. a thermostat trying to keep the indoor temperature steady, a model of the heat dynamics is difficult to obtain without any excitation of the output dynamics. So an aggregator can identify an aggregated model of the units with set points and disturbances as inputs and the actuated power consumption as output. This can be done online and the aggregator problem (5.1) can be solved based on an aggregated model of all unit's behavior. In this section, we present the method from Paper D that deals with the aggregator balancing problem through such a model. The method uses an aggregated model that describes the total power consumption response to a control signal from the aggregator. This control signal communicates the need for balancing and is also referred to as a control price. The control price is linearly linked to the unit set points and therefore indirectly influences the total power consumption of an aggregated group of units. The aggregator broadcasts the current control price, which is translated by each unit individually into a local set point to be followed by the local integral controllers. This control hierarchy is sketched in Fig. 5.7, while the local control loops are shown in Fig. 5.6.

The method assumes that each unit is controlled by a local temperature integral controller with a flexible set point within some comfort bounds. The aggregator could model all the control loops and calculate all set points. But it turns out that a SISO model of the aggregated behavior is sufficient. We used a linear tracking MPC based on a low-order SISO auto-regressive (AR) model.

$$\begin{aligned} \text{minimize} \quad & \frac{1}{2}||p-q||_2^2 + \lambda||\Delta c||_2^2 \\ \text{subject to} \quad & c \in \hat{\mathcal{M}}_c \\ & p = Su \end{aligned} \tag{5.14}$$

The model input is the control price, and the total aggregated power consumption is the output. Moreover, an integrator model is added to eliminate model and forecast

errors and to achieve offset-free tracking. Tuning of the controller matters considerably when subject to noise. The aggregator model $\hat{\mathcal{M}}_c$ captures the estimated control price response and the model may be very small compared to a centralized model that includes detailed information about all units $\mathcal{M}_j \ \forall j$. Fig. 5.8 shows the control price step response.

A Kalman filter estimates the state of the aggregated model from measurements of the controlled total power consumption. Thus the individual unit power consumptions do not need to be measured or communicated in real-time, but must of course be registered for later billing.

The aggregator MPC controls the total power consumption of all units indirectly through one-way communication, i.e. broadcasting of the real-time control price. Based on a model of the aggregated consumption response to the control price, closed-loop feedback is provided at the aggregator level by measuring the total power consumption in the grid. In this way the aggregator is able to balance instantaneous power and track an amount of power already bought from a market.

The MPC also handles the unit temperature constraints through constraints on the control price. The control price is a scalar that is broadcast to all loads, reflecting the need for balancing. Each unit must map the control price to an individual temperature set point. This mapping is done by the affine function $f_j(p)$ defined for each unit

$$f_j(p) = -a_j p + b_j \tag{5.15}$$

When the price is constrained to ± 1 the function $f_j(p)$ also constrains the individual unit set point to a certain interval defined by a_j and b_j. Fig. 5.9 illustrates this mapping and is key to understanding the role of the control price. Individual units can set their own desired upper and lower bounds by choosing a_j and b_j independently from the aggregator.

The MPC incorporates forecasts of disturbances and power production, e.g. time-varying wind power forecasts, in order to react ahead of time. Added integral control eliminates model and forecast errors, while feedback is provided by measuring total load power consumption. Through simulation of general thermal storage units the method showed the load-following-ability where consumption follows a changing production.

5.4.1 Simulation example

Ten different thermal storage units with a first-order transfer function $G(s)$ from power consumption u to temperature y are modeled as

$$G(s) = \frac{K}{\tau s + 1} \tag{5.16}$$

τ is the time constant and K is the gain. Some process noise was added to simulate unmodeled disturbances. A simulation of the MPC price control with the estimated models is shown in Fig. 5.10. The upper plot of Fig. 5.10(a) shows the aggregated response and how the aggregator MPC tracks the power reference nicely with no offset errors despite of the aggregated model mismatch, forecast errors, and noisy disturbances. The consumption reference r_a is known to the MPC, and control prices which indirectly change power consumption are broadcast ahead of time in order to minimize the tracking error. Notice how the requested consumption plan forces the control price to its limits over the whole flexibility range. Also the control price is not constant when the total reference power consumption is constant, i.e. tracking a constant power requires a ramping of the price due to the dynamics of the loads. Fig. 5.10(b) shows the temperatures of the units. Some units are more flexible than others and allow a wider temperature interval, i.e. a large a_j, indicated by the various dashed lines at different levels. Consequently, a more flexible load will have a more varying temperature. However, the temperature is still ensured to lie within the predefined interval, $b \pm a$, due to the constrained control price. As intended, each unit's power consumption mainly occurs when the price is low. This is evident when comparing to the control price in Fig. 5.10(a).

5.5 Indirect Dual Decomposition

In this section we solve the aggregator balancing problem (5.5) with a decomposition method based on price signals. Controlling power systems using prices first proposed in [SCTB88] and is often referred to as *indirect control*. A price concept is easy to understand for consumers as they are charged a price that is often equal to the actual cost of energy at the time of consumption. Another important advantage is the simple control signal, i.e. a global price signal broadcast unidirectionally to the units. Using one-way incentive signals from the aggregator to the units simplifies communication, and closed loop feedback can be established by the measurements of the total consumption through the grid. One price signal also creates an appealing opportunity to manage a diverse portfolio of units in the same simple manner. Therefore, it is also difficult to control the power accurately and good models of the system dynamics is crucial. Luckily the reliability of the models and behavior predictions increase with a large portfolio [COMP12].

We again apply dual decomposition for all decoupled units in a distributed manner. But this time the aggregator uses a low order model of the unit dynamics like in the set point method in Section 5.4 and we broadcast the resulting dual variable as a price signal to all units. We reformulate the centralized problem (5.5) to include a balance constraint (5.17b)

$$\begin{aligned} \text{minimize} \quad & g(e) + \sum_{j=1}^{n} \phi_j(u_j, s_j) && \text{(5.17a)} \\ \text{subject to} \quad & e = Su - q && \text{(5.17b)} \\ & \{u_j, s_j\} \in \mathcal{M}_j, \quad j = 1, 2, ..., n && \text{(5.17c)} \end{aligned}$$

The objective contains local control objectives and costs associated with operating the unit. In our case we add a strictly convex regularization term and a slack variable penalty

$$\phi_j(u_j, s_j) = \lambda_j ||\Delta u_j||_2^2 + \rho_j^T s_j \tag{5.18}$$

The soft constrained slack variable s_j must be heavily penalized to prevent output constraint violations, e.g. by setting $\rho_j \gg 1$. Finally, we choose the aggregator objective (5.6) that minimizes the power imbalance e. Only the total power consumption response p is measured for feedback control. The aggregator control signal is a price of consuming power such that each unit minimizes its own cost of operation. With this assumption the subproblems are exactly the same as in the normal dual decomposition method from Section 5.3.3. We let each unit cooperate by minimizing their cost of consumption by using an Economic MPC on the form

$$\begin{aligned} \text{minimize} \quad & c^T u_j + \phi_j(u_j, s_j) \\ \text{subject to} \quad & \{u_j, s_j\} \in \mathcal{M}_j \end{aligned} \tag{5.19}$$

The objective has to be strictly convex for the dual decomposition method to converge. When each unit locally adopts this Economic MPC control strategy their total power consumption can be controlled in a predictable manner. The aggregator is decoupled from the units in the original problem (5.17) but coordinates control action through a global price signal c. From dual decomposition we know that this signal is the dual variable $z \in \mathbf{R}^N$ associated with the equality constraint (5.17b). That constraint is the actual power balance. The aggregator still needs to solve (5.17) with all model and state information and then broadcast the dual variable. But if we apply a Kalman filter, integral control, and use an aggregated model of the power consumption analogue to the method presented in Section 5.4 we only need measurements of the total power consumption. Each unit determines its own control action based on the globally broadcast dual variable and its local model. The aggregated model must contain the dynamics of the units to be controlled, not their price response. When the aggregator have solved the problem with a low-order model the optimal dual variable is broadcast by setting $c = z$ in the subproblems (5.19). Each unit

then solves an Economic MPC with this dual variable as the price. The dual variable can be interpreted as a price, and can be negative with the interpretation that units receive money to consume power.

The aggregated model of the unit dynamics and their constraints is denoted $\mathcal{M}$, while the estimated low-order model is denoted, $\hat{\mathcal{M}}$. This low-order model represents the flexibility of the aggregated units. Low-order models have fewer parameters and also reduce MPC computation time significantly compared to solving the centralized problem with all local unit models. Model mismatch is always present in real control problems and is justified by the use of feedback to eliminate offsets.

The estimated aggregator problem is

$$\begin{aligned} \text{minimize} \quad & \frac{1}{2}||e||_2^2 + \hat{\lambda}||\Delta\hat{u}||_2^2 + \rho^T\hat{s} \\ \text{subject to} \quad & e = \hat{u} - q \\ & \{\hat{u}, \hat{s}\} \in \hat{\mathcal{M}} \end{aligned} \tag{5.20}$$

Let $\hat{\mathcal{M}}$ be an average model of the units. The average model consumption $\hat{u}$ is scaled through its state space model to match the maximum total aggregated consumption.

We calculate the dual variable z by solving the dual problem subject to the estimated model $\hat{\mathcal{M}}$. We set

$$c = z \tag{5.21}$$

and broadcast the price c to all units that individually solve the following Economic MPC with their local models.

5.5.1 Simulation

A first order model of the units has the transfer function

$$\mathcal{M}_j: \quad T_j(s) = \frac{1}{\tau_j s + 1} \tag{5.22}$$

where τ_j is the time constant, e.g. normal distributed as $\tau_j \in N(10, 2)$. A simple estimated population model $\hat{\mathcal{M}}$ would then be the average, i.e. $\hat{\tau} = 10$. Furthermore, scaled constraints should be estimated as well. However, for consumption units the lower bound on power consumption is always zero. Fig. 5.13 shows a similar case study with EVs.

The aggregator model of the dynamics does not have to be very accurate as we control the unit inputs, i.e. the power consumption that can change instantaneously, and not

the outputs. The output constraints that represents the amount of flexibility is more important than the actual dynamics from input to output. Especially on short time scales where the outputs do not change much. As in previous described methods that use aggregated models a state estimator should be applied.

5.6 Warm starting

MPC requires solution of optimization problems in real-time. Consequently, until recently MPC has been limited to slow systems with ample time for solution of the optimization problem. For large-scale MPC we can increase the number of units by lowering the real-time computation time. In MPC, an optimization problem - most often either a Linear Program (LP) or Quadratic Program (QP) - must be solved in each sampling instant. Since each problem usually does not differ much from the next, the entire solution process involves solving a sequence of closely related optimization problems. In case online solution of the optimization problem is needed, an obvious idea to reduce computation time is to utilize the information contained in the previous solution of the problem when solving the next problem in the sequence. [SFS+14] implements this idea by using *warmstarting* of the homogeneous and self-dual interior-point method (IPM) for linear optimization.

Recently, a new warmstarting strategy for the homogeneous and self-dual IPM for mixed linear and conic quadratic optimization was introduced [SAY12]. For further information about previous work on warmstarting IPMs, see the thorough overview in [EAV10]. The following results are based on the method described in [SFS+14] but are independent from this work and based on the simulation from Section 4.6.

In this section we show an example of how the warmstarting strategy of [SAY12] can be applied to the sequences of problems that arise from Economic MPC. Also the decomposition methods from Section 5.3 benefit from warmstarting since they require fast evaluation of repeated closely related QPs. The bottom plot of Fig. 4.7 shows the number of iterations used by the warmstart algorithm when coldstarting (C) and warmstarting (W). The results are also shown in Table 5.1. We notice a relatively large variety in the improvement of using warmstarting over the individual problems. For some problems the iteration count is halved while it for other problems cuts away about 25%. Overall, the total work reduction is about 37%. We remark further, that the gain from warmstarting for these problems is quite sensitive to the parameters involved. If, for example, the sampling time is reduced, the neighboring problems are more alike, and warmstarting is even more useful. Another example is the initial state of charge of the EVs which, if relatively high, results in few charging periods and thus less varying predictions. This also improves warmstarting performance. Generally, warmstarting is most useful when the simulation is “uneventful” in the

P	$\mathcal{I}^{\text{cold}}$	$\mathcal{I}^{\text{warm}}$	$\mathcal{R}$
1	11	11	1.00
2	13	11	0.85
3	11	10	0.91
.	.	.	.
13	12	10	0.83
14	12	11	0.92
15	11	12	1.09
16	13	14	1.08
17	13	12	0.92
.	.	.	.
69	13	7	0.54
70	12	7	0.58
71	12	8	0.67
72	12	8	0.67
$\mathcal{G}$	12.2	9.3	**0.76**

Table 5.1: LPs from the case study in Section 4.6. Columns two and three show iteration counts and the fourth column their ratio. The last row shows geometric means.

sense that few changes occur. These considerations suggest an adaptive strategy: When model predictions are relatively uneventful, use warmstarting. In the opposite case, use coldstart.

5.7 Comparison

In this chapter, we formulated a large-scale control problem that coordinates the active power consumption of different flexible units. Table 5.2 compares the different control strategies presented in this thesis. Their common goal is to minimize the imbalance e. The first column of the table indicates in which paper the method was applied. The * indicates that the aggregator does not know the local unit models, i.e. the units calculate their own response in a completely distributed manner. Two of these distributed methods require fast two-way communication since the problem is solved iteratively through real-time negotiations between aggregator and units. The methods with no * indicates that the aggregator holds all models. These methods force the units to apply the provided consumption plan and communicate any state measurements back to the aggregator. This requires fast and reliable two-way communication, all model information for each unit, and fast solving times. The Indirect dual method, listed in the last row, indirectly controls the units through the price c. The centralized controller, listed in the first row, directly controls all units and calculate individual consumption profiles u_j for all units. These methods require the unit to solve either a an LP or a QP subproblem.

The different methods introduce different update steps for the aggregator as indicated in the *Aggregator*-column of Table 5.2. In the centralized method the aggregator solves the entire large-scale problem for all units. The decomposition method based on Douglas-Rachford (DR) splitting evaluates the prox-operators associated with the aggregator objective. The aggregator update in the dual decomposition method is a simple subgradient step. The last two methods solve small-scale QP problems as they both use a low-order aggregated model as indicated in the last column $\hat{\mathcal{M}}$. They are also the only two methods that work with one-way communication to the units, i.e. the aggregator controller broadcasts a price signal and retrieve aggregated measurements for closed loop feedback. The required feedback signal is indicated in the *Feedback*-column.

Three of the methods are based on prices. The dual decomposition methods obviously use the dual variable (shadow price) as the price. In the set point method the price is merely a global set point. If consumers are charged a price that is often equal to the actual cost of consumption, then the benefits of making flexibility available to the system is more transparent. So a control-by-price concept is easy to comprehend for consumers, but these price strategies work best when fully automated without human intervention. Methods based on price significantly reduces communication requirements and the computational burden for the aggregator. Note that warmstarting as described in Section 5.6 can be applied to all the methods, but in particular to the centralized controller where warmstarting will have the biggest impact on solving times.

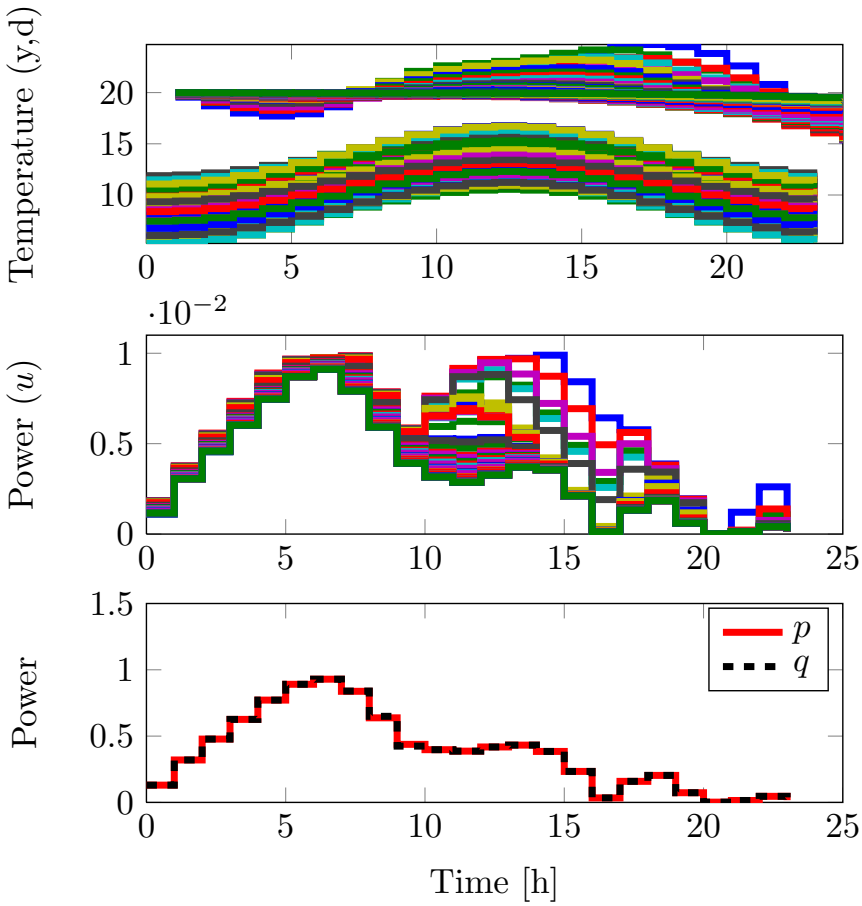

Figure 5.4: *Open loop simulation of power balancing with $n = 100$ thermal storage units.*

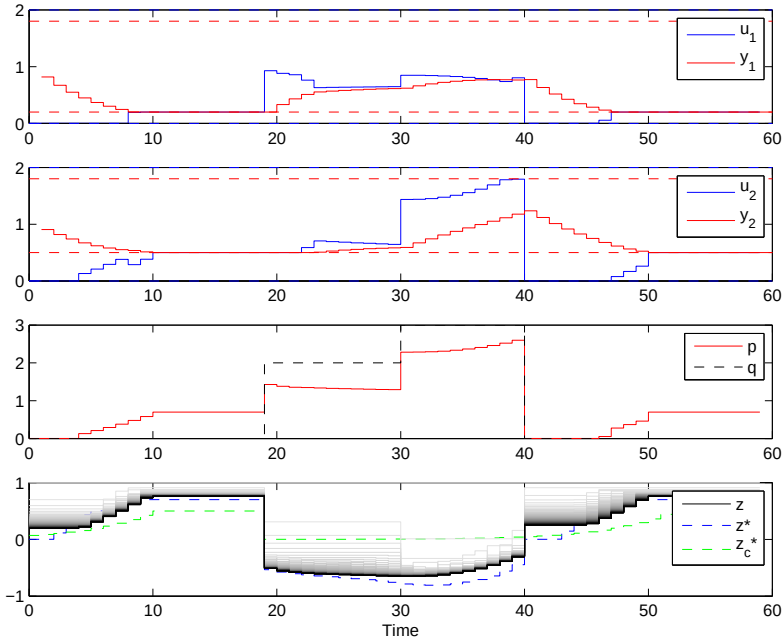

Figure 5.5: *Simulation of power balancing with two first order systems. The two input/output pairs (blue/red) with constraints (dotted) are shown above the resulting power tracking profile. The lower plot shows the converged dual variable (black), its iterations (gray), and the optimal dual variable of the original problem (dotted blue).*

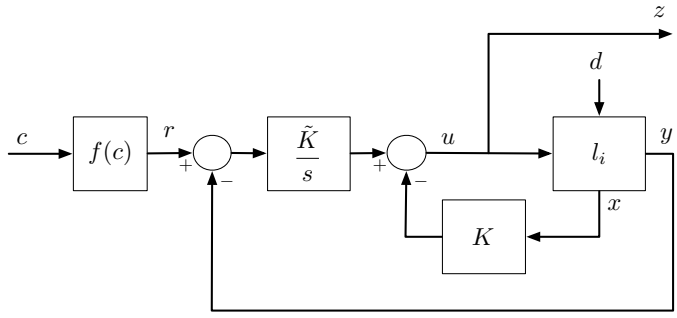

Figure 5.6: *Unit i with system $l_i : (A_i, B_i, C_i, E_i)$ and LQ integral controller.*

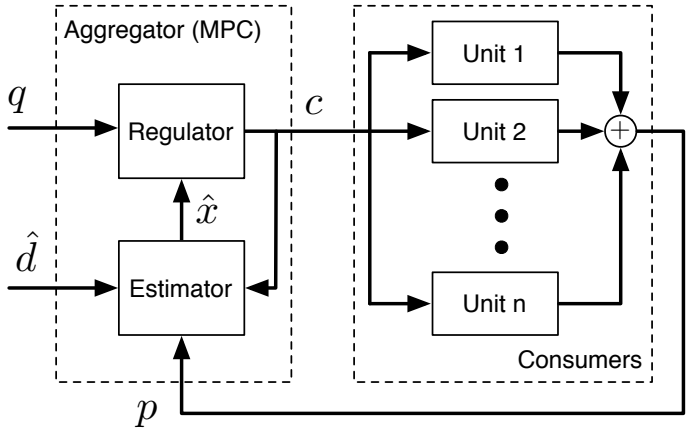

Figure 5.7: *System overview of aggregator and loads.*

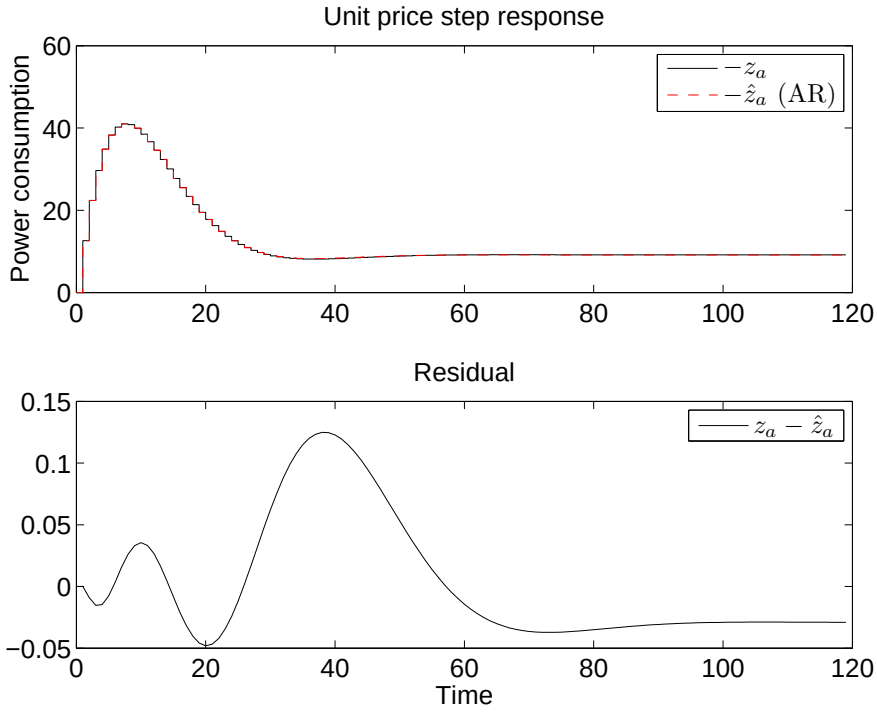

Figure 5.8: *Power consumption response and estimated response to unit price step (upper) and their residual (lower).*

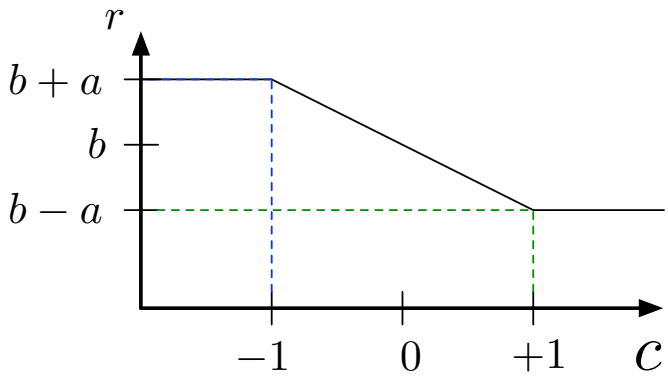

Figure 5.9: *Function $f(p)$ from control price to temperature set point*

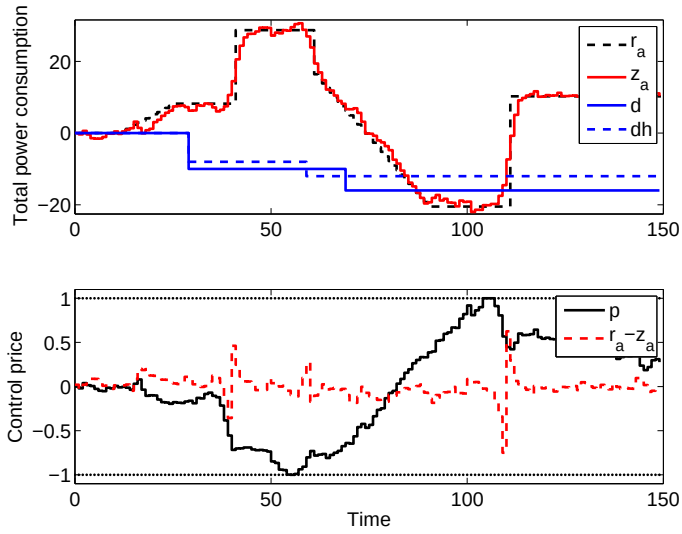

(a) Simulation of the aggregator tracking a power consumption r_a by controlling an aggregation of thermal loads. Total power consumption z_a is plotted around zero as the deviation from the stationary consumption z_a^0. The normalized residual is plotted below along with the control price p. As intended, load consumption is highest when the price is low. The disturbance is forecast dh and eliminated by the MPC. The disturbance shown here is scaled and does not match the units of the y-axis.

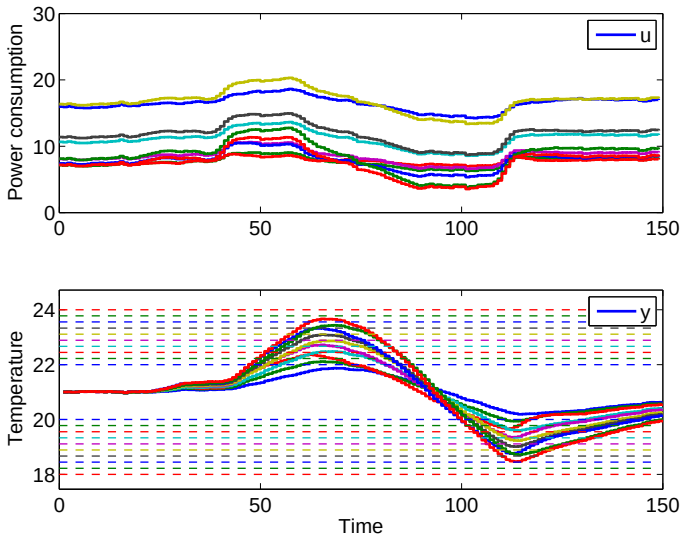

(b) Unit output temperatures y_i (lower) and their temperature intervals $b_i \pm a_i$ (dashed lines). Also their power consumptions u_i are plotted (upper).

Figure 5.10: Closed loop simulation of aggregator balancing with thermal storage units

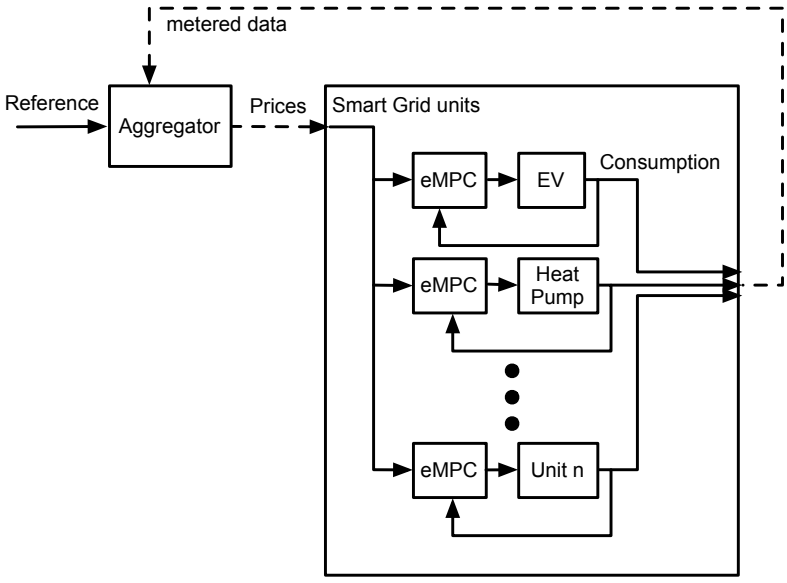

Figure 5.11: *Indirect Dual Decomposition method block diagram*

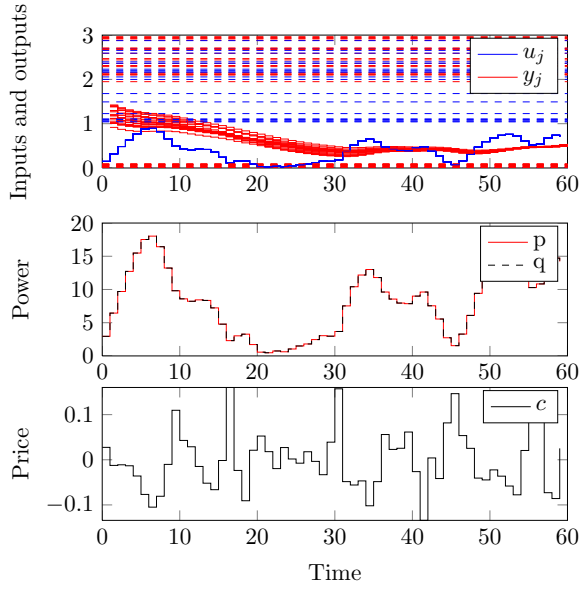

Figure 5.12: *Simulation and price response of 10 thermal storage units.*

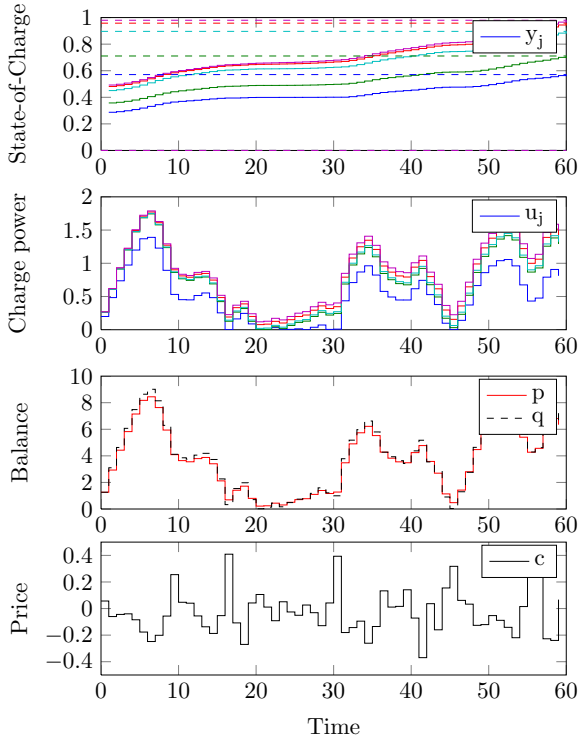

Figure 5.13: *Simulation and price response of five EVs.*

Table 5.2: Comparison of aggregator control strategies.

	Method	Aggregator	Unit	Comm.	Feedback	Price	$\hat{\mathcal{M}}$
	Centralized	$\min_{u_j \in \mathcal{M}_j} g(e)\ \forall j$	actuate u_j	two-way	y_j	N	N
F	DR	prox_{tg^*}, (5.7b)-(5.7e)	actuate u_j	two-way	y_j	N	N
F	DR*	prox_{tg^*}, (5.7b)-(5.7e)	$u_j^+ = \text{prox}_{tf}(v_j^+)$	two-way	u_j^+	N	N
G	Dual	$c^+ = c + t\nabla g(e)$	actuate u_j	two-way	u_j^+	N	N
G	Dual*	$c^+ = c + t\nabla g(e)$	$\underset{u_j^+ \in \mathcal{M}_j}{\text{argmin}}\, c^{T+} u_j^+$	two-way	u_j^+	Y	N
E	Set point*	$\min_{c \in \hat{\mathcal{M}}_c} g(e)$	$\underset{u_j \in \mathcal{M}_j}{\text{argmin}}\, \|\|f_j(c) - y_j\|\|$	one-way	$\sum_{j=1}^n u_j$	"Y"	Y
	Indirect dual*	$\min_{\hat{u} \in \hat{\mathcal{M}}} g(e)$	$\underset{u_j \in \mathcal{M}_j}{\text{argmin}}\, c^T u_j$	one-way	$\sum_{j=1}^n u_j$	Y	Y

Chapter 6

Conclusions and Perspectives

The green transition to an intelligent energy system – a *Smart Grid* – is currently fueled by ambitious energy policies, especially in Denmark. Distributed energy resources such as heat pumps in buildings or electrical vehicle batteries are expected to participate flexibly in the future Smart Grid. In this thesis, we briefly introduced the power system actors and markets to identify how Model Predictive Control (MPC) can enable the flexibility of these units. One objective of MPC is to coordinate a large portfolio of units in the role of an *Aggregator*. If the power consumption and production can be controlled, a large portfolio of units might help balance the power without sacrificing much of their own objectives. We investigated different aggregator control strategies ranging from centralized to decentralized strategies based on prices. All strategies were based on MPC including related control tasks such as state estimation, filtering and prediction of the variables.

6.1 Models of Smart Grid units

In this thesis, we provide realistic linear dynamical models of the flexible units described in Chapter 2: heat pumps in buildings, heat storage tanks, electrical vehicle battery charging/discharging, refrigeration systems, wind turbine parks, and power plants. Different formulations of linear dynamical models can all be realized as discrete time state space models that fit into a predictive control framework. We showed

how to enable control of the flexible units with an Economic Model Predictive Control (MPC) in Chapter 4. This chapter sums up the main contributions of Papers A, B, and C. The simulation results showed the expected load shifting capabilities of the units that adapts to realistic electricity market prices fed to the Economic MPC. The performance showed large potential economic savings around 20-50% compared to control strategies that do not consider prices. We integrated state-of-the-art forecasts of disturbances, e.g. temperatures and solar radiation, in the controller to evaluate the performance and the prediction horizons needed. Even simple linear predictors showed only very little performance decrease in terms of savings. Furthermore, simulations conclude that the units consume *more* energy when taking prices into account. However, if the prices reflect the amount of wind power, the units might use more energy, but they use it at the right time. In this way consumers save money from flexibility while helping the grid.

6.2 Model Predictive Control

We expect the units and controllers to enter in to real-time large-scale control systems where speed is of the essence. The choice of certainty equivalent MPC keeps the computational burden and memory requirements very low. A time varying sampling period can be applied to reduce computations in systems with different time scales. Also warm starting of the optimization algorithms involved lowers the computation time of the repetitive optimization problems that arise in MPC. Chapter 3 introduced the principles of MPC, including stability, state estimation, filtering and prediction that are important in practical predictive control systems subject to noise. We briefly introduced three different objective functions related to MPC: The traditional linear quadratic regulator, a linear economic objective, and a combined trade-off between the two, namely a mean-variance objective. Finally, we showed how to solve the underlying optimization problems that arise in certainty equivalent economic MPC.

6.3 Large-scale control algorithms

Enabling flexible consumers on a large scale require efficient control and coordination strategies. These strategies are expected to be handled in the future by new market players referred to as aggregators. In Chapter 1 we introduced aggregators and sketched the current power system architecture, its main actors, their objectives, and the markets they act on. Here we also reviewed current aggregator strategies and their role in the future power system. Our different control strategies were compared in Chapter 5 that also summarize the main contributions of Papers D, E, and F. The

control strategies are based on MPC, state-estimation, classical control principles, and decomposition methods such as dual decomposition and operator splitting. The decomposition methods can handle more units than naive implementations by breaking down the large-scale control problem into smaller subproblems that can be solved independently and in parallel. The suggested Douglas-Rachford splitting method is very general and apply to a broad range of aggregator objectives. One common objective for the control strategies is to track a given power reference. This is crucial to the demand response capabilities and will enable flexible units as reserves and on the regulating power markets.

6.4 Price-based control

Two of the aggregator control strategies are based on prices and a simple aggregated model of the portfolio of units. A price is a control signal. A predictable price-response control policy for each unit is therefore crucial for the aggregator to accurately control the aggregated consumption. It is therefore important that the units let a controller respond autonomously to the prices. Our first approach, the indirect set point method, manipulated the power consumption indirectly through the temperature set points of a portfolio of thermal storage units. Our second approach, the indirect dual method, modeled the aggregated dynamics of the units and broadcast the dual variables as prices. Intuitively consumers want to minimize costs and the Economic MPC at each unit does exactly this. To make both methods work, state estimation and off-set free control are an essential part of the MPC.

6.5 Contributions

The scientific contributions in this thesis are:

- Linear dynamic models of heat pumps in buildings, heat storage tanks, electric vehicles, refrigeration systems, power plants, and wind farms.
- Two models of a heat pump heating a low-energy building and a modern residential house.
- Economic MPC that demonstrates load shifting capabilities of these flexible units.
- Economic MPC as a control strategy to balance consumption and production and minimize costs.

- Distributed large-scale aggregation methods based on MPC, convex optimization, and decomposition methods.
- Several novel strategies for controlling the power consumption of a large portfolio of flexible consumers using a tracking MPC and prices.
- Demonstration of warm starting an Interior Point algorithm to reduce computation time in the large-scale control strategies.
- A Matlab toolbox including the presented models for simulating a Smart Energy System with Economic MPC.

6.6 Future work

As of today, economic incentives and feasible business models slow down the employment of Smart Grid technologies. The sales of Electric Vehicles and heat pumps in Denmark are not increasing as rapidly as hoped. Industrial consumers, e.g. district heating and the process industries, have large load shifting capabilities and should be engaged more. We showed that Economic MPC is indeed an appealing method to enable this functionality. MPC was applied to process industries before gaining the tremendous traction in academia as it has today. Models, tuning, and verification of robustness and performance are challenges that now limit the implementation of MPC. Stochastic MPC and fast numerical algorithms will also be a big part of future research in this field.

Given the complexity of the energy system, i.e. its hierarchy, timescale and markets, one centralized real-time controller is not likely to control the entire system dynamics in the near future. Decentralized approaches based on modern control and optimization methods must be integrated to take full advantage of the anticipated smaller distributed energy resources. Critical infrastructure, such as the power system must work reliably around the clock. Unfortunately, the gap between research and practice in Smart Grid technology is huge. Both Smart Grids and distributed MPC are still young research fields and we still haven't seen a lot of advanced Smart Grid projects demonstrating some of the more advanced control mechanisms.

Bibliography

[AA99] Erling D Andersen and K D Andersen. *The MOSEK interior point optimization for linear programming: an implementation of the homogeneous algorithm*, pages 197–232. Kluwer Academic Publishers, 1999.

[AAR12] David Angeli, Rishi Amrit, and James B. Rawlings. On Average Performance and Stability of Economic Model Predictive Control. *IEEE Transactions on Automatic Control*, 57(7):1615–1626, 2012.

[AB09] Alessandro Alessio and Alberto Bemporad. A Survey on Explicit Model Predictive Control. In Lalo Magni, Davide Raimondo, and Frank Allgöwer, editors, *Nonlinear Model Predictive Control*, volume 384 of *Lecture Notes in Control and Information Sciences*, pages 345–369. Springer Berlin / Heidelberg, 2009.

[ADD+11] Alessandro Agnetis, Gabriella Dellino, Gianluca De Pascale, Giacomo Innocenti, Marco Pranzo, and Antonio Vicino. Optimization models for consumer flexibility aggregation in smart grids: The ADDRESS approach. In *2011 IEEE 1st International Workshop on Smart Grid Modeling and Simulation (SGMS)*, pages 96–101. IEEE, October 2011.

[AES08] M. H. Albadi and E. F El-Saadany. The role of distributed generation in restructured power systems. In *2008 40th North American Power Symposium*, September 2008.

[AHJS97] C. Audet, P. Hansen, B. Jaumard, and G. Savard. Links Between Linear Bilevel and Mixed 0-1 Programming Problems. *Journal of Optimization Theory and Applications*, 93(2):273–300, 1997.

[AHV13] Martin S. Andersen, Anders Hansson, and Lieven Vandenberghe. Reduced-Complexity Semidefinite Relaxations of Optimal Power Flow Problems. August 2013.

[AJRM13] Philip Delff Andersen, María José Jiménez, Carsten Rode, and Henrik Madsen. Characterization of heat dynamics of an arctic low-energy house with floor heating. 2013.

[ANAS10] Michèle Arnold, Rudy R. Negenborn, Göran Andersson, and Bart De Schutter. Distributed Predictive Control for Energy Hub Coordination in Coupled Electricity and Gas Networks. In Rudy R. Negenborn, Zofia Lukszo, and Hans Hellendoorn, editors, *Intelligent Infrastructures*, chapter 1, pages 235–273. Springer Netherlands, Dordrecht, 2010.

[Ang04] B.W Ang. Decomposition analysis for policymaking in energy:, 2004.

[Ara78] Samir A. Arafeh. Hierarchical Control of Power. *IEEE Transactions on Automatic Control*, AC-23(2):333–343, 1978.

[ARB13] Rishi Amrit, James B. Rawlings, and Lorenz T. Biegler. Optimizing process economics online using model predictive control. *Computers & Chemical Engineering*, 58:334–343, November 2013.

[Åst70] Karl Johan Åstrøm. *Introduction to stochastic control theory*. Academic Press, 1970.

[BB06] Roscoe A. Bartlett and Lorenz T. Biegler. QPSchur: A dual, active-set, Schur-complement method for large-scale and structured convex quadratic programming. *Optimization and Engineering*, 7(1):5–32, March 2006.

[BB10] Alberto Bemporad and Davide Barcelli. Decentralized Model Predictive Control. In *Lecture Notes in Control and Information Sciences*, chapter 5, pages 149–178. Springer-Verlag Berlin Heidelberg, 2010.

[Ber00] Dimitri P. Bertsekas. *Dynamic Progarmming and Optimal Control*. Athena Scientific, 3rd edition, 2000.

[BGW13] Andrea Boccia, Lars Grüne, and Karl Worthmann. Stability and Feasibility of State Constrained MPC without Stabilizing Terminal Constraints. *Submitted to Elsevier*, 2013.

[Bix12] Robert E. Bixby. A Brief History of Linear and Mixed-Integer Programming Computation. *Documenta Mathematica*, I:107–121, 2012.

[BKP11] E. Bitar, P. P. Khargonekar, and Kameshwar Poolla. Systems and Control Opportunities in the Integration of Renewable Energy into the Smart Grid. In Bittanti Sergio, editor, *18th IFAC World Congress*, volume 18, pages 4927–4932, August 2011.

[BM99] Alberto Bemporad and Manfred Morari. Robust model predictive control: A survey. *Robustness in identification and control*, 245:207—-226, 1999.

[BMDP02] Alberto Bemporad, Manfred Morari, V. Dua, and E. N. Pistikopoulos. The explicit linear quadratic regulator for constrained systems. *Automatica*, 38(1):3–20, 2002.

[BMP11] Peder Bacher, Henrik Madsen, and Bengt Perers. Short-term solar collector power forecasting. In *In proceedings of ISES Solar World Conference*, 2011.

[BPC+11] Stephen Boyd, Neal Parikh, Eric Chu, B. Peleato, and Jonathan Eckstein. Distributed Optimization and Statistical Learning via the Alternating Direction Method of Multipliers. *Foundations and Trends in Machine Learning*, 3(1):1–122, 2011.

[BS08] Martin Braun and Philipp Strauss. A review on aggregation approaches of controllable distributed energy units in electrical power systems. *International Journal of Distributed Energy Resources*, 4:297–319, 2008.

[BT09] Amir Beck and Marc Teboulle. A Fast and Iterative Shrinkage-Thresholding and Algorithm and for Linear and Inverse Problems. *SIAM J. IMAGING SCIENCES Society for Industrial and Applied Mathematics*, 2(1):183–202, 2009.

[BV04] Stephen Boyd and Lieven Vandenberghe. *Convex Optimization*. Cambridge University Press, 2004.

[Cal11] Duncan S. Callaway. Can smaller loads be profitably engaged in power system services? In *2011 IEEE Power and Energy Society General Meeting*, pages 1–3. IEEE, July 2011.

[Cap14] Andrea Capolei. *Nonlinear Model Predictive Control for Oil Reservoirs Management*. PhD thesis, Technical University of Denmark, 2014.

[CB07] E. F. Camacho and Carlos Bordons. *Model Predictive Control*. Springer, London, 2nd edition, 2007.

[CC09] S. P. Chowdhury and P. Crossley. Distributed Energy Resources. In *Microgrids and Active Distribution Networks*, pages 15–34. IET, The Institution of Engineering and Technology, Michael Faraday House, Six Hills Way, Stevenage SG1 2AY, UK, January 2009.

[CCMGB06] Antonio J. Conejo, Enrique Castillo, Roberto Minguez, and Raquel Garcia-Bertrand. *Decomposition Techniques in Mathematical Programming*. Springer, 2006.

[CI12] Aranya Chakrabortty and Marija D. Illic. *Power Electronics and Power Systems*. Springer, 2012.

[CMT87] D. W. Clarke, C. Mohtadi, and P. S. Tuffs. Generalized predictive control. I. The basic algorithm. *Automatica*, 23(2):137–148, 1987.

[COMP12] Olivier Corradi, Henning Ochsenfeld, Henrik Madsen, and Pierre Pinson. Controlling Electricity Consumption by Forecasting its Response to Varying Prices. *IEEE Transactions on Power Systems*, PP:1, 2012.

[CSZ+12] Christian Conte, Tyler H Summers, Melanie Nicole Zeilinger, Manfred Morari, and Colin Neil Jones. Computational aspects of distributed optimization in model predictive control. In *2012 IEEE 51st IEEE Conference on Decision and Control (CDC)*, pages 6819–6824, December 2012.

[CVX12] CVX Research Inc. CVX: Matlab Software for Disciplined Convex Programming, version 2.0. http://cvxr.com/cvx, August 2012.

[Dan10] Danish Commission on Climate Change Policy. Green energy - the road to a Danish energy system without fossil fuels. Technical report, 2010.

[DAR11] Moritz Diehl, Rishi Amrit, and James B. Rawlings. A Lyapunov Function for Economic Optimizing Model Predictive Control. *IEEE Transactions on Automatic Control*, 56(3):703–707, 2011.

[DSE+12] Chris Diduch, Mostafa Shaad, Rachid Errouissi, M E Kaye, Julian Meng, and Liuchen Chang. Aggregated Domestic Electric Water Heater Control - Building on Smart Grid Infrastructure. In *IEEE 7th International Power Electronics and Motion Control Conference (ECCE Asia)*, pages 128–135, 2012.

[DT78] E. Davison and N. Tripathi. The optimal decentralized control of a large power system: Load and frequency control. *IEEE Transactions on Automatic Control*, 23(2):312–325, April 1978.

[DW61] George B Dantzig and Philip Wolfe. The Decomposition Algorithm for Linear Programs. *Econometrica*, 29(4):767–778, October 1961.

[DZZ+12] Alex Domahidi, A. Zgraggen, Melanie Nicole Zeilinger, Manfred Morari, and Colin Neil Jones. Efficient interior point Methods for Multistage Problems Arising in Receding Horizon Control. In *IEEE Conference on Decision and Control (CDC)*, pages 668–674, Maui, HI, USA, December 2012.

[EAV10] Alexander Engau, Miguel F Anjos, and Anthony Vannelli. On Interior-Point Warmstarts for Linear and Combinatorial Optimization. *SIAM Journal on Optimization*, 20(4):1828–1861, January 2010.

[EB92] Jonathan Eckstein and Dimitri P. Bertsekas. On the Douglas-Rachford splitting method and the proximal point algorithm for maximal monotone operators. *Mathematical Programming*, 55(1-3):293–318, April 1992.

[ED10] Energinet.dk and Dansk Energi. Smart Grid i Danmark. Technical report, 2010.

[EMB09] Kristian Edlund, Tommy Mølbak, and Jan Dimon Bendtsen. Simple models for model-based portfolio load balancing controller synthesis. In *IFAC Symphosium on Power Plants and Power System Control*, 2009.

[ESJ09] Kristian Edlund, Leo Emil Sokoler, and John Bagterp Jørgensen. A Primal-Dual Interior-Point Linear Programming Algorithm for MPC. In *Joint 48th IEEE Conference on Decision and Control and 28th Chinese Control Conference*, pages 351–356, 2009.

[FBD08] H J Ferreau, Hans G. Bock, and Moritz Diehl. An online active set strategy to overcome the limitations of explicit MPC. *International Journal of Robust and Nonlinear Control*, 18(8):816–830, 2008.

[FJ13] Gianluca Frison and John Bagterp Jørgensen. Efficient Implementation of the Riccati Recursion for Solving Linear-Quadratic Control Problems. In *2013 IEEE Multi-conference on Systems and Control (MSC)*, pages pp. 1117–1122, 2013.

[FM10] Heinz Frank and Sidonia Mesentean. Efficient Communication Interfaces for Distributed Energy Resources. *International Journal of Grid and High Performance Computing*, 2(2):23–36, January 2010.

[GA07] Martin Geidl and Göran Andersson. Optimal Power Flow of Multiple Energy Carriers, 2007.

[Gis12] Pontus Giselsson. *Gradient-Based Distributed Model Predictive Control*. PhD thesis, Lund University, 2012.

[GKS13] Lazaros Gkatzikis, Iordanis Koutsopoulos, and Theodoros Salonidis. The Role of Aggregators in Smart Grid Demand Response Markets. *IEEE Journal on Selected Areas in Communications*, 31(7):1247–1257, 2013.

[GOJ10] Ravi Gondhalekar, Frauke Oldewurtel, and Colin Neil Jones. Least-restrictive robust MPC of periodic affine systems with application to building climate control. In *49th IEEE Conference on Decision and Control (CDC)*, pages 5257–5263. IEEE, 2010.

[GPM89] Carlos E. Garcia, David M. Prett, and Manfred Morari. Model Predictive Control: Theory and Practice – a Survey. *Automatica*, 25(3):335–348, 1989.

[GPSW12] Lars Grüne, Jürgen Pannek, Martin Seehafer, and Karl Worthmann. Analysis of Unconstrained Nonlinear MPC Schemes with Time Varying Control Horizon. 2012.

[Grü12a] Lars Grüne. Economic receding horizon control without terminal constraints. *Submitted to Automatica*, 49(3):725–734, March 2012.

[Grü12b] Lars Grüne. Economic receding horizon control without terminal constraints. *Submitted to Automatica*, 49(3):725–734, March 2012.

[GTSJ13] Euhanna Ghadimi, André Teixeira, Iman Shames, and Mikael Johansson. Optimal parameter selection for the alternating direction method of multipliers (ADMM): quadratic problems. June 2013.

[HBLJ13] Tobias Gybel Hovgaard, Stephen Boyd, Lars F. S. Larsen, and John Bagterp Jørgensen. Nonconvex model predictive control for commercial refrigeration. *International Journal of Control*, 86(8):1349–1366, August 2013.

[HEJ10] Tobias Gybel Hovgaard, Kristian Edlund, and John Bagterp Jørgensen. The Potential of Economic MPC for Power Management. In *49th IEEE Conference on Decision and Control (CDC)*, pages 7533–7538, 2010.

[HF] Jørgen Horstmann and Frank Nørgaard. Wind Optimized Charging of Electric Vehicles.

[HHLJ11] Tobias Gybel Hovgaard, Rasmus Halvgaard, Lars F. S. Larsen, and John Bagterp Jørgensen. Energy Efficient Refrigeration and Flexible Power Consumption in a Smart Grid. In *Proceedings of Risø International Energy Conference*, pages 164–175, 2011.

[HHM11] M. Hashmi, S. Hanninen, and K. Maki. Survey of smart grid concepts, architectures, and technological demonstrations worldwide. In *2011 IEEE PES Innovative Smart Grid Technologies (ISGT) Latin America*, October 2011.

[HM11] Karsten Hedegaard and Peter Meibom. Wind power impacts and electricity storage - A time scale perspective. *Renewable Energy*, 37(1):318–324, 2011.

[Hov13] Tobias Gybel Hovgaard. *Power Management for Energy Systems*. PhD thesis, Technical University of Denmark, 2013.

[HPJJ10] Jakob Kjøbsted Huusom, Niels Kjølstad Poulsen, Sten Bay Jørgensen, and John Bagterp Jørgensen. ARX-Model based Model and Predictive Control and with Offset-Free and Tracking. In *Proceedings of the 20th European Symposium on Computer Aided Process Engineering (ESCAPE)*, 2010.

[HPMJ12] Rasmus Halvgaard, Niels Kjølstad Poulsen, Henrik Madsen, and John Bagterp Jørgensen. Economic Model Predictive Control for Building Climate Control in a Smart Grid. In *Proceedings of 2012 IEEE PES Innovative Smart Grid Technologies (ISGT)*, 2012.

[HYB+12] Kai Heussen, Shi You, Benjamin Biegel, Lars Henrik Hansen, and K. B. Andersen. Indirect control for demand side management - A conceptual introduction. In *2012 3rd IEEE PES Innovative Smart Grid Technologies Europe (ISGT Europe)*, pages 1–8. IEEE, October 2012.

[JFGND12] John Bagterp Jørgensen, Gianluca Frison, Nicolai Fog Gade-Nielsen, and Bernd Damman. Numerical Methods for Solution of the Extended Linear Quadratic Control Problem. In *4th IFAC Nonlinear Model Predictive Control Conference International Federation of Automatic Control*, 2012.

[JHR11] John Bagterp Jørgensen, Jakob Kjøbsted Huusom, and James B. Rawlings. Finite Horizon MPC for Systems in Innovation Form. In *50th IEEE Conference on Decision and Control and European Control Conference (CDC-ECC)*, pages 1896–1903, 2011.

[JL11] Libin Jiang and Steven Low. Real-time demand response with uncertain renewable energy in smart grid. In *49th Annual Allerton Conference on Communication, Control, and Computing*, pages 1334–1341, September 2011.

[Jør05] John Bagterp Jørgensen. *Moving Horizon Estimation and Control*. PhD thesis, Technical University of Denmark, 2005.

[JRJ96] John Bagterp Jørgensen, James B. Rawlings, and Sten Bay Jørgensen. Numerical Methods for Large Scale Moving Horizon Estimation and Control. In *7th International Symposium on Dynamics and Control of Process Systems (DYCOPS)*, 1996.

[KA12] Arman Kiani and Anuradha Annaswamy. Distributed hierarchical control for renewable energy integration in a Smart Grid. *2012 IEEE PES Innovative Smart Grid Technologies (ISGT)*, pages 1–8, January 2012.

[KCLB14] Matt Kraning, Eric Chu, Javad Lavaei, and Stephen Boyd. Message Passing for Dynamic Network Energy Management. *Foundations and Trends in Optimization*, 1(2):70–122, 2014.

[KF12] Markus Kögel and Rolf Findeisen. Parallel solution of model predictive control using the alternating direction multiplier. In *4th IFAC Nonlinear Model Predictive Control Conference International Federation of Automatic Control*, 2012.

[KH05] Wook Hyun Kwon and Soo Hee Han. *Receding Horizon Control: Model Predictive Control for State Models (Advanced Textbooks in Control and Signal Processing)*. Springer, 2005.

[KL97] Willett Kempton and Steven E. Letendre. Electric vehicles as a new power source for electric utilities. *Transportation Research Part D: Transport and Environment*, 2(3):157–175, September 1997.

[KMJ04] Niels Rode Kristensen, Henrik Madsen, and Sten Bay Jørgensen. Parameter estimation in stochastic grey-box models. *Automatica*, 40(2):225–237, February 2004.

[KO13] Pardis Khayyer and Umit Ozguner. Decentralized control of smart grid with fixed and moving loads. In *2013 IEEE Power and Energy Conference at Illinois (PECI)*, pages 72–75. IEEE, February 2013.

[KSH00] T Kailath, A H Sayed, and B Hassibi. *Linear estimation*. Prentice Hall, 2000.

[LM67] Ernest Bruce Lee and Lawrence Markus. *Foundations of optimal control theory*. Wiley, 1967.

[LSD+11] Shuai Lu, Nader Samaan, Ruisheng Diao, Marcelo Elizondo, Chunlian Jin, Ebony Mayhorn, Yu Zhang, and Harold Kirkham. Centralized and decentralized control for demand response. In *2011 IEEE PES Innovative Smart Grid Technologies (ISGT)*, January 2011.

[LYM06] K. V. Ling, S. P. Yue, and Jan M. Maciejowski. A FPGA implementation of model predictive control. In *2006 American Control Conference*, pages 1930–1935, 2006.

[MAA13] Matthias A. Müller, David Angeli, and Frank Allgöwer. Economic model predictive control with self-tuning terminal weight. In *European Control Conference (ECC)*, pages 2044–2049, 2013.

[Mac02] Jan M. Maciejowski. Predictive control with constraints. 2002.

[Mar52] Harry Markowitz. Portfolio Selection. *The Journal of Finance*, 7(1):77–91, March 1952.

[MB12] Jacob Mattingley and Stephen Boyd. CVXGEN: A Code Generator for Embedded Convex Optimization. *Optimization and Engineering*, 13(1):1–27, 2012.

[MCM+14] Juan Miguel Morales, Antonio J. Conejo, Henrik Madsen, Pierre Pinson, and Marco Zugno. *Integrating Renewables in Electricity Markets*. Springer, 2014.

[MH99] Manfred Morari and Jay H. Lee. Model predictive control: past, present and future. *Computers & Chemical Engineering*, 23(4-5):667–682, May 1999.

[MHMV13] Peter Meibom, Klaus Baggesen Hilger, Henrik Madsen, and Dorthe Vinther. Energy Comes Together in Denmark. *IEEE Power and Energy Magazine*, 11(5):46–55, 2013.

[MN14] José M. Maestre and Rudy R. Negenborn. *Distributed Model Predictive Control Made Easy*. Springer, 2014.

[MRRS00] David Q. Mayne, James B. Rawlings, Christopher V. Rao, and P. O. M. Scokaert. Constrained model predictive control: Stability and optimality. *Automatica*, 36:789–814, 2000.

[MSPM12] E. D. Mehleri, Haralambos Sarimveis, L. G. Papageorgiou, and N. C. Markatos. Model Predictive Control of distributed energy resources. In *20th Mediterranean Conference on Control & Automation (MED)*, pages 672–678, July 2012.

[Nes07] Yurii Nesterov. Primal-dual subgradient methods for convex problems. *Mathematical Programming*, 120(1):221–259, June 2007.

[Nor] NordPool. www.nordpoolspot.com/How-does-it-work/Day-ahead-market-Elspot-/Price-calculation/.

[OEC13] OECD. *World Energy Outlook 2013*. OECD Publishing, 2013.

[OPJ+10] Frauke Oldewurtel, Alessandra Parisio, Colin Neil Jones, Manfred Morari, Dimitrios Gyalistras, Markus Gwerder, Vanessa Stauch, Beat Lehmann, and Katharina Wirth. Energy Efficient Building Climate Control using Stochastic Model Predictive Control and Weather Predictions. In *American Control Conference (ACC)*, pages 5100–5105, 2010.

[OPMO13] Niamh O'Connell, Pierre Pinson, Henrik Madsen, and M. O'Malley. Benefits and challenges of electric demand response: A critical review. 2013.

[PBM+12] Panagiotis Patrinos, Daniele Bernardini, Alessandro Maffei, Andrej Jokic, and Alberto Bemporad. Two-time-scale MPC for Economically Optimal Real-time Operation of Balance Responsible Parties. *IFAC Proceedings Volumes (IFAC-PapersOnline)*, 8:741–746, 2012.

[PHB+13] Mette K. Petersen, Lars Henrik Hansen, Jan Dimon Bendtsen, Kristian Edlund, and Jakob Stoustrup. Market Integration of Virtual Power Plants. In *52nd IEEE Conference on Decision and Control*, pages 2319–2325, 2013.

[PJ08] Guru Prasath and John Bagterp Jørgensen. Model Predictive Control based on Finite Impulse Response Models. In *Proceedings of 2008 American Control Conference (ACC)*, pages 441–446, 2008.

[PLOP08] Luis Pérez-Lombard, José Ortiz, and Christine Pout. A review on buildings energy consumption information. *Energy and Buildings*, 40(3):394–398, January 2008.

[PSS+13] Rasmus Pedersen, John Schwensen, Senthuran Sivabalan, Chiara Corazzol, Seyed Ehsan Shafiei, Kasper Vinther, and Jakob Stoustrup. Direct Control Implementation of a Refrigeration System in Smart Grid. In *2013 American Control Conference (ACC)*, pages 3954–3959, 2013.

[QB03] S. Joe Qin and Thomas A. Badgwell. A survey of industrial model predictive control technology. *Control Engineering Practice*, 11(7):733–764, 2003.

[RAB12] James B. Rawlings, David Angeli, and Cuyler N. Bates. Fundamentals of economic model predictive control. *2012 IEEE 51st IEEE Conference on Decision and Control (CDC)*, pages 3851–3861, December 2012.

[Ran09] Anders Rantzer. Dynamic Dual Decomposition for Distributed Control. In *American Control Conference (ACC)*, pages 884–888, St. Louis, MO, 2009. Ieee.

[RBJ+08] James B. Rawlings, Dennis Bonné, John Bagterp Jørgensen, Aswin N. Venkat, and Sten Bay Jørgensen. Unreachable Setpoints in Model Predictive Control. *IEEE Transactions on Automatic Control*, 53(9):2209–2215, 2008.

[RJM12] Stefan Richter, Colin Neil Jones, and Manfred Morari. Computational Complexity Certification for Real-Time MPC With Input Constraints Based on the Fast Gradient Method. *IEEE Transactions on Automatic Control*, 57(6):1391–1403, June 2012.

[RM93] James B. Rawlings and Kenneth R. Muske. The stability of constrained receding horizon control. *IEEE Transactions on Automatic Control*, 38(10), 1993.

[RRG11] Harry Rose, Alex Rogers, and Enrico H Gerding. Mechanism Design for Aggregated Demand Prediction in the Smart Grid. In *Artificial Intelligence and Smarter Living – The Conquest of Complexity: Papers from the 2011 AAAI Workshop (WS-11-07)*, pages 38–43, 2011.

[RSR13] Samira Rahnama, Jakob Stoustrup, and Henrik Rasmussen. Model predictive control for integration of industrial consumers to the smart grid under a direct control policy. *2013 IEEE International Conference on Control Applications (CCA)*, pages 515–520, August 2013.

[RWR98] Christopher V. Rao, Stephen J. Wright, and James B. Rawlings. Application of Interior-Point Methods to Model Predictive Control. *Journal of Optimization Theory*, 99(3):723–757, December 1998.

[SAY12] Anders Skajaa, Erling D Andersen, and Yinyu Ye. Warmstarting the homogeneous and self-dual interior point method for linear and conic quadratic problems. *Mathematical Programming Computation*, 5(1):1–25, August 2012.

[SB04] Takayuki Shiina and John R. Birge. Stochastic unit commitment problem. *International Transactions in Operational Research*, 11(1):19–32, January 2004.

[SC12] Masoud Soroush and Donald J. Chmielewski. Process Systems Opportunities in Power Generation, Storage and Distribution. In *Invited Session: Renewable Energy Systems and Sustainable Processes, Chemical Process Control (CPC VIII), Savannah, GA, 2012*, 2012.

[Sca09] Riccardo Scattolini. Architectures for distributed and hierarchical Model Predictive Control - A review. *Journal of Process Control*, 19(5):723–731, 2009.

[SCTB88] Fred C. Schweppe, M. Caramanis, R. Tabors, and R. Bohn. *Spot pricing of electricity*. Springer, 1988.

[SFS+14] Leo Emil Sokoler, Gianluca Frison, Anders Skajaa, Rasmus Halvgaard, and John Bagterp Jørgensen. A Homogeneous and Self-Dual Interior-Point Linear Programming Algorithm for Economic Model Predictive Control. *Submitted to IEEE Transactions on Automatic Control*, 2014.

[SIS12] Stephen Frank, Ingrida Steponavice, and Steffen Rebennack. Optimal power flow: a bibliographic survey I. *Energy Systems*, 3(3):221–258, 2012.

[SKC10] Amir Shahzad, Eric C. Kerrigan, and George A. Constantinides. A fast well-conditioned interior point method for predictive control. In *49th IEEE Conference on Decision and Control (CDC)*, pages 508–513. IEEE, December 2010.

[Sko02] Sigurd Skogestad. Plantwide control: Towards a systematic procedure. In *European Symposium on Computer Aided Process Engineering (ESCAPE)*, pages 57–69, 2002.

[SM72] Fred C. Schweppe and Sanjoy K. Mitter. Hierarchical System Theory and Electric Power Systems. In *Proceedings of the symposium on real-time control of electric power systems*, pages 259–277, 1972.

[SN12] Tomoharu Suehiro and Toru Namerikawa. Decentralized Control of Smart Grid by using Overlapping Information. In *SICE Annual Conference*, pages 125–130, 2012.

[Sok12] Leo Emil Sokoler. Second-Order Cone Programming for Probabilistic MPC in Power Production Management. Master's thesis, DTU Informatics, Technical University of Denmark, 2012.

[Sve06] Jørgen Svensson. *Active Distributed Power Systems*. Phd thesis, Lund University, 2006.

[SY05] M. Shahidehopour and Yong Fu. Benders decomposition: applying Benders decomposition to power systems, 2005.

[Taf12] Jeffrey Taft. Ultra Large Scale Power System Control Architecture. Technical Report October, CISCO Connected Energy Networks Business Unit, 2012.

[TBS11] Klaus Trangbæk, Jan Dimon Bendtsen, and Jakob Stoustrup. Hierarchical Control for Smart Grids. In *Proceedings of the 18th IFAC World Congress*, 2011.

[TLW13] Luminita C. Totu, John Leth, and Rafel Wisniewski. Control for large scale demand response of thermostatic loads. *2013 American Control Conference (ACC)*, pages 5023–5028, 2013.

[TNM+12] Hermen A. Toersche, S. Nykamp, A. Molderink, J. L. Hurink, and G. J. M. Smit. Controlling smart grid adaptivity. In *2012 3rd IEEE PES Innovative Smart Grid Technologies Europe (ISGT) Europe*, October 2012.

[UACA11] Andreas Ulbig, Michèle Arnold, Spyros Chatzivasileiadis, and Göran Andersson. Framework for Multiple Time-Scale Cascaded MPC Application in Power Systems. In *18th IFAC World Congress*, pages 10472–10480, 2011.

[VPM+11] Z. A. Vale, T. Pinto, H. Morais, I. Praca, and P. Faria. VPP's multilevel negotiation in smart grids and competitive electricity markets. In *2011 IEEE Power and Energy Society General Meeting*, July 2011.

[WÅÅ02] Bjørn Wittenmark, Karl Johan Åstrøm, and Karl Erik Årzen. Computer Control: An Overview. *IFAC Professional Brief*, pages 1–82, 2002.

[Wan07] Ivar Wangensteen. *Power System Economics - the Nordic Electricity Market*. Tapir Academic Press, Trondheim, 2007.

[WB10] Yang Wang and Stephen Boyd. Fast Model Predictive Control Using Online Optimization. *IEEE Transactions on Control Systems Technology*, 18(2):267–278, 2010.

[WdG10] Chen Wang and Martin de Groot. Managing end-user preferences in the smart grid. In *1st International Conference on Energy-Efficient Computing and Networking*, New York, New York, USA, 2010. ACM Press.

[WLJ12] Qingsi Wang, Mingyan Liu, and Rahul Jain. Dynamic Pricing of Power in Smart-Grid Networks. 2012.

[WNØ+10] Qiuwei Wu, Arne H Nielsen, Jacob Østergaard, Seung Tae Cha, Francesco Marra, Yu Chen, and Chresten Træholt. Driving Pattern Analysis for Electric Vehicle (EV) Grid Integration Study. In *Innovative Smart Grid Technologies Conference Europe (ISGT Europe), 2010 IEEE PES*, pages 1–6, 2010.

[ZJM10] Melanie Nicole Zeilinger, Colin Neil Jones, and Manfred Morari. Robust stability properties of soft constrained MPC. In *49th IEEE Conference on Decision and Control (CDC)*, pages 5276–5282. IEEE, December 2010.

[ZMPM12] Marco Zugno, Juan Miguel Morales, Pierre Pinson, and Henrik Madsen. Modeling Demand Response in Electricity Retail Markets as a Stackelberg Game. In *Proceedings of IAEE conference*, 2012.

[ZT11] Y. Zhu and K. Tomsovic. Analysis and control of Distributed Energy Resources. In *2011 IEEE Power and Energy Society General Meeting*, July 2011.

[Zug13] Marco Zugno. *Optimization under Uncertainty for Management of Renewables in Electricity Markets*. PhD thesis, Technical University of Denmark, 2013.

Part II

Papers

Paper A

Economic Model Predictive Control for Building Climate Control in a Smart Grid

Published in *Proceedings of 2012 IEEE PES Innovative Smart Grid Technologies (ISGT), 2012.*

Economic Model Predictive Control for Building Climate Control in a Smart Grid

Rasmus Halvgaard, Niels Kjølstad Poulsen, Henrik Madsen and John Bagterp Jørgensen

***Abstract*—Model Predictive Control (MPC) can be used to control a system of energy producers and consumers in a Smart Grid. In this paper, we use heat pumps for heating residential buildings with a floor heating system. We use the thermal capacity of the building to shift the energy consumption to periods with low electricity prices. In this way the heating system of the house becomes a flexible power consumer in the Smart Grid. This scenario is relevant for systems with a significant share of stochastic energy producers, e.g. wind turbines, where the ability to shift power consumption according to production is crucial. We present a model for a house with a ground source based heat pump used for supplying thermal energy to a water based floor heating system. The model is a linear state space model and the resulting controller is an Economic MPC formulated as a linear program. The model includes forecasts of both weather and electricity price. Simulation studies demonstrate the capabilities of the proposed model and algorithm. Compared to traditional operation of heat pumps with constant electricity prices, the optimized operating strategy saves 25-35% of the electricity cost.**

I. Introduction

The energy policies in the Nordic countries stipulate that 50% of the energy consumed by 2025 should come from renewable and CO_2-free energy sources. By 2050 the aim is to be independent of fossil fuels. This transformation of the energy system is needed to reduce CO_2 emissions and global warming as well as to protect the Nordic economies from the consequences of sharply rising prices of fossil fuels due to an increasing world population and depletion of fossil fuel resources. Not only the Nordic countries but the entire world and industrialized world in particular are facing this grand challenge. Reducing the fossil fuel consumption from 80% of the energy consumption to 0% in 40 years, requires introduction of a significant amount of renewable energy sources and an efficient utilization of energy in buildings, the process industries, and transportation. In the Nordic countries, a major part of the renewable energy will be produced by hydro power and offshore wind turbines. On the consumption side, residential and commercial buildings will use heat pumps for heating and electrical vehicles will replace vehicles based on combustion engines.

Accordingly, electricity will be the main energy carrier in such an energy system independent of fossil fuels. Depending on the rate of adoption of electrified vehicles, 40-70% of the energy consumption will originate from electricity in 2050. Currently, 20% of the energy consumption is electricity. As it is more difficult to store electricity than fossil fuels, such a large share of stochastic electricity production requires an intelligent power system - also referred to as a Smart Grid - that continuously balances the power consumption and the power production. This balancing requires control of the power consumption from heat pumps and electrical vehicles such that surplus of cheap wind energy is used as it is produced. Heat tanks in residential homes as well as in district heating plants must be established such that heat pumps can store electricity as heat in periods with low electricity prices. The power consumption by the process industries and retail industry, e.g. refrigeration in supermarkets and large cooling houses, must also be made flexible. Such a system is a large-scale complex system that must be coordinated to balance consumption and production of electricity.

Buildings account for approximately 40% of the total energy use in Europe. Therefore, intelligent control of the energy use in buildings is a necessity for the future smart energy system. In the Nordic countries, the energy is mainly used for heating, lighting, and electrical appliances. Heat pumps combined with water based floor heating systems will be one of the main sources for heating of buildings [1]–[4]. By themselves, these heat pumps are very energy efficient as their coefficient of performance is typically 3 or larger, i.e. for each kWh electricity supplied, they deliver more than 3 kWh heat. As heat pumps are driven by electricity and can be connected to floors with large thermal capacity, they have a large potential to shift the electricity consumption and adapt to the stochastic electricity production from wind turbines. The adoption of heat pumps could very well accelerate in the coming years. Especially for buildings situated outside district heating areas. They can benefit from heating using electric heat pumps instead of the current oil and natural gas. Heat pumps connected to the district heating system can benefit from a large store of heat and can be used to shift electricity consumption on a 24-hour or weekly basis. Furthermore, large electric heat pumps can be installed at a number of district heating plants. The large heat pumps can better exploit heat from the sea, lakes or waste heat, while small heat pumps can exploit geothermal heat.

The use of Model Predictive Control to provide indoor thermal comfort in heating systems of buildings has been reported in [5]–[7]. In the future energy systems with a large share of stochastic power producers such as wind turbines, the ability to shift the load of electricity is just as important as providing indoor thermal comfort in a heating system based on heat pumps. Different control strategies have been suggested for load balancing and load shifting in electrical grids [8]. For

R. Halvgaard, N. K. Poulsen, H. Madsen and J. B. Jørgensen are with DTU Informatics, Technical University of Denmark, Richard Petersens Plads, Building 321, DK-2800 Kgs. Lyngby, Denmark {rhal,nkp,hm,jbj}@imm.dtu.dk

978-1-4577-2159-5/12/$31.00 ©2011 IEEE

heat pumps, these strategies can be summarized as

1) **Frequency based control**. The heat pump senses the grid frequency, which in Europe has the nominal value of 50 Hz. When demand exceeds supply, the frequency falls. When supply exceeds demand, the frequency increases. Depending on a measured difference from the nominal value of the frequency, the heat pump can decide to pre-heat by starting the compressor or to delay the activation of the compressor for a short time. The advantage of this type of control is the low price of the controller, because no additional communication between the utility and the heat pump is necessary. However, there is no way to integrate the device into an intended schedule as it responds completely autonomously.
2) **Price based control**. The heat pump controller computes a schedule for the compressor based on dynamic price information given by the utility. This enables the heat pump to shift its load to times with low electricity price. It requires a communication infrastructure between utilities and households. The drawback of this control strategy is that it is relatively complex and the fact that effects of sent tariff information to affect the load are not completely sure for the utility.
3) **Direct control**. Given the communication infrastructure required for the price based control, utilities can send control signals to the heat pump to raise or reduce the demand. This allows the utility a more direct control of the demand. Furthermore, it allows the controller in the heat pump to be quite simple as it only sends information and receives commands from the utility. The drawback of course is that the utility must solve large-scale optimization problems to coordinate a large number of heat pumps.

[9] use Economic Model Predictive Control (MPC) in a direct control case to shift the electricity load of refrigeration systems. In this paper, we use Economic MPC based on price signals to control a heat pump such that certain temperature limits in a building with a floor heating system are respected. By using price signals, both current and future prices, the optimization of the energy consumption of each individual residential building decouples from the energy consumption of all other agents in the system. However, we do not specify how to determine this price but assume that it is given based on market principles of supply and demand. Consequently, each individual house is a price taker.

Simple weather conditions such as outdoor temperature and solar radiation are included in the model. By adding forecasts of prices and weather conditions to the heat pump control problem, the energy consumption is made flexible. It is thus possible to predict where to place the heat pump energy consumption and minimize the electricity cost of operating the heat pump to meet a certain indoor thermal comfort, i.e. a desired temperature interval. The temperature interval can be time varying. We exploit that the dynamics of the temperatures in the house floor heating system and indoor air are slow while the power consumption can be changed rapidly. The thermal capacity of the residential building determines how much of the electricity consumption that can be shifted to times with cheap electricity.

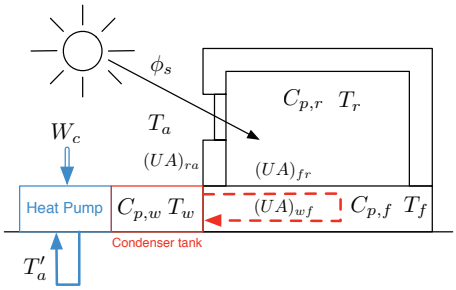

Fig. 1. House and heat pump floor heating system and its thermal properties. The dashed line represents the floor heating pipes.

MPC is increasingly being considered for building climate control [10]–[12]. Traditionally, MPC is designed using objective functions penalizing deviations from a given setpoint. Recently Economic MPC has emerged as a general methodology with efficient numerical implementations and provable stability properties [13], [14].

This paper is organized as follows. In Section II, we develop and discuss a model for a heat pump connected to a floor heating system of a building. Section III states and discusses the Economic MPC. Simulation results for the Economic MPC applied to the model are described in Section IV. Section V provides conclusions.

II. Model

In this section, we develop a model of the heat dynamics of a house floor heating system connected to a ground source based heat pump. The system is illustrated in Fig. 1. The model is a linear third order model. Table I lists the variables and parameters of the model.

TABLE I
Description of variables

Variable	Unit	Description
T_r	°C	Room air temperature
T_f	°C	Floor temperature
T_w	°C	Water temperature in floor heating pipes
T_a	°C	Ambient temperature
T'_a	°C	Ground temperature
W_c	W	Heat pump compressor input power
ϕ_s	W	Solar radiation power

A. Energy Balances and Heat Conduction

In this subsection we develop energy balances for the air in the room, the floor and the water in the floor heating pipes

and condenser water tank. In the simple model developed in this paper, the house is considered to be one big room. Furthermore, we make the following simplifying assumptions: 1) One uniform air temperature, 2) no ventilation, 3) no influence from humidity of the air, 4) no influence from the heat released from people in the room, 5) no influence from wind.

In [15] a model of the indoor temperature in buildings is identified and suggests at least two dominating heat accumulating media in order to capture the short-term and long-term variations of the heat dynamics. In our model two heat accumulating media are thus included, namely the room air and the floor. The resulting energy balances are

$$C_{p,r}\dot{T}_r = Q_{fr} - Q_{ra} + (1-p)\phi_s \tag{1}$$
$$C_{p,f}\dot{T}_f = Q_{wf} - Q_{fr} + p\,\phi_s \tag{2}$$

The disturbances are the ambient temperature and the solar radiation through a window. These disturbances are also illustrated in Fig. 1.

The energy balance for the water circulating in the floor heating pipes can be stated as

$$C_{p,w}\dot{T}_w = Q_c - Q_{wf} \tag{3}$$

in which Q_c is the heat transferred to the water from the condenser in the heat pump. Q_{wf} is the heat transferred from the water to the floor.

The conductive heat transfer rates are

$$Q_{ra} = (UA)_{ra}(T_r - T_a) \tag{4a}$$
$$Q_{fr} = (UA)_{fr}(T_f - T_r) \tag{4b}$$
$$Q_{wf} = (UA)_{wf}(T_w - T_f) \tag{4c}$$

Q_{ra} is the heat transferred from the air in the room to the surroundings, Q_{fr} is the heat transferred from the floor to the air in the room, and Q_{wf} is the heat transferred from the water in the floor heating pipes to the floor. The term $U \cdot A$ is a product of the heat conductivity and the surface area of the layer between two heat exchanging media. Its reciprocal value $R = 1/(UA)$ is often used since it can be interpreted as a resistance against heat flow [16].

B. Heat Pump

A heat pump is a device that transfers heat from a low temperature zone to a higher temperature zone using mechanical work. A heat pump can provide both heating or cooling, but in cooler climates heating is of course more common. Heat pumps normally draw heat from the air or from the ground and uses a vapor compression refrigeration cycle. This cycle requires the four basic components as sketched in Fig. 2. The components are a compressor, an expansion valve, a condenser converting the working fluid from its gaseous state to its liquid state, and an evaporator converting the working fluid from its liquid state to its gaseous state [17], [18].

As the heat pump dynamics is much faster than the thermodynamics of the building, we can assume a static model for the heat pump. The amount of heat transferred from the condenser to the water, Q_c, is related to the work of the compressor, W_c, using the coefficient of performance

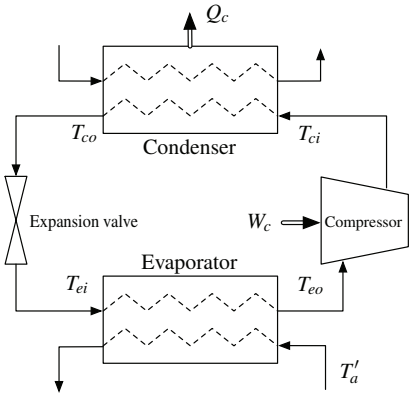

Fig. 2. Heat pump vapor compression refrigeration cycle. The temperatures are denoted T with subscript c or e for condenser or evaporator, respectively, while i or o denotes input or output.

$$Q_c = \eta W_c \tag{5}$$

The coefficient of performance η for heat pumps varies with type, outdoor ground temperature, and the condenser temperature. As the outdoor ground temperature and the condenser temperature are approximately constant, we can assume that the coefficient of performance is constant. For ground source based heat pumps η is typically around 3 in the specified operating range.

The model consists of (1)-(5). Consequently, a third order linear model can be stated as

$$\begin{aligned} C_{p,r}\dot{T}_r = (UA)_{fr}(T_f - T_r)\ldots \\ -(UA)_{ra}(T_r - T_a) + (1-p)\phi_s \end{aligned} \tag{6a}$$
$$\begin{aligned} C_{p,f}\dot{T}_f = (UA)_{wf}(T_w - T_f)\ldots \\ -(UA)_{fr}(T_f - T_r) + p\phi_s \end{aligned} \tag{6b}$$
$$C_{p,w}\dot{T}_w = \eta W_c - (UA)_{wf}(T_w - T_f) \tag{6c}$$

C. State space model

The model (6) can be expressed as a continuous-time state space model

$$\dot{x} = Ax + Bu + Ed \tag{7a}$$
$$y = Cx \tag{7b}$$

x is the states, u is the manipulated variables, d is the disturbances, and y is the controlled variable. In the case studied, the states are $x = \begin{bmatrix} T_r & T_f & T_w \end{bmatrix}^T$; the manipulate variable is the power used by the compressor in the heat pump, $u = W_c$; the disturbances are the ambient temperature and the sun radiation such that $d = \begin{bmatrix} T_a & \phi_s \end{bmatrix}^T$; and the controlled

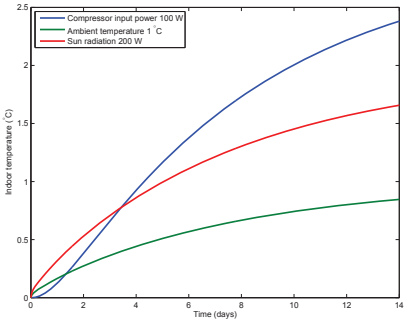

Fig. 3. Step responses from inputs and disturbances to indoor temperature T_r. Step size is noted in the plot legend.

variable is the indoor temperature $y = T_r$. The matrices in the state space model (7) are

$$A = \begin{bmatrix} a_{11} & a_{12} & 0 \\ a_{21} & a_{22} & a_{23} \\ 0 & a_{32} & a_{33} \end{bmatrix} \quad E = \begin{bmatrix} \frac{(UA)_{ra}}{C_{p,r}} & \frac{1-p}{C_{p,r}} \\ 0 & \frac{p}{C_{p,f}} \\ 0 & 0 \end{bmatrix}$$

$$C = \begin{bmatrix} 1 & 0 & 0 \end{bmatrix} \quad B = \begin{bmatrix} 0 & 0 & \frac{\eta}{C_{p,w}} \end{bmatrix}^T$$

with the coefficients

$$a_{11} = (-(UA)_{fr} - (UA)_{ra})/C_{p,r}$$
$$a_{22} = (-(UA)_{wf} - (UA)_{fr})/C_{p,f} \quad a_{33} = -(UA)_{wf}/C_{p,w}$$
$$a_{12} = (UA)_{fr}/C_{p,r} \quad a_{23} = (UA)_{wf}/C_{p,f}$$
$$a_{21} = (UA)_{fr}/C_{p,f} \quad a_{32} = (UA)_{wf}/C_{p,w}$$

[19] provides values for building heat capacities and thermal conductivities obtained from system identification methods. The values of these parameters for a representative building are listed in Table II. The water tank heat capacity is estimated as $C_{p,w} = m_w c_w$ for a 200 liter tank filled with water having the specific heat capacity c_w and mass m_w. The resulting time constants of the third order model are 1, 24, and 186 hours for the room air, water condenser tank, and the floor, respectively. This is also observed from the step responses seen in Fig. 3.

III. Economic MPC

The state space model (7) is converted to a discrete-time state space model using zero-order-hold sampling of the input signals

$$x_{k+1} = A_d x_k + B_d u_k + E_d d_k \tag{8a}$$
$$y_k = C_d x_k \tag{8b}$$

Using this discrete-time linear state space formulation to predict the future outputs, we may formulate a linear program that minimizes the electricity cost for operating the heat pump while keeping the indoor room temperature in prespecified intervals

$$\min_{\{x,u,y\}} \quad \phi = \sum_{k\in\mathcal{N}} c_{u,k} u_k + \rho_v v_k \tag{9a}$$
$$s.t. \quad x_{k+1} = A_d x_k + B_d u_k + E_d d_k \quad k \in \mathcal{N} \tag{9b}$$
$$y_k = C_d x_k \quad k \in \mathcal{N} \tag{9c}$$
$$u_{\min} \le u_k \le u_{\max} \quad k \in \mathcal{N} \tag{9d}$$
$$\Delta u_{\min} \le \Delta u_k \le \Delta u_{\max} \quad k \in \mathcal{N} \tag{9e}$$
$$y_{k,\min} \le y_k + v_k \quad k \in \mathcal{N} \tag{9f}$$
$$y_{k,\max} \ge y_k - v_k \quad k \in \mathcal{N} \tag{9g}$$
$$v_k \ge 0 \quad k \in \mathcal{N} \tag{9h}$$

$\mathcal{N} \in \{0, 1, \ldots, N\}$ and N is the prediction horizon. The electricity prices enter the optimization problem as the cost coefficients $c_{u,k}$. It may not always be possible to meet the temperature demand. Therefore, the MPC problem is relaxed by introduction of slack variable v_k and the associated penalty cost ρ_v. The penalties can be set sufficiently large, such that the output constraints are met whenever possible. The Economic MPC also contains bound constraints and rate-of-movement constraints on the manipulated variables. The rate-of-movement is defined in discrete time as $\Delta u_k = u_{k+1} - u_k$ and adds to robustness of the numerical optimization routine.

The prediction horizon, N, is normally selected large to avoid discrepancies between open-loop and closed-loop profiles. However, long horizons increases computation speed rapidly and uncertainties in the forecasts grow larger and larger with time. At each sampling time, we solve the linear program (9) to obtain $\{u_k^*\}_{k=0}^{N-1}$. We implement u_0^* on the process. As new information becomes available at the next sampling time, we redo the process of solving the linear program using a moving horizon and implementing the first part, u_0^*, of the solution.

The electricity prices, $\{c_{u,k}\}_{k=0}^{N-1}$, as well as the ambient temperature and sun radiation, $\{d_k\}_{k=0}^{N-1}$, must be forecasted. In this paper we assume that we have perfect forecasts.

IV. Results

The Economic MPC has been implemented in Matlab calling a primal active set solver. To illustrate the potential of the Economic MPC for controlling heat pumps, we simulate scenarios using day-ahead electricity prices from Nordpool, the Nordic power exchange market. These electricity prices are available in one hour intervals. We also discretize the system using a sample time of 30 minutes, i.e. $T_s = 0.5$ hour. Both the outdoor temperature, T_a, and solar radiation ϕ_s are modeled as diurnal cycles with added noise [10]. We aim to minimize the total electricity cost in a given period while keeping the indoor temperature, T_r, in predefined intervals. In the case studied, we assume that the forecasts are perfect, i.e. that the forecasts are without uncertainty. We simulate a five day period using a prediction horizon $N = 96$ (= 48 hours). The optimal control signal is calculated at every time step over the prediction horizon to obtain a closed loop profile.

Fig. 4 illustrates the optimal compressor schedule and the predicted indoor temperature for a five day horizon. The lower

TABLE II
ESTIMATED MODEL PARAMETERS

	Value	Unit	Description
$C_{p,r}$	810	kJ/°C	Heat capacity of room air
$C_{p,f}$	3315	kJ/°C	Heat capacity of floor
$C_{p,w}$	836	kJ/°C	Heat capacity of water in floor heating pipes
$(UA)_{ra}$	28	kJ/(°C h)	Heat transfer coefficient between room air and ambient
$(UA)_{fr}$	624	kJ/(°C h)	Heat transfer coefficient between floor and room air
$(UA)_{wf}$	28	kJ/(°C h)	Heat transfer coefficient between water and floor
c_w	4.181	kJ/(°C kg)	Specific heat capacity of water
m_w	200	kg	Mass of water in floor heating system
p	0.1		Fraction of incident solar radiation on floor
η	3		Compressor coefficient of performance (COP)
ρ_v	10^4		Slack variable penalty

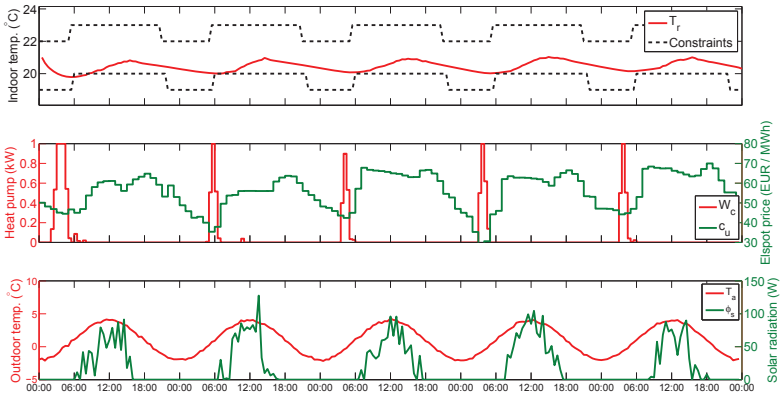

Fig. 4. Temperature in a house with time varying soft constraints, time varying electricity prices, and time varying outdoor temperatures. The simulation time is five days starting 20 JAN 2011 00:00. The upper figure shows the indoor temperature, the middle figure contains the electricity spot price and the optimal schedule for the heat pump, and the lower figure contains the ambient temperature and solar radiation. The compressor is on when the electricity spot price is low.

plot shows the outdoor temperature, T_a, and the solar radiation, ϕ_s. The outdoor temperature reflects a cold climate, i.e. the outdoor temperature is lower than the indoor temperature. The solar radiation has a peak around noon contributing to heating the building. The middle plot shows the actual electricity prices in Western Denmark. The middle plot also contains the computed optimal heat pump power input, W_c. The upper plot shows the predicted indoor temperature along with the predefined time varying constraints. The constraints indicate that during night time the temperature is allowed to be lower than at day time. The figure reveals clearly that the power consumption is moved to periods with cheap electricity and that the thermal capacity of the house floor is able to store enough energy such that the heat pump can be left off during day time. This demonstrates that the slow heat dynamics of the floor can be used to shift the energy consumption to periods with low electricity prices and still maintain acceptable indoor temperatures. Notice that the soft constraints are violated in the beginning due to the initial conditions. We allow for such violations by using reasonable moderate penalty costs for violation of the soft constraints. Consequently, the controller will find cheaper optimal solutions while the comfort level is compromized very little.

We also conducted a simulation with constant electricity prices. In this case, the heat pump now is turned on to just keep the indoor temperature at its lower limit. This implies that there is no load shifting from the heat pump in this case. By comparing the case with varying electricity price, $\{u_k^*\}_{k=0}^{N-1}$, to the case with constant electricity price, $\{u_{k,cst}^*\}_{k=0}^{N-1}$, we observe economic savings around 35%. We obtained this figure

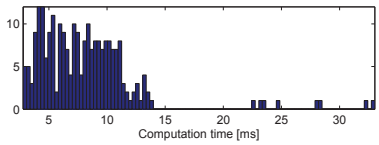

Fig. 5. Computation time distribution for all open loop profiles calculated in the five days closed loop simulation with prediction horizon 48 hours.

by comparing the total electricity expenses using the true time varying electricity prices $\{c_{u,k}\}_{k=0}^{N-1}$ such that the savings S are calculated as

$$S = -\frac{c_u^T u_{cst}^* - c_u^T u^*}{c_u^T u_{cst}^*} \tag{10}$$

Using a simulation study with hard constraints on the indoor temperature, the saving by load shifting was 25%.

Figure 5 shows the computation times of solving the open loop optimization problems for the given simulation using a PC with Intel Core i7 2.67 GHz. The average computation time is seen to be around 8 ms. Using hard constraints the average computation time reduces to 1 ms.

V. Conclusions

In this paper, we have presented a model for the temperature in a residential building with a floor heating system and a heat pump. We used an Economic Model Predictive Controller (Economic MPC) to manipulate the compressor in the heat pump such that the total electricity cost is minimized, while keeping the indoor temperature in a predefined interval. Using actual electricity prices and weather conditions, we demonstrated that the Economic MPC is able to shift the power consumption load to periods with low electricity prices. As the Nordic Electricity spot prices reflect the amount of wind power in the system, the large thermal capacity of the house floor can essentially be used to store cheap electricity from renewable energy sources such as wind turbines. We also observed that the load shifting ability of the Economic MPC can exploit weather forecasts to reduce the total cost of operating a heat pump.

The Economic MPC concept was proofed using perfect forecasts. In the future, we will use real forecast to investigate cases with uncertainty.

References

[1] A. Hepbasli and Y. Kalinci, "A review of heat pump water heating systems," *Renewable and Sustainable Energy Reviews*, vol. 13, pp. 1211–1229, 2009.

[2] F. Karlsson and P. Fahlén, "Impact of design and thermal intertia on the energy saving potential of capacity controlled heat pump heating systems," *International Journal of Refrigeration*, vol. 31, pp. 1094–1103, 2008.

[3] Z. Han, M. Zheng, F. Kong, F. Wang, Z. Li, and T. Bai, "Numerical simulation of solar assisted ground-source heat pump heating system with latent heat energy storage in severly cold area," *Applied Thermal Engineering*, vol. 28, pp. 1427–1436, 2008.

[4] A. Molyneaux, G. Leyland, and D. Favrat, "Environomic multi-objective optimisation of a district heating network considering centralized and decentralized heat pumps," *Energy*, vol. 35, pp. 751–758, 2010.

[5] T. Y. Chen, "Application of adaptive predictive control to a floor heating system with a large thermal lag," *Energy and Buildings*, vol. 34, pp. 45–51, 2001.

[6] H. Karlsson and C.-E. Hagentoft, "Application of model based predictive control for water-based floor heating in low energy residential buildings," *Building and Environment*, vol. 46, pp. 556–569, 2011.

[7] S. Privara, J. Siroky, L. Ferkl, and J. Cigler, "Model predictive control of a building heating system: The first experience," *Energy and Buildings*, vol. 43, pp. 564–572, 2011.

[8] M. Stadler, W. Krause, M. Sonnenschein, and U. Vogel, "Modelling and evaluation of control schemes for enhancing load shift of electricity demand for cooling devices," *Environmental Modelling & Software*, vol. 24, pp. 285–295, 2009.

[9] T. G. Hovgaard, K. Edlund, and J. B. Jørgensen, "The potential of economic MPC for power management," in *49th IEEE Conference on Decision and Control*, 2010, pp. 7533–7538.

[10] F. Oldewurtel, A. Ulbig, A. Parisio, G. Andersson, and M. Morari, "Reducing peak electricity demand in building climate control using real-time pricing and model predictive control," *IEEE Conference on Decision and Control*, 2010.

[11] F. Oldewurtel, A. Parisio, C. N. Jones, M. Morari, D. Gyalistras, M. Gwerder, V. Stauch, B. Lehmann, and K. Wirth, "Energy efficient building climate control using stochastic model predictive control and weather predictions," *Proceedings of ACC*, 2010.

[12] V. M. Zavala, E. M. Constantinescu, and T. K. amd Mihai Anitescu, "On-line economic optimization of energy systems using weather forecast information," *Journal of Process Control*, no. 19, pp. 1725–1736, 2009.

[13] J. B. Rawlings and R. Amrit, "Optimizing process economic performance using model predictive control," in *Nonlinear Model Predictive Control: Towards New Challenging Applications*. Springer, 2009, pp. 119–138.

[14] M. Diehl, R. Amrit, and J. B. Rawlings, "A lyapunov function for economic optimizing model predictive control," *IEEE Transactions on Automatic Control*, 2009.

[15] H. Madsen and J. Holst, "Estimation of continuous-time models for the heat dynamics of a building," *Energy and Buildings*, vol. 22, no. 1, pp. 67–79, 1995.

[16] A. Thavlov, "Dynamic optimization of power consumption," Master's thesis, Dept. of Informatics and Mathematical Modelling, Technical University of Denmark, 2008.

[17] A. Schijndel and M. de Wit, "Advanced simulation of building systems and control with simulink," *Building Simulation*, pp. 1185–1192, 2003.

[18] B. P. Rasmussen, "Dynamic modeling and advanced control of air conditioning and refrigeration systems," Ph.D. dissertation, University of Illinois, 2000.

[19] K. K. Andersen, H. Madsen, and L. H. Hansen, "Modelling the heat dynamics of a building using stochastic differential equations," *Energy and Buildings*, vol. 13, pp. 13–24, 2000.

Paper B

Electric Vehicle charge planning using Economic Model Predictive Control

Published in *Proceedings of 2012 IEEE International Electric Vehicle Conference (IEVC), 2012.*

Electric Vehicle Charge Planning using Economic Model Predictive Control

Rasmus Halvgaard, Niels K. Poulsen
Henrik Madsen and John B. Jørgensen
Department of Informatics and Mathematical Modelling
Technical University of Denmark
Richard Petersens Plads
2800 Kgs. Lyngby, Denmark
Email:{rhal,nkp,hm,jbj}@imm.dtu.dk

Francesco Marra
and Daniel Esteban Morales Bondy
Department of Electrical Engineering
Technical University of Denmark
Elektrovej, building 325
2800 Kgs. Lyngby, Denmark
Email: {fm,bondy}@elektro.dtu.dk

***Abstract*—Economic Model Predictive Control (MPC) is very well suited for controlling smart energy systems since electricity price and demand forecasts are easily integrated in the controller. Electric vehicles (EVs) are expected to play a large role in the future Smart Grid. They are expected to provide grid services, both for peak reduction and for ancillary services, by absorbing short term variations in the electricity production. In this paper the Economic MPC minimizes the cost of electricity consumption for a single EV. Simulations show savings of 50-60% of the electricity costs compared to uncontrolled charging from load shifting based on driving pattern predictions. The future energy system in Denmark will most likely be based on renewable energy sources e.g. wind and solar power. These green energy sources introduce stochastic fluctuations in the electricity production. Therefore, energy should be consumed as soon as it is produced to avoid the need for energy storage as this is expensive, limited and introduces efficiency losses. The Economic MPC for EVs described in this paper may contribute to facilitating transition to a fossil free energy system.**

I. INTRODUCTION

Reducing CO_2 emissions and becoming independent of fossil fuels are both major economic and political drivers for switching from traditional combustion engines to electrification of the transport sector through the introduction of Electric Vehicles (EVs). To facilitate the fossil free electrification of the transport sector, the amount of renewable energy sources in the energy system must be increased significantly. By nature, renewable energy sources like wind and solar power are stochastic and introduce fluctuations in the otherwise predictable and stable power system.

In Denmark the penetration of wind power is beyond 20% and calls for either huge storage solutions or a highly flexible demand that can be controlled in order to consume power as it is produced. Electric storage is very expensive, introduces efficiency losses and is not feasible everywhere. However, the development and penetration of EVs seems inevitable, and their batteries could potentially provide a storage opportunity. The idea is that if the EVs are intelligently charged, they could become a controllable asset to the grid rather than a traditional load disturbance. They could help absorb variations in the power system and help move consumption to off-peak periods. When parked and plugged into the grid, EVs are expected to either charge intelligently or discharge, i.e. feed power back into the grid. However, handling the probabilistic load behavior of EVs present is a challenge to the balance responsible.

In the future, large fleets of EVs will be available, and could potentially provide flexible services to the grid, e.g. load shifting, balancing power, and frequency response. Another of these services could be delivery of electricity to the grid by discharging the EV battery, also known as Vehicle-to-Grid (V2G). This was first proposed by [1] and is the main reason why EVs are expected to play an important role in the future power system. The charging impact of EVs on the power grid has also been reported in the literature, e.g. [2]. Emphasis is mainly on the services EVs can provide to the electric energy system. Currently, it is not clearly understood if a centralized or decentralized strategy should be applied, and what actual services EV users require. However, it is clear that there must be an incentive for EV users to help the balance the power production and charge during off-peak periods.

Fig. 1 illustrates the Virtual Power Plant (VPP) approach for handling a fleet of EVs. In a centralized strategy, the aggregator performs the optimal charge scheduling calculations and sends out the individual charge plans to EVs. A decentralized approach could be to broadcast a price signal and let the individual EV optimize its own charging based on this price. Less communication is required at the expense of a larger computation task for the EV. In Denmark EV charging is billed with the same tariffs as for the standard domestic loads. So in this paper the price signal is the Elspot price, a Time of Use (TOU) price for the customer, taken from the Nordpool day ahead market. This price is settled every day at noon for the coming day and is thus known 12 to 36 hours in advance. The amount of wind power in the power grid is thus also reflected in this signal. Furthermore, since feed-in tariffs do not yet exist for LV grid producers vehicle-to-grid (V2G) operation will not be addressed in this study.

[3] considers a decentralized strategy where the charging costs are minimized for each EV user individually. In addition,

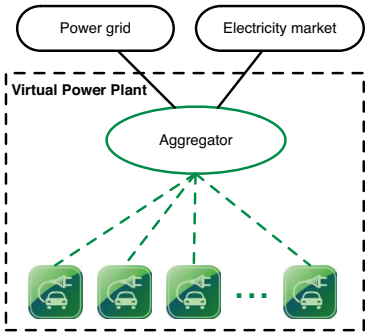

Fig. 1. Virtual Power Plant framework with EVs. The dashed green line is the price signal from the aggregator.

a penalty on the deviation from the average EV fleet charge behavior is added to the objective function. By sending out the average optimal charging plans to all EVs, the charge strategy is negotiated by an iteration procedure that is guaranteed to converge towards a Nash equilibrium.

In practice, when charging a large fleet of EVs in periods where electricity prices are low, typically at night time, the price will in the long run start to increase in these periods reflecting new demand patterns. This price elasticity effect has been modeled for an EV demand response and a price flattening was observed [4].

An optimal charge strategy for EVs optimization of both energy cost and battery health has also been investigated [5]. The proposed battery model is based on a first principles chemical battery model and a battery degradation map was determined by simulation. This map was used to determine at what rates the battery suffers the most. Battery degradation in detail will not be taken into account in this paper but general guidelines for improving the life time will.

In [6], [7] methods for planning the individual charging schedules of a large EV fleet while respecting the constraints in the low-voltage distribution grid are proposed. Another proposed ancillary service is to minimize the load variance of the power system by queuing up charge requests [8]. In this way, uncertainty in the load and price forecasts are avoided. However, in this approach the comfort of the EV user is not taken into consideration.

In this paper, we consider several decentralized EV charging strategies based on Model Predictive Control (MPC) [9]–[11]. Minimizing the electricity costs of EV charging fits directly into an Economic MPC framework where the battery model is formulated as a linear discrete time dynamic state space model. Forecasts of the load, i.e. the driving pattern, and handling of the battery storage constraints are handled natively by the MPC. Electricity prices are assumed to be known and could be any price signal that is set by an aggregator. It could

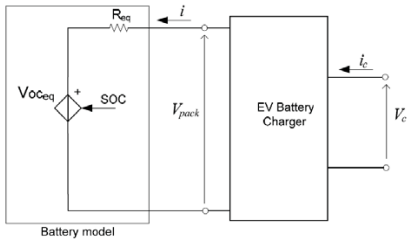

Fig. 2. Equivalent electrical circuit model of an EV battery.

also be a price that is the deviation from the day-ahead price making sure that the load follows the plan. The MPC algorithm incorporates feedback by its moving horizon implementation. In this way, forecast errors are compensated for by the MPC algorithm.

This paper is organized as follows. Section II models an electric vehicle battery. The battery side behavior is described as well. In section III, the EV driving pattern used for simulation is defined based on real data. The Economic MPC optimization problem is formulated in IV, while different Economic MPC charge strategies are compared in Section V. Finally, section VI provides conclusions.

II. Electric Vehicle Battery Model

In this study, an EV is modeled as a flexible energy storage resource that is capable of exchanging power with the grid under a predefined charging schedule. EVs have been modeled in many different manners, depending on the detail and scope of the study in question. In this paper a model of the State of Charge (SOC) is used based on [12].

A. Battery model

A simple battery model can be composed of an electric equivalent circuit with a voltage source in series with the ohmic impedance [13], see also Fig.2. The only state variable of this model is the State of Charge (SOC) $\zeta \in [0;1]$, i.e. the normalized battery capacity at time t, that can be modeled as a simple integrator with loss

$$\dot{\zeta}(t) = \frac{V_{pack} i(t)}{Q_n} = \frac{1}{Q_n}(\eta^+ P_c^+(t) - \eta^- P_c^-(t)) \qquad (1)$$

P_c is the power flowing in or out of the battery during charging or discharging; Q_n is the nominal capacity of the battery, denoted with a $+$ and $-$ respectively; η is the charger efficiency. The actual power is bounded by

$$P_{min} \leq P_c \leq P_{max} \qquad (2)$$

The maximum power is limited by the maximum charge current. Leaving a margin for other household appliances the maximum charge power P_{max} is set to

$$P_{max} = V_c i_{max} = 230 \text{ V} \cdot 10 \text{ A} = 2.3 \text{ kW} \qquad (3)$$

TABLE I
DESCRIPTION OF VARIABLES AND MODEL PARAMETERS

	Description	Value	Unit
ζ	State of Charge (SOC)	[0;1]	
V_c	Grid voltage	230	V
i_c	Charge current		A
P_c	Charge power ($P_c = V_c i_c$)		W
i_{max}	Maximum charge current	10	A
i_{min}	Minimum charge current	0	A
Δi_{min}	Minimum ramp constraint	-10	A/h
Δi_{max}	Maximum ramp constraint	10	A/h
Q_n	Nominal battery capacity	40	Ah
η	Charger efficiency	0.9	
η_{EV}	EV energy efficiency	150	Wh/km
p	Electricity price		EUR/MWh
ρ	Slack variable penalty	10^5	
T_s	Model sampling period	0.5	h
N	No. of steps in prediction horizon		

The charging power of 2.3 kW (230 V, 10 A) is chosen as the charging rate for this study, as this is the most common residential use case for EV charging in Denmark today. Considering standard household electric installations, most grid connection points only allow charging rates up to 10 A, while other appliances are running. Furthermore a small EV fleet consisting of 12% households in a generic LV grid charging at 6 pm with 2.4 kW can lead to overload of the distribution transformer [14]. The lower bound, P_{min}, could be negative and equal to $-P_{max}$ if Vehicle to Grid (V2G) is considered. Otherwise $P_{min} = 0$.

For the case study in this paper the battery chemistry is assumed to be Lithium-ion with capacity $Q_n = 24$ kWh. The SOC of the EV battery is equal to its normed capacity such that $\zeta \in [0; 1]$. The model (1) is suitable for a generic battery modeling study. In the context of EV charging management, the model has been tuned to common EV use conditions. The choice of Lithium-ion is related to market trend reports for EV batteries [15], where Li-ion batteries are expected to dominate the whole EV battery market sector with a 70-80% share by 2015.

Based on the main life time recommendations for optimal SOC management in [16] and common practice of EV manufacturer's [17] the SOC of the EV battery is limited to

$$\zeta \in [0.2; 0.9] \tag{4}$$

Other external conditions such as temperature behavior during operation are not taken into account.

B. Modeling the Charging/Discharging operation

The linear model in section II-A will be used for both simulation purposes and as the controller model. The nonlinear behavior outside the region (4) can be modeled by the open circuit voltage as

$$V_{oc_{eq}}(\zeta, Q) = V_0 - \frac{K}{1-\zeta} + a \cdot \exp\left(-\frac{Q}{\tau}\right) \tag{5}$$

- a is the exponential zone amplitude [V]
- τ is the exponential zone time constant [Ah]
- V_0 is the battery voltage constant [V]
- K is the polarization voltage [V]
- Q is the instant battery capacity [Ah] obtained from $\dot{Q} = i$, where i is the DC current during charging

The real-time EV battery voltage is $V_{pack} = V_{oc} + R_{eq} \cdot i$, where i is the current used to charge or discharge the battery. The voltage drop is considered positive during charging and negative during discharging. The resistive impedance of a lithium-iron phosphate (LFP) battery cell, a common class of Li-ion batteries, has been measured using impedance spectroscopy. A resulting intrinsic resistance of about 10 mΩ per battery cell was found from measurements [18]. The charger has been modeled as a single-phase 230V power converter. The charger operates in either Constant Current (CC) or Constant Voltage (CV) mode. During charging/discharging, the battery cell voltage is continuously monitored and maintained within a safe operational zone for the battery according to [19]. The safe voltage region of the LFP 3.3 V - 40 Ah battery cell is $[2.8; 4.0]$ V, which entails the SOC window 20-90%. The EV battery is only in discharging mode when driving.

C. State Space Model

The EV battery model in section II-A can be formulated as a discrete time state space model that fits into the MPC framework.

$$x_{k+1} = Ax_k + Bu_k + Ed_k \tag{6a}$$

$$z_k = Cx_k \tag{6b}$$

where $k \in \{0, 1, ..., N\}$. Defining the manipulable u, disturbance d and output z. The EV charge control signal is equal to the charging power $u = P_c^+$ while the only state is the SOC, also equal to the output $x = z = \zeta$. The demand d_k, i.e. battery usage from driving, is modeled as a disturbance to the battery SOC according to the description in section III. The state space matrices for the SISO model (6) are

$$A = 1 \qquad B = \frac{\eta}{Q_n} T_s \qquad C = 1 \qquad E = -T_s \tag{7}$$

This result follows from discretization of the state space matrices obtained from (1). Note that the efficiency and capacity is not in E but will be included in the signal d_k. u is kept constant between samples.

III. DRIVING PATTERNS

In order to estimate the driving pattern of the average EV driver, survey data from [20] including a group of observed commuters in Denmark was investigated. In Fig. 3 the total number of parked cars with 5 minute resolution for different weekdays, i.e. cars that could potentially charge if connected to the grid, have been plotted. The amount of trips is also shown as a function of time. The morning and afternoon peaks at 7:30 am and 4:00 pm are both clearly visible. Based on the presented data, an EV commuter driving pattern scenario was defined for simulation purposes such that

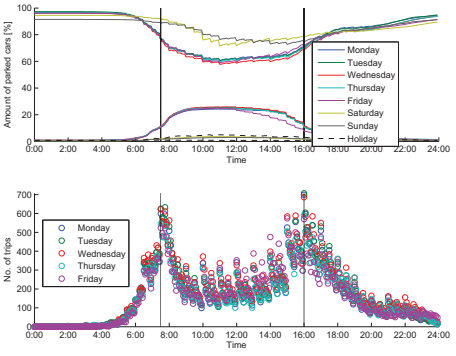

Fig. 3. The lower plot shows the no. of trips for difference weekdays. The upper plot shows the availability, i.e. the amount of parked cars at home (upper) and at work (lower).

- The average driving distance to work is $d_w = 18.92$ km
- The average driving time to work is $t_w = 22.6$ min
- Two trips of length $d_w + 5$ km and $d_w + 10$ km, and duration $t_w + 10$ min and $t_w + 20$ min
- The start time of the two daily trips is at 7:00 am and 4:00 pm

We assume that the EV is connected and able to charge whenever it is not driving. Furthermore, the estimated energy efficiency for typical EVs are $\eta_{EV} \in [120; 180]$ Wh/km [20]. As a compromise we use a fixed average value of $\eta_{EV} = 150$ Wh/km in simulations.

In the simulations in section V, the actual demand d_k when driving is constant for each trip and is equal to the average energy used for every trip. The actual demand depends on the driving behavior, i.e. the acceleration of the EV. When integrated the simulated demand will give exactly the amount of energy used at the end of the trip.

The minimum charge time is dependent on the sampling period and, since the price signal is available every hour, this should be the largest sampling period. In this way a decision whether to charge or not can be placed at all available price levels. This paper is a feasibility study intended to demonstrate Economic MPC. Therefore all simulations use $T_s = 30$ min. In practice, we would recommend significantly shorter sample times.

IV. Economic Model Predictive Control

In this paper Economic MPC will be applied for EV charge scheduling. Economic MPC for intelligent energy systems has previously been proposed in [21], [22]. MPC will minimize the electricity costs of charging a single EV based on predictions of the electricity price and the expected driving pattern over the prediction horizon of N samples. The objective function to be minimized is ϕ and the linear MPC can be formulated as

$$\begin{aligned}
\text{minimize} \quad & \phi = \sum_{k=0}^{N-1} p_k u_k + \rho w_k && && \text{(8a)}\\
\text{subject to} \quad & x_{k+1} = Ax_k + Bu_k + Ed_k && k \in \mathcal{N} && \text{(8b)}\\
& z_k = Cx_k && k \in \mathcal{N} && \text{(8c)}\\
& u_{\min} \le u_k \le u_{\max,k} && k \in \mathcal{N} && \text{(8d)}\\
& \Delta u_{\min} \le \Delta u_k \le \Delta u_{\max} && k \in \mathcal{N} && \text{(8e)}\\
& z_k \ge z_{\min,k} - w_k && k \in \mathcal{N} && \text{(8f)}\\
& z_k \le z_{\max} + w_k && k \in \mathcal{N} && \text{(8g)}\\
& w_k \ge 0 && k \in \mathcal{N} && \text{(8h)}
\end{aligned}$$

where $\mathcal{N} \in \{0, 1, \ldots, N\}$ and N is the prediction horizon. The output $z = \zeta$ is constrained by the battery capacity limits, but the constraints in this problem are softened, i.e. the SOC is allowed to lie outside the band of operation defined by (4). This constraint violation is defined by the slack variable w_k that is heavily penalized by the slack variable penalty ρ. Also note that the lower bound on the output, $z_{min,k}$, is time varying and represents a safety margin to absorb prediction errors. It can thus be set according to what degree of flexibility is needed for the individual EV user. When operation decreases so does flexibility, and the possibility of shifting consumption and saving money is reduced. However, in this paper we use $z_{min,k} \ge 0.2$ (see section II-A). p is the electricity price and u is the input equal to the charge power P_c. The EV is not able to charge when disconnected from the grid, i.e. when driving, resulting in a time varying input constraint

$$u_{max,k} = \begin{cases} P_{max} & \text{for } d_k = 0 \\ 0 & \text{otherwise} \end{cases}$$

Likewise, $u_{min,k}$, could be time varying and negative if V2G is considered. $\Delta u_k = u_k - u_{k-1}$ is the discrete time rate of movement input constraint. The input charge current can change very quickly compared to the time horizons considered, so these rate limits can be set very high, e.g. $\Delta u_{min} \ge u_{min}$ and $\Delta u_{max} \ge u_{max}$, and can in theory be neglected. However, when a stochastic model is used they help to smoothen out the charging and adds robustness against forecast errors.

The optimal EV charging plan within the prediction horizon is the solution to (8) and is denoted $U^* = \{u_k^*\}_{k=0}^{N-1}$. This charging plan is calculated at every time step k and represents a decision plan, stating when to charge and how much power should be used. It is optimal in terms of economy, and is the cheapest solution based on the predictions and model assumptions available at time $k = 0$. The first decision of the plan, u_0^*, is implemented, i.e. a certain amount of power is delivered to the battery at the present time step $k = 0$. This process is repeated at every time step and constitutes the principle of a model predictive controller also known as receding horizon control.

V. Simulation

Fig. 4 and 5 show the closed loop MPC charge plan simulated over one week. Based on the perfect forecasts of

the electricity el-spot price and the demand, i.e. the driving pattern, the controller charges just the right amount of energy prior to each trip. The first simulation uses a prediction horizon of $N = 24$ h, while the latter uses $N = 48$ h. The advantage of using a 48 h horizon is clearly seen; this controller is able to pick the cheapest charging period seen over a larger time window. For example, if energy is expensive on Friday morning, it is cheaper to fill up the battery on Thursday morning in order to cover the next two days' consumption. Knowing more about prices and demand in advance, allows for a better charging plan and ultimately more money can be saved. However, forecasts will always contain uncertainty, so a balance must be found between long prediction horizons, i.e. more computation time, and how much money can be saved. Even if a perfect forecast is used, the increase in savings is very small when the prediction horizon is increased. This is due to the nature of the day ahead price and the limited capacity of the battery, i.e. charging all energy needs during the summer to cover the whole winter period is not possible. The battery capacity thus limits the amount of energy that can be shifted using a large number of EVs.

The Economic MPC strategy can be compared to other strategies like uncontrolled charging, also referred to as *dumb charging*, where the EV starts charging whenever it is plugged in. This can easily be simulated with the MPC controller by setting the soft lower output bound to $\{z_{\min}\}_{k=0}^{N} = \{z_{\max}\}_{k=0}^{N}$. It is observed from Fig. 6 that the EV charges to full capacity after every trip and unfortunately charging takes place in the most expensive periods.

Another optimal charge strategy could be a fixed cost strategy where the electricity price remains the same throughout the entire interval. The response using this strategy is seen on Fig. 7. Obviously the controller does ensure charging takes place in the cheap periods, since it is cheap during the entire interval. It does, however, minimize the energy consumption and charges just enough energy for each trip just before the EV leaves. A third strategy could be to take advantage of the deterministic part of electricity price and use a simple timer to delay the dumb charging to periods where the electricity price is usually low. However, a charging scenario that is reactive to a price signal is desired in the decentralized approach.

Comparing the simulation results, it is found that using MPC with fixed costs saves around 39% of the costs compared to dumb charging. If Economic MPC with the varying prices is considered, savings increase to almost 60%. Using the longer prediction horizon another 0.5% is gained. The computation time for solving the individual open loop problems are within micro seconds.

The proposed Economic MPC was also simulated for a period of one year with the real day ahead price from 2010, and the results were compared to dumb charging. For the dumb charging simulation the total energy consumption was found to be 2.6 MWh. The annual energy consumption obtained from simulation is very close to the estimates for an average household in Denmark [23]. The Economic MPC saves an annual 47% of the electricity costs associated with the Elspot price.

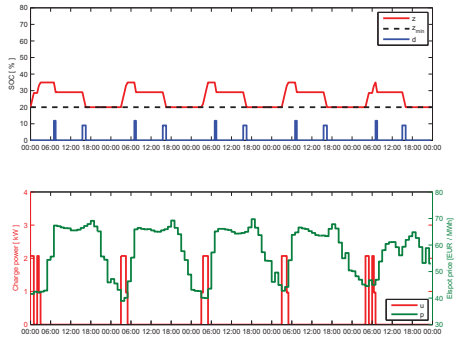

Fig. 4. Optimal charging of EV for five days using Economic MPC with prediction horizon $N = 24$ h. The upper plot shows the SOC ζ and the driving pattern or demand d_k. The lower plot shows the electricity price variation and the charge power.

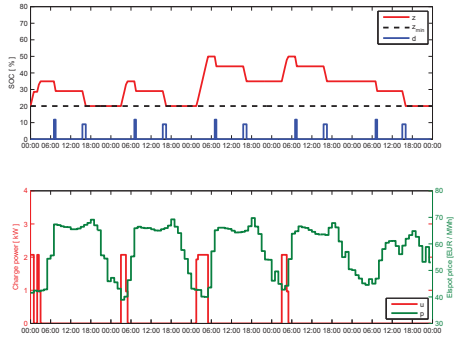

Fig. 5. Economic MPC charging with $N = 48$ h.

VI. Conclusion

Economic MPC was introduced as a method for charging EVs in Smart Grid using varying prices. A suitable EV battery model was derived to be used in the optimization of EV charge scheduling in a Smart Grid. Realistic commuter driving patterns were analyzed from real data and used in simulations along with electricity prices taken from the day-ahead market. A comparison of different charging strategies were compared clearly showing the potential of using Economic MPC to shift the load in a cost efficient way. Perfect forecasts were used in the simulations. Future work will address the inherent stochastics of the driving pattern and electricity prices.

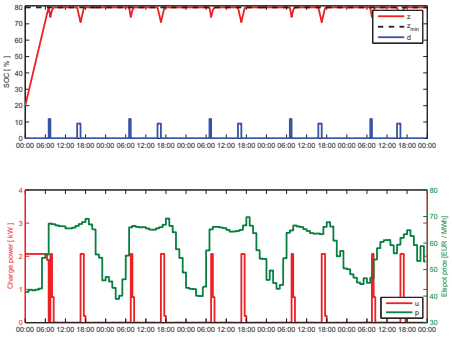

Fig. 6. Uncontrolled *dumb* charging. $\{z_{\min}\}_{k=0}^{N} = \{z_{\max}\}_{k=0}^{N}$

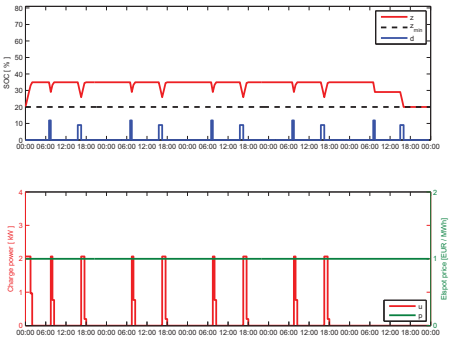

Fig. 7. MPC fixed unity price charging with $N = 24$ h.

REFERENCES

[1] W. Kempton and S. E. Letendre, "Electric vehicles as a new power source for electric utilities," *Transportation Research Part D: Transport and Environment*, vol. 2, no. 3, pp. 157–175, 1997.

[2] D. K. C., J. Østergaard, E. Larsen, C. Kern, T. Wittmann, and M. Weinhold, "Integration of electric drive vehicles in the Danish electricity network with high wind power penetration," *European Transactions on Electrical Power*, vol. 20, no. 7, pp. 872–883, 2010. [Online]. Available: http://dx.doi.org/10.1002/etep.371

[3] Z. Ma, D. Callaway, and I. Hiskens, "Decentralized charging control for large populations of plug-in electric vehicles: Application of the Nash certainty equivalence principle," in *2010 IEEE International Conference on Control Applications (CCA)*, sept. 2010, pp. 191–195.

[4] M. Doostizadeh, M. Khanabadi, A. Esmaeilian, and M. Mohseninezhad, "Optimal energy management of a retailer with smart metering and Plug-in Hybrid Electric Vehicle," in *Environment and Electrical Engineering (EEEIC), 2011 10th International Conference on*, may 2011, pp. 1–5.

[5] S. Bashash, S. Moura, and H. Fathy, "Charge trajectory optimization of plug-in hybrid electric vehicles for energy cost reduction and battery health enhancement," in *American Control Conference (ACC), 2010*, 30 2010-july 2 2010, pp. 5824–5831.

[6] O. Sundström and C. Binding, "Planning electric-drive vehicle charging under constrained grid conditions," in *2010 International Conference on Power System Technology (POWERCON)*, oct. 2010, pp. 1–6.

[7] ——, "Charging Service Elements for an Electric Vehicle Charging Service Provider," in *Proc. IEEE Power & Energy Society General Meeting, Detroit*, 2011.

[8] Q. Li, T. Cui, R. Negi, F. Franchetti, and M. D. Illic, "On-line Decentralized Charging of Plug-In Electric Vehicles in Power Systems," *[submitted]*, 2011.

[9] M. Diehl, R. Amrit, and J. B. Rawlings, "A Lyapunov Function for Economic Optimizing Model Predictive Control," *IEEE Transactions on Automatic Control*, vol. 56, no. 3, pp. 703–707, march 2011.

[10] J. B. Rawlings, D. Bonne, J. B. Jørgensen, A. Venkat, and S. B. Jørgensen, "Unreachable Setpoints in Model Predictive Control," *IEEE Transactions on Automatic Control*, vol. 53, no. 9, pp. 2209–2215, oct. 2008.

[11] K. Edlund, J. D. Bendtsen, and J. B. Jørgensen, "Hierarchical model-based predictive control of a power plant portfolio," *Control Engineering Practice*, vol. 19, no. 10, pp. 1126–1136, 2011. [Online]. Available: http://www.sciencedirect.com/science/article/pii/S0967066111001171

[12] O. Tremblay, L. Dessaint, and A. Dekkiche, "A Generic Battery Model for the Dynamic Simulation of Hybrid Electric Vehicles," in *Vehicle Power and Propulsion Conference, 2007. VPPC 2007. IEEE*, sept. 2007, pp. 284 –289.

[13] D. Haifeng, W. Xuezhe, and S. Zechang, "A new SOH prediction concept for the power lithium-ion battery used on HEVs," in *Vehicle Power and Propulsion Conference, 2009. VPPC '09. IEEE*, sept. 2009, pp. 1649 –1653.

[14] N. Butcher, S. Felsenstein, S. Stoeter, and C. Flon, "Dawn of a new age," ABB, Tech. Rep., 2010.

[15] Frost&Sullivan, "M5B6-Global Electric Vehicles Lithium-ion Battery Second Life and Recycling Market AnalysisM5B6-Global Electric Vehicles Lithium-ion Battery Second Life and Recycling Market Analysis," Tech. Rep., 2010.

[16] F. Marra, C. Traholt, E. Larsen, and Q. Wu, "Average behavior of battery-electric vehicles for distributed energy studies," in *Innovative Smart Grid Technologies Conference Europe (ISGT Europe), 2010 IEEE PES*, oct. 2010, pp. 1–7.

[17] "Nissan Leaf Features and Specs, www.nissanusa.com," 2012.

[18] S. H. Jensen, A. Hauch, P. V. Hendriksen, M. Mogensen, N. Bonanos, and T. Jacobsen, "A Method to Separate Process Conributions in impedance Spectra by Variation of Test Conditions," *Journal of the Electrochemical Society*, vol. 154, pp. 1325–1330, 2007.

[19] ThunderSky, "LFP Battery User Manual," Tech. Rep.

[20] Q. Wu, A. H. Nielsen, J. Østergaard, S. T. Cha, F. Marra, Y. Chen, and C. Træholt, "Driving Pattern Analysis for Electric Vehicle (EV) Grid Integration Study," in *Innovative Smart Grid Technologies Conference Europe (ISGT Europe), 2010 IEEE PES*, oct. 2010, pp. 1–6.

[21] R. Halvgaard, N. K. Poulsen, H. Madsen, and J. B. Jørgensen, "Economic Model Predictive Control for Building Climate Control in a Smart Grid," in *IEEE PES Innovative Smart Grid Technologies Conference [Accepted]*, 2012.

[22] T. G. Hovgaard, K. Edlund, and J. B. Jørgensen, "The Potential of Economic MPC for Power Management," in *Proc. of 49th IEEE Conference on Decision and Control, 2010*, 2010, pp. 7533–7538.

[23] C. Hay, M. Togeby, N. C. Bang, C. Søndergren, and L. H. Hansen, "Introducing Electric Vehicles Into The Current Electricity Markets," Electric Vehicles in a Distributed and Integrated Market Using Sustainable Energy and Open Networks (EDISON), Tech. Rep., May 25 2010.

Paper C

Model Predictive Control for a Smart Solar Tank based on Weather and Consumption Forecasts

---

Published in *Energy Procedia, vol. 30, pp. 270-278, 2012.*

Available online at www.sciencedirect.com

SciVerse ScienceDirect

Energy Procedia 30 (2012) 270 – 278

Energy Procedia

SHC 2012

Model predictive control for a smart solar tank based on weather and consumption forecasts

Rasmus Halvgaard[a*], Peder Bacher[a], Bengt Perers[b], Elsa Andersen[b], Simon Furbo[b], John B. Jørgensen[a], Niels K. Poulsen[a], Henrik Madsen[a]

[a]*Technical University of Denmark, Department of Informatics, Richard Petersens Plads, Kgs. Lyngby 2800, Denmark*
[b]*Technical University of Denmark, Department of Civil Engineering, Brovej, Kgs. Lyngby 2800, Denmark*

Abstract

In this work the heat dynamics of a storage tank were modelled on the basis of data and maximum likelihood methods. The resulting grey-box model was used for Economic Model Predictive Control (MPC) of the energy in the tank. The control objective was to balance the energy from a solar collector and the heat consumption in a residential house. The storage tank provides heat in periods where there is low solar radiation and stores heat when there is surplus solar heat. The forecasts of consumption patterns were based on data obtained from meters in a group of single-family houses in Denmark. The tank can also be heated by electric heating elements if necessary, but the electricity costs of operating these heating elements should be minimized. Consequently, the heating elements should be used in periods with cheap electricity. It is proposed to integrate a price-sensitive control to enable the storage tank to serve a smart energy system in which flexible consumers are expected to help balance fluctuating renewable energy sources like wind and solar. Through simulations, the impact of applying Economic MPC shows annual electricity cost savings up to 25-30%.

Keywords: Model predictive control; solar heating; smart solar tank; smart energy systems

1. Introduction

Economic Model Predictive Control (MPC) has previously been used to reduce the electricity costs of heating and cooling in buildings [1,2,3]. For a smart solar tank [4] the same MPC framework can be

* Rasmus Halvgaard. Tel.: +45 45255281; fax: +45 45882673.
E-mail address: rhal@imm.dtu.dk

1876-6102 © 2012 The Authors. Published by Elsevier Ltd.
Selection and peer-review under responsibility of the PSE AG
doi:10.1016/j.egypro.2012.11.032

applied in order to save energy and reduce electricity costs. For the system considered in this paper, the electricity consumption of the auxiliary heating elements in a storage tank must be controlled. The heating elements can be turned on in periods when the amount of solar energy alone cannot meet the heat demand, e.g. hot water and space heating in a residential house.

The MPC exploits knowledge about the future inputs, so to minimize electricity costs a good tank model is required, along with excellent forecasts of both solar radiation and consumption patterns. In this paper we estimate the parameters in a storage tank model from measured data with a maximum likelihood method. With this model we design an Economic MPC to control the power consumption of the heating elements according to a price. By adding a price signal to the objective of the controller, the MPC will minimize the electricity costs for the individual tank by shifting power consumption to periods with cheap electricity. As the electricity costs are reduced the trade-off of considering prices and not power consumption alone is to use more power, but at the right time.

The performance of the MPC in terms of power consumption and electricity costs is investigated for different consumption patterns in a one-year simulation period. The influence of uncertainty in the forecasts of both solar radiation and consumption is also examined. We assume that electricity prices are known each hour at least 12 hours ahead, which is true for the day-ahead Elspot market in Denmark [5]. These prices reflect the power demand of the overall energy system and also indicate the amount of cheap renewable energy sources available, such as wind power.

2. Solar thermal collector and storage tank

The smart solar tank consists of a solar collector with area of 9 m^2, and a storage tank with a total volume of 788 l. The tank itself contains an inner tank for domestic hot water and a pressureless outer tank for space heating. The tank can be heated by the solar collectors. To help cover the remaining heat demand, three smaller electric heating elements of 3 kW each are installed in the tank, as shown in Figure 1b.

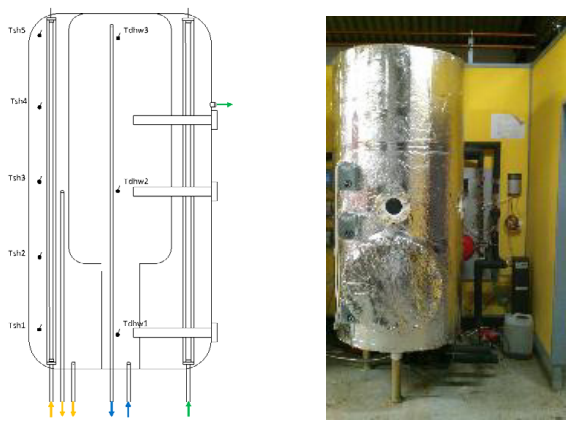

Fig. 1. (a) Sketch of the tank with inlets, outlets and eight temperature measurement points. (b) Photo of storage tank in lab

Solar energy is transferred to the tank by feeding water into the tank through a stratification device. In this way, beneficial thermal stratification is built up during solar collector operation [4,6]. Space heating is transferred from the upper part of the tank and the return inlet to the tank goes through another stratification device.

2.1. Tank model

We model the storage tank separated from the solar collector such that the energy balance is

$$Q_{\text{tank}} = Q_{heater} + Q_{solar} - Q_{consumption} - Q_{loss} \quad (1)$$

The contribution from the solar collector Q_{solar} and heat consumption $Q_{consumption}$ are forecasted inputs. The heating element input power consumption Q_{heater} is controllable. The loss is modelled as proportional to the temperature difference between the internal tank temperature and the ambient room temperature. The actual energy in the tank Q_{tank} cannot be physically measured, but is assumed to be dependent on the measured tank temperatures. Eight temperature measurements from different layers of the tank are combined to represent an overall tank temperature (T_t) proportional to the stored energy. Using an average from the eight sensors (n = 8) we get the tank temperature

$$T_t = \frac{1}{n}\sum_{j=1}^{n} T_j \quad (2)$$

Based on (1), the heat dynamics of the tank can be described as a simple first order differential equation

$$C_t \cdot \dot{T}_t = Q_h + \hat{Q}_s - \hat{Q}_c - UA \cdot (T_t - \hat{T}_i) \quad (3)$$

Q_h is the controllable power consumption for the electric heating elements with efficiency η. C_t is the specific heat capacity of the tank, while the energy contribution from the solar collector Q_s and the house consumption Q_c are both forecasted inputs. We use the forecasts computed from measurements in domestic households in southern Denmark based on [7,8]. The ambient temperature T_i should also be forecast, but is assumed to be a constant 20°C in further simulations.

The model data to be used for model estimation was based on a storage tank that uses stratification pipes for optimal injection of the return water. Therefore a layered model with more than one temperature state should possibly be considered. However, for the given data set and a time scale of minutes, a first order model with only one layer was found sufficient for describing the heat dynamics of the tank.

The solar thermal power is simulated from measured climate data recorded at the local district heating plant in Sønderborg. A standard flat-plate collector is used as the simulation model, as described in [9]. The solar thermal power is forecast with the method described in [7], where a conditional parametric model is applied for forecasting the hourly solar thermal power up to 36 hours ahead. The forecasting model takes numerical weather predictions of global radiation as input. Based on past data, the collector thermal performance is modelled and takes local effects into account, such as the orientation of the collector and shading from objects in the surroundings.

2.2. Model parameter estimation

CTSM was used to estimate the unknown parameters of a continuous discrete stochastic state space model. The model consists of a set of stochastic differential equations describing the dynamics of a

system in continuous time and a set of algebraic equations describing how measurements are obtained at discrete time instants.

$$\begin{aligned} \mathrm{d}x &= (A(\theta)x + B(\theta)u + E(\theta)d)\mathrm{d}t + \sigma \mathrm{d}w \\ \mathrm{y} &= C(\theta)x + e \end{aligned} \tag{4}$$

The model includes a diffusion term to account for random effects, but otherwise it is structurally similar to ordinary differential equations. Therefore conventional modelling principles can be applied to set up the model structure. Given the model structure, any unknown model parameters can be estimated from data, including the parameters of the diffusion term. The parameter estimation method is a *maximum likelihood* (ML) method and a *maximum a posteriori* (MAP) method [10,11,12,13].

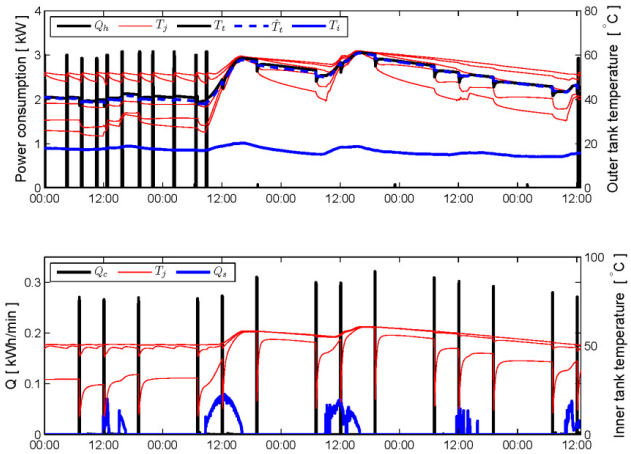

Fig. 2. Data measurements from real storage tank used for parameter estimation. The estimated tank temperature has been also been plotted

The model parameters $\theta = [C_t \quad UA \quad \eta]$ were estimated in the continuous time stochastic state space model (4) with $x = y = T_t$ and $d = [Q_s \quad Q_c \quad T_i]$ that contains the forecast disturbances from (3). It is assumed that the measurement error is normal-distributed. with a variance of 1°C such that $e \in N(0,1)$. The process noise was assumed to have standard deviation $\sigma = 0.001$.

The parameter estimation was based on the data shown in Fig. 2. The estimated parameters of (3) were found to be:

$$UA = 8.29\ (\pm\ 0.0278)\ \mathrm{W/K} \qquad C_t = 3881.3\ (\pm\ 0.00167)\ \mathrm{kJ/K} \tag{5}$$

It should be noted that the heating element efficiency was fixed at $\eta = 1$ and the tank temperature representing the stored energy was assumed to be an average of all eight temperature measurements. The fit of the resulting estimated tank temperature $\hat{T}_t$ is also compared to the average tank temperature T_t in

Fig. 2, and reveals a nice match. Note that the consumption pattern Q_c in this data set is deterministic and the same amount of energy is deliberately drawn from the tank at 7 am, 12 pm, and 7 pm.

3. Economic MPC

Traditionally the heating elements in a storage tank are controlled by a thermostat that is either on or off and keeps the temperature close to a temperature set point in a hysteresis loop. Instead of specifying a temperature set point for the tank, a set of constraints on the tank temperature and on power consumption is specified. For the MPC strategy, as long as the temperature is within some bounds, there is no need to force it to a certain temperature. In this way knowledge about the future weather and heat consumption can help to minimize the power consumption of the heating elements. Adding a price signal to the objective will then not only try to minimize the power consumption, but also the electricity costs. So the finite static MPC optimization problem to be solved at every sampling time t is

$$\begin{aligned} \text{minimize} \quad & \sum_{k=t}^{t+N-1} p_k u_k \\ \text{s.t.} \quad & x_{k+1} = Ax_k + Bu_k + Ed_k \\ & y_k = Cx_k \\ & 0\text{kW} \le u_k \le 9\,\text{kW} \\ & 50°\text{C} \le y_k \le 95°\text{C} \end{aligned} \tag{6}$$

At each sampling time, t, we minimize the electricity costs over the prediction horizon N, given the forecasts available at time t. The first control action u_0 of the solution is implemented on the process and the procedure is repeated at the next sampling instant. This is usually referred to as receding horizon control. The model (3) is discretized into a discrete time state space model defined by the matrices (A,B,E,C) with the estimated parameters (5). The constraints on temperature and power consumption must also be satisfied.

4. Simulation

Fig. 3 shows a simulation of the resulting MPC with the estimated tank model. The scenario is based on real measured solar radiation and consumption patterns from residential houses in southern Denmark during a whole year from May 17 2010. The simulation is a closed loop simulation with a 24-hour prediction horizon based on forecasts subject to uncertainty and actual electricity prices from the Nordic Elspot market [5].

In Fig. 4, one week in March 2011 of the simulation from Fig. 3 has been extracted. During the first few days the heating elements mostly use power during night-time when the prices are low. In the remaining period a lot of solar radiation heats up the tank and the heating elements are practically not used. The temperature stays within the predefined interval that defines the storage capability.

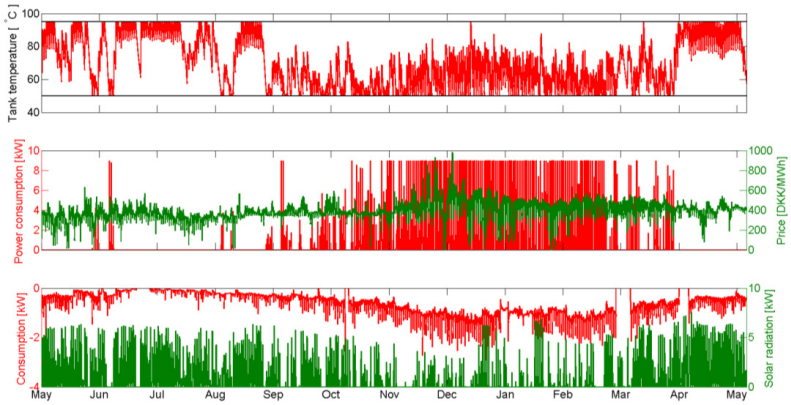

Fig. 3. A one-year simulation starting May 17 2010 with 24 h prediction horizon using uncertain forecasts. The upper plot shows the tank temperature, the middle plot contains the electricity price and the optimal power consumption for the heating element, and the lower plot contains the solar heat input and the house consumption demand. The heating element is turned on when the electricity price is low.

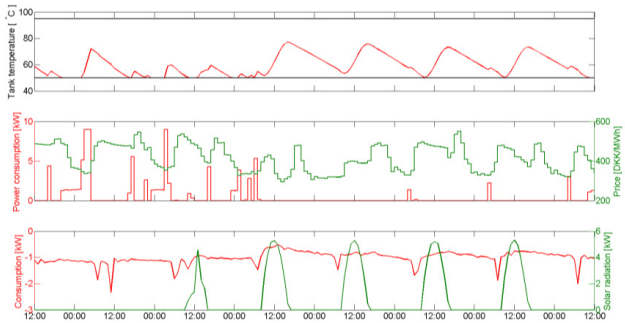

Fig. 4. Shows the same as Fig. 3. but contains only one week in March 2011 to make it easier to read the details.

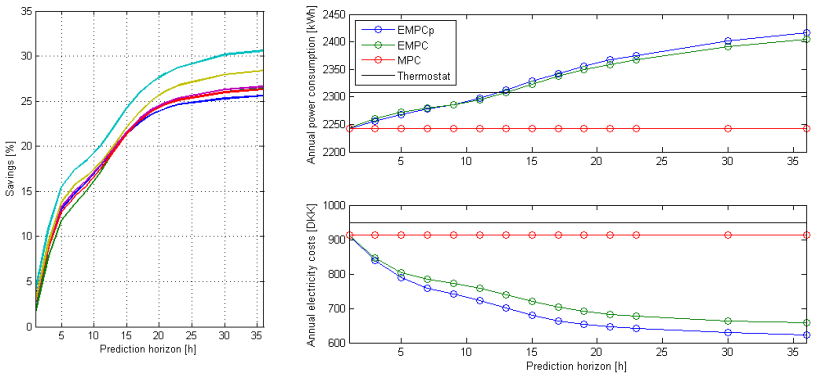

Fig. 5. (a) Annual savings in percent compared to conventional thermostat control for the six different houses. (b) Annual power consumption (upper) and electricity costs (lower) for house #2 as a function of the prediction horizon N for four different control strategies. Closed loop Economic MPC with perfect forecasts (EMPCp), with real forecasts subject to uncertainty (EMPC), a constant electricity price of 1 (MPC) and a Thermostat control keeping the temperature at 60°C.

5. Results and discussion

For a whole year the annual power consumption and electricity costs were found from closed loop MPC simulations for four different control strategies. The results can be found in Fig. 5a, while a simulation for one of the houses is shown in Fig. 5b. For a prediction horizon N larger than 24 hours, the cost savings do not increase by much as the prediction horizon increases further. This is mainly due to the maximum input power and the storage capacity of the system. Information about the solar radiation or the consumption next week will not change the optimal power consumption due to these system constraints. Furthermore, using perfect forecasts, i.e. knowing the future inputs exactly, does not increase the savings significantly. The annual savings of considering the price with an Economic MPC are 25-30% for the given simulation scenarios for six different houses.

Note that the power consumption for the Economic MPC grows larger than for the ordinary thermostat control as the prediction horizon increases. However the costs go down. Consequently, to save more money, more electricity must be used for control. However, the increased power consumption can be justified when the electricity price reflects the amount of renewable energy in the power system.

Another result of the investigations is that in the MPC strategy in which only power consumption is minimized and where prices are not considered, the annual power consumption is constant regardless of the prediction horizon. Since the sampling period is so high (1 h) compared to the dynamics (< 5 min), the amount of power (9 kW) that can be delivered instantaneously in every one-hour sampling period is higher than the instantaneous demand at any time. So the control signal matches the consumption at every sampling time even for a one-hour prediction horizon. Also the control is only active at the lower temperature bound, because it is not possible to actively cool the tank.

Similar results were obtained for the five other houses, with the same conclusions.

Any missing data in the forecasts was ignored by setting it to zero. This means that some periods in the annual simulation have no solar input or no consumption at all. For the six different houses the total missing number of samples in the consumption data sets was around 510 (~21 days) for all houses except

house 1, where 1800 samples were missing (~78 days). For the solar data that were used for every house, 351 samples were missing (~14 days). An example of the missing data in the consumption forecast can easily be seen in Fig. 3.

Computation times for solving the individual open loop MPC problem are in the millisecond range. Simulating a whole year takes around 5-10 seconds for a prediction horizon of 24 hours running Matlab on an Intel i7 2.67 GHz laptop.

6. Conclusion

The heat dynamics of a smart solar storage tank were modelled and its parameters were found from maximum likelihood estimation procedures. An Economic MPC was designed to control the power consumption of the auxiliary heating elements in the storage tank. The MPC minimizes electricity costs given the price and forecasts of the solar radiation and consumption. Electricity cost savings of 25-30% compared to current thermostat control strategy were found for six different houses.

Acknowledgements

Acknowledgements are given to the The Danish Council for Strategic Research, which have provided the financial support for the project ”Solar/electric heating systems in the future energy system” (2104-07-0021) under which the work was carried out. The heat load and climate data was very kindly provided by Sønderborg Fjernvarme and the Danish Meteorological Institute is thanked for making their numerical weather predictions available.

References

[1] R. Halvgaard, N. K. Poulsen, H. Madsen and J. B. Jørgensen, “Economic Model Predictive Control for Building Climate Control in a Smart Grid”, *IEEE PES Innovative Smart Grid Technologies,* 2012.

[2] F. Oldewurtel, A. Ulbig, A. Parisio, G. Andersson and M. Morari “*Reducing Peak Electricity Demand in Building Climate Control using Real-Time Pricing and Model Predictive Control”, IEEE Conference on Decision and Control*, 2010

[3] T.G. Hovgaard, L. F.S. Larsen, K. Edlund, J. B. Jørgensen, “*Model predictive control technologies for efficient and flexible power consumption in refrigeration systems”,* Energy, 2012

[4] J. Fan, E. Andersen, S. Furbo and B. Perers, 2010, “Detailed Modelling of Charging Behaviour of Smart Solar Tanks”, *Proceedings of EuroSun 2010: International Conference on Solar Heating, Coolings and Buildings*.

[5] http://www.nordpoolspot.com/Market-data1/Elspot/Area-Prices/ALL1/Hourly/

[6] Elsa Andersen, Simon Furbo, Bengt Perers, Jianhua Fan, Ziqian Chen, “Experimental investigations of intelligent solar heating systems for single family houses”, SHC Conference, San Francisco, USA, July 2012

[7] P. Bacher, H. Madsen, and B. Perers, “Short-term solar collector power forecasting”, in proceedings of *ISES Solar World Conference*, 2011.

[8] P. Bacher, H. Madsen, H. Aalborg and B. Perers, “Short-term heat load forecasting for single family houses”, Submitted to Buildings and Energy, 2012.

[9] B. Perers, S. Furbo, E. Andersen, J. Fan, “Solar/electric heating systems using smart solar tanks and variable electricity costs”, *Eurosun Conference 2010 Graz Austria*, 2010.

[10] Continous Time Stochastic Modeling www2.imm.dtu.dk/~ctsm/

[11] Niels Rode Kristensen and Henrik Madsen and Sten Bay Jørgensen, ”Parameter estimation in stochastic grey-box models”, Automatica, volume 40, p.225-237, 2004.

[12] Niels Rode Kristensen and Henrik Madsen and Sten Bay Jørgensen, "A method for systematic improvement of stochastic grey-box models", Computers & Chemical Engineering, volume 28, p. 1431-1449, 2004.

[13] John B. Jørgensen and Sten B. Jørgensen, "MPC-Relevant Prediction-Error Identification", *Proceedings of the 2007 American Control Conference*, p.128-133, 2007.

Paper D

Thermal Storage Power Balancing with Model Predictive Control

Published in *Proceedings of 2013 European Control Conference (ECC), pp. 2567-2572, 2013.*

2013 European Control Conference (ECC)
July 17-19, 2013, Zürich, Switzerland.

Thermal Storage Power Balancing with Model Predictive Control

Rasmus Halvgaard, Niels K. Poulsen, Henrik Madsen and John B. Jørgensen

Abstract— **The method described in this paper balances power production and consumption with a large number of thermal loads. Linear controllers are used for the loads to track a temperature set point, while Model Predictive Control (MPC) and model estimation of the load behavior are used for coordination. The total power consumption of all loads is controlled indirectly through a real-time price. The MPC incorporates forecasts of the power production and disturbances that influence the loads, e.g. time-varying weather forecasts, in order to react ahead of time. A simulation scenario demonstrates that the method allows for the integration of flexible thermal loads in a smart energy system in which consumption follows the changing production.**

I. Introduction

Integration of large amounts of renewable energy sources in the power system, such as wind and solar energy, introduces large fluctuations in power production. This type of green energy must be either stored or consumed right away. Consuming all of it as it is produced requires a very flexible and controllable power consumption. Thermal loads, in particular, consume power and often have flexible operating temperatures and thermal storage capacity. Examples of controllable electric thermal loads are heat pumps in buildings [1], auxiliary heating in solar collector storage tanks [2], and commercial and domestic refrigeration systems [3]. In a smart energy system these loads can potentially offer flexibility if they are pooled together into a large-scale system with large power consumption. With the right control scheme this large-scale system of flexible thermal loads can help balance changing power production levels by adjusting the consumption of the loads accordingly [4]. However, an incentive to help balance the power and a method for coordinating must be established.

In this paper an indirect control strategy is proposed where a control signal, referred to as a control price, communicates the need for balancing. The control price is linearly linked to the temperature set points and therefore indirectly influences the total power consumption of a group of thermal loads. This group is often referred to as an *aggregation* of loads, and all loads are connected to an *aggregator* [5]. The aggregator broadcasts the current control price, which is translated by each load individually into a local temperature set point to be followed. Based on a model of the aggregated consumption response to the control price, closed-loop feedback is provided at the aggregator level by measuring the total power consumption. In this way the aggregator is able to balance instantaneous power or track an amount of power already bought from a market [6]. In this paper the aggregator controller is based on Model Predictive Control (MPC) [7]. The MPC uses an estimated low-order autoregressive (ARX) model for real-time power balancing. Moreover, an integrator model is added to eliminate model and forecast errors and to achieve offset-free tracking.

For control, the MPC needs a model of the aggregated thermal loads. This model should predict the effect of a price change and calculate a single control price, which is broadcast to all loads. The aggregator model is estimated from the price response and may be very small compared to a centralized model that includes detailed information about all loads.

Compared to a centralized direct control strategy, the decentralized indirect method described in this paper reduces the aggregator problem complexity considerably. The computation efforts are decreased dramatically and the need for two-way communication is eliminated. The relationship between control price and set point in this paper was inspired by [8]. A similar concept of balancing is found in [9], where simple hysteresis control is used. In [10] an indirect price strategy based on bilevel programming and a large centralized model is proposed to minimize power imbalances accounting for the load's response to the price signal. An example of a centralized direct control strategy can be found in [11]. Note that most centralized formulations can be solved more efficiently through decomposition of the optimization problem into smaller subproblems. However, two-way communication is still needed for coordination and as the number of loads increase a decentralized approach is needed. A completely decentralized approach, where optimization variables are exchanged between loads as dynamic prices, is considered in [12].

This paper is organized as follows. In Section II we formulate an aggregated model of a large-scale system of thermal loads. Section III describes the MPC that controls the aggregated loads. In Section IV the control method is demonstrated through simulation. The *control price* concept is discussed further in Section V, while Section VI provides conclusions.

II. Modeling

First we model the dynamics of the thermal loads and their closed loop behavior with Linear Quadratic (LQ) controllers. Then connection to the aggregator and the estimated aggregated model is described. For notational simplicity,

*This work was partly supported by the DSF iPower (Strategic Platform for Innovation and Research in Intelligent Power) project.

R. Halvgaard, N. K. Poulsen, H. Madsen, and J. B. Jørgensen are with Department of Applied Mathematics and Computer Science, Technical University of Denmark, Matematiktorvet, 2800 Kgs. Lyngby, Denmark {rhal,nkpo,hmad,jbjo}@dtu.dk

the discrete time step subscript k has been omitted in the following while the superscript $^+$ denotes $k+1$.

A. Thermal load

Each thermal load is modeled by the discrete-time state space model

$$x^+ = Ax + Bu + Ed + w \tag{1a}$$
$$y = Cx \tag{1b}$$

y is the output temperature, u is the power consumption, d and $w \in N(0, \sigma_w^2)$ are disturbances influencing the states x. The disturbance d could be an outdoor temperature acting on a building, or solar radiation, while w is the unmodeled process noise. For the method described in this paper we design LQ controllers to track a temperature set point r . When choosing linear controllers, the aggregated model is also linear and allows for a linear MPC at the aggregator level. The unconstrained LQ controller should be able to track the set point with no offset by rejecting any disturbances. Offset-free integral control is achieved by augmenting the state vector x with an integrating state $\tilde{x}$, such that $x_i = \begin{bmatrix} x^T & \tilde{x}^T \end{bmatrix}^T$. From now on the different loads are subscripted i to denote the L different loads. With integral control the ith load is then modeled by

$$x_i^+ = A_i x_i + B_i u_i + F_i r_i + E_i d_i + G_i w_i \tag{2a}$$
$$y_i = C_i x_i \tag{2b}$$

with

$$A_i = \begin{bmatrix} A & 0 \\ -C & I \end{bmatrix} \qquad B_i = \begin{bmatrix} B \\ 0 \end{bmatrix} \qquad C_i = \begin{bmatrix} C & 0 \end{bmatrix} \tag{3a}$$
$$F_i = \begin{bmatrix} 0 \\ I \end{bmatrix} \qquad E_i = \begin{bmatrix} E \\ 0 \end{bmatrix} \qquad G_i = \begin{bmatrix} I \\ 0 \end{bmatrix} \tag{3b}$$

The following linear control law is applied to track the temperature set point r_i

$$u_i = -K_i x_i \qquad K_i = \begin{bmatrix} K & -\tilde{K} \end{bmatrix} \tag{4}$$

A stationary control gain K_i has been designed for each load with the weights $Q_i \geq 0$ and $R_i \geq 0$ on the states x_i and control action u_i, respectively. All loads are assumed stable and controllable. The assumption of full-state feedback is justified by the use of SISO models later in the numerical example in Section IV. Alternatively, a Kalman filter could be applied to estimate any unmeasured states. The controller weights should be tuned separately for each load to trade off long settling times for temperature overshoot and power consumption.

As the aggregator objective is to manipulate power consumption indirectly through the set point, the relationship between u_i and r_i must be modeled. In our case a linear expression for power consumption is readily available from the control law (4). Inserting (4) in (2) gives us the closed-loop model

$$x_i^+ = (A_i - B_i K_i) x_i + F_i f_i(p) + E_i d_i + G_i w_i \tag{5a}$$
$$z_i = u_i = -K_i x_i \tag{5b}$$

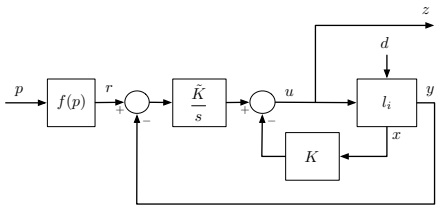

Fig. 1. Load i with system $l_i : (A_i, B_i, C_i, E_i)$ and LQ integral controller.

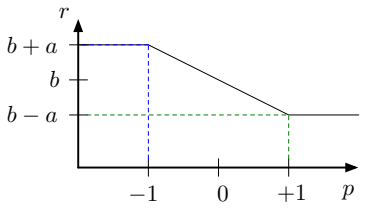

Fig. 2. Function $f(p)$ from control price to temperature set point

The aggregator measures the power consumption and not the temperature.Therefore, power consumption is now defined as the model output z_i from the ith load. y_i still indicates the temperature output. In (5) the temperature set point r_i has been replaced by a function f_i with the aggregator control price p as argument. The control price is a scalar that is broadcast to all loads, reflecting the need for balancing. A block diagram of the controlled load is shown in Fig. 1. Here it is seen how the control price is added as input to the closed-loop model. Each load must map the control price to an individual temperature set point. This mapping is done by the affine function $f_i(p)$ defined for each load

$$r_i = f_i(p) = -\frac{\overline{r_i} - \underline{r_i}}{\overline{p} - \underline{p}}(p - \underline{p}) + \overline{r_i} \tag{6}$$

When $(\underline{p}, \overline{p}) = (-1, 1)$ and $(\underline{r_i}, \overline{r_i}) = (b_i - a_i, b_i + a_i)$, (6) reduces to

$$f_i(p) = -a_i p + b_i \tag{7}$$

When the price is constrained the function $f_i(p)$ also constrains the temperature set point to a certain interval defined by a_i and b_i. This mapping is illustrated in Fig. 2 and is key to understanding the role of the control price. Note that for cooling systems the sign on the slope a will be chosen opposite of (7).

B. Aggregated model

We can put all the closed-loop models from (5) together to get a large linear model of all L loads. This augmented state space model subscripted a is then

$$x_a^+ = A_a x_a + B_a(p) + E_a d + G_a w_a \tag{8a}$$
$$z_a = C_a x_a \tag{8b}$$

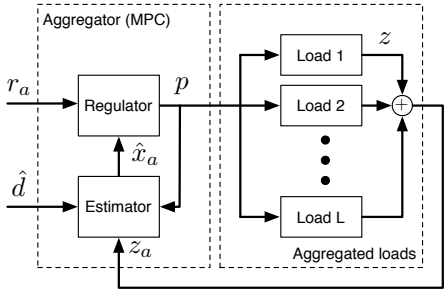

Fig. 3. System overview of aggregator and loads.

with $B_a(p) = F_a f_a(p)$ and

$$
\begin{aligned}
A_a &= \text{blkdiag}(A_1 - B_1K_1, A_2 - B_2K_2, \ldots, A_L - B_LK_L) \\
F_a &= \text{blkdiag}(F_1, F_2, \ldots, F_L) \\
G_a &= \text{blkdiag}(G_1, G_2, \ldots, G_L) \\
f_a(p) &= \begin{bmatrix} f_1(p) & f_2(p) & \cdots & f_L(p) \end{bmatrix}^T \\
x_a &= \begin{bmatrix} x_1^T & x_2^T & \cdots & x_L^T \end{bmatrix}^T \\
w_a &= \begin{bmatrix} w_1^T & w_2^T & \cdots & w_L^T \end{bmatrix}^T \\
E_a &= \begin{bmatrix} E_1^T & E_2^T & \cdots & E_L^T \end{bmatrix}^T \\
C_a &= -\begin{bmatrix} K_1^T & K_2^T & \cdots & K_L^T \end{bmatrix} \cdot \mathbf{1}
\end{aligned}
$$

The derived closed-loop model (8) of all loads describes the aggregated response from price to power consumption. The desired SISO model with $z_a \in \mathbb{R}^1$ and $p \in \mathbb{R}^1$ is here formed by the output matrix C_a, which sums all power consumption contributions $z_a = \sum_{i=1}^{L} z_i$. The disturbance, $d \in \mathbb{R}^1$, is assumed from now on to be a scalar influencing all loads. It is assumed that the main component of this disturbance can be forecast, while the remaining tracking errors from disturbances are assumed to be eliminated by the MPC integral controller.

As the number of loads increase, so does model complexity and, ultimately, controller computation time. However, this high dimensional model can be well approximated by a lower-order model [13], [14]. In our method, we reduce the model by estimating a low-order AR model from the simulated response

$$A_{ar}(q^{-1})\hat{z}_a = B_{ar}(q^{-1})p + E_{ar}(q^{-1})\hat{d} + \eta \tag{9}$$

η is the unmodeled disturbances. The model (9) can be used for model estimation and control. It is assumed to be accurate enough to enable the aggregator MPC to eliminate model mismatch errors through an observer and stable closed-loop feedback. Forecasts of the load disturbance $\hat{d}$ is also added to the model with the term E_{ar}.

III. Aggregator controller

The MPC is well suited for control at the aggregator level due to the following reasons. It handles capacity constraints indirectly through a limit on the price. It rejects disturbances and is able to track the power consumption reference r_a with a small error, since r_a is known ahead of time so the MPC can react in advance. In practice, r_a could be a time-varying forecast of wind power production, and at every time step the MPC takes continuously updated forecasts into account.

A. Aggregator objective

The method presented in this paper will indirectly change the power consumption of all thermal loads through a price that is linearly related to the temperature set points. In this way the aggregator puts a price on heating or cooling, and indirectly on electricity as well. The set points will be set at a high temperature set point when the price is low, and at a low temperature when the price is high. However, the interval within which the temperature set point is allowed to vary and is up to the individual load, e.g. it could be the temperature comfort interval in a building heated by a heat pump [1]. The temperature interval could even be set at zero by setting $a_i = 0$ in (7), but then the aggregator would have no flexibility to exploit. Note that the same method holds for refrigeration systems. However, in this case the set points should set at a low temperature when the price is low. Controlling the loads through a price requires a model of the price response as well as models of the thermal load behavior. The loads are connected to the aggregator through a control price p as shown in Fig. 3. The total power consumption of the loads z_a is measured by the aggregator that estimates an aggregated model and provides closed-loop feedback with an MPC for tracking the power consumption reference r_a.

B. Offset-free ARX MPC

We assume the model (8) to be estimated from data as an ARX model on the form (9). To obtain offset-free tracking we replace the unmodeled term η by an integrator model [15]

$$\eta = \frac{1 - \alpha q^{-1}}{1 - q^{-1}} e \tag{10}$$

α is a tuning parameter [15]. The observer error $e = z_a - \hat{z}_a$ is obtained from measurements of the aggregated response z_a (8). Adding the integrator model (10) to (9) yields the controller model in ARMAX form

$$A_{c,ar} = (1 - q^{-1})A_{ar} \qquad E_{c,ar} = (1 - q^{-1})E_{ar} \tag{11a}$$

$$B_{c,ar} = (1 - q^{-1})B_{ar} \qquad C_{c,ar} = 1 - \alpha q^{-1} \tag{11b}$$

The final controller model used as a predictor is obtained by realizing (11) as a discrete state-space model in innovation form

$$\hat{x}_a^+ = A_c\hat{x}_a + B_c p + E_c\hat{d} + K_c e \tag{12a}$$

$$\hat{z}_a = C_c\hat{x}_a \tag{12b}$$

This is the one-step predictor. For predicting j-steps ahead the term $K_c e$ is omitted.

Algorithm 1 MPC algorithm

For every time step find the optimal control price p_k^*
Require $\mathscr{P} = \left(\hat{x}_{a,k}, p_{k-1}, \{\hat{d}_{k+j}\}_{j=0}^{N-1}, \{r_{a,k+j}\}_{j=0}^{N-1}\right)$
$z_{a,k} = C_a x_{a,k}$ {Measure}
$e_k = z_{a,k} - C_c \hat{x}_{a,k}$ {Estimate error}
$\{p_{k+j}\}_{j=0}^{N-1} = \mu(\mathscr{P})$ {Solve QP}
$x_{a,k+1} = A_a x_{a,k} + F_a f_a(p_k) + E_a d_k + G_a w_{a,k}$ {Actuate}
$\hat{x}_{a,k+1} = A_c \hat{x}_{a,k} + B_c p_k + E_c \hat{d}_k + K_c e_k$ {Predict}
return p_k^*

C. Model Predictive Control

We use the tracking MPC formulation from [16] and minimize the residual by solving the following optimization problem at every time step k

$$\begin{aligned} \text{minimize} \quad & \frac{1}{2}\sum_{j=0}^{N-1} ||\hat{z}_{a,k+1+j} - r_{a,k+1+j}||_2^2 + \lambda ||\Delta p_{k+j}||_2^2 \\ \text{subject to} \quad & (12) \\ & \hat{x}_{a,k+1+j} = A_c \hat{x}_{a,k+j} + B_c p_{k+j} + E_c \hat{d}_{k+j} \\ & \hat{z}_{a,k+j} = C_c \hat{x}_{a,k+j} \\ & -1 \le p_{k+j} \le 1 \\ & \Delta p_{min} \le \Delta p_{k+j} \le \Delta p_{max} \end{aligned} \tag{13}$$

The optimal control price $\{p_k^*\}_{j=0}^{N-1}$ is found over the prediction horizon $j = 0, 1, \ldots, N-1$. The control price minimizes the deviations from the power consumption reference based on model predictions of the aggregated thermal loads. The first control price p_0^* is broadcast to all loads and the process is repeated at the next time step. Only the optimal control price at the current time step is implemented, e.g. the current price, and consequently closed-loop feedback is obtained. This is often referred to as the receding horizon principle. A regularization term is also added to the objective with penalty λ on the price rate Δp to enforce stability.

Algorithm 1 shows the closed-loop MPC algorithm that runs at every time step [16]. The MPC control law $p = \mu(\mathscr{P})$ is evaluated by solving (13), and real-time computation is enabled from the low-order aggregated controller model.

IV. Numerical Example

We model the individual load with a first-order transfer function $G(s)$ from power consumption u to temperature y

$$G(s) = \frac{c}{\tau s + 1} \tag{14}$$

τ is the time constant and c is the gain. The same model is used to model the disturbance response from d to y. We discretize with a zero-order hold and sampling period $T_s = 1$. As an example we set up a portfolio of $L = 10$ loads, each modeled with (14) and the parameters from Table I. We select different price scalings in a, but use the same temperature interval bias b. The tuning weight R is set rather high to minimize control action and is not tuned separately for each load.

i	τ	c	a	b	Q	R
1	55.4	1.32	1.00	21	1	2
2	68.3	2.94	1.22	21	1	2
3	27.4	2.91	1.44	21	1	2
4	58.6	1.97	1.67	21	1	2
5	53.2	2.60	1.89	21	1	2
6	36.9	1.28	2.11	21	1	2
7	45.7	1.84	2.33	21	1	2
8	53.4	2.83	2.56	21	1	2
9	85.8	2.58	2.78	21	1	2
10	77.7	2.92	3.00	21	1	2

TABLE I
Parameters for numerical example with $L = 10$

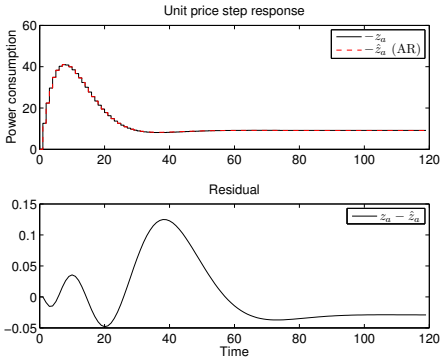

Fig. 4. Power consumption response and estimated response to unit price step (upper) and their residual (lower).

A. Estimated controller model

Fig. 4 depicts the unit price step response of the chosen model. The response fits an AR(2,2) model quite well, except for a small stationary error, even though the response is the sum of $L = 10$ different first-order models. For the chosen numerical parameters in Table I we find the following model

$$\hat{A}_{ar}(q^{-1}) = 1 - 1.756q^{-1} + 0.7798q^{-2} \tag{15a}$$
$$\hat{B}_{ar}(q^{-1}) = -12.62q^{-1} + 12.40q^{-2} \tag{15b}$$
$$\hat{E}_{ar}(q^{-1}) = -2.286q^{-1} + 2.038q^{-2} \tag{15c}$$

Also a response from the disturbance to power consumption was used to estimate the polynomial $\hat{E}_a(q^{-1})$. The final controller model is obtained by adding the integrator model as in (11).

In this numerical example some process noise was added to simulate unmodeled disturbances with $w_a \in N(0, 0.01)$. We tune the controller with the parameters to $\alpha = 0.7$, $\lambda = 10^3$ and $(\Delta p_{min}, \Delta p_{max}) = (-1, 1)$. These parameters matter considerably when the plant is subject to stochastics [17].

B. Simulation results

A simulation of the MPC price control with the estimated models is shown in Fig. 5 and 6. The upper plot of Fig. 5 shows the aggregated response and how the power reference is tracked by the aggregator MPC with no offset errors. Since prediction of the reference r_a is available to the MPC, control prices which indirectly change power consumption are broadcast ahead of time in order to minimize the residual. The residual is plotted below, along with the control price. After 55 time steps the control price constraint is active at -1. At this point the power reference is very high and the aggregator demands all available power from the thermal loads. Note that the control price is not constant when the total reference power consumption is constant, i.e. tracking a constant power requires a ramping of the price due to the dynamics of the loads.

There is a small stationary offset error during ramping of the reference. A double integrator can be added to (10) to eliminate the error. However, this requires the LQ load controllers to increase their order as well. This means the response will be more sensitive to noise and the tuning parameter α becomes extremely important [17]. In this work we accept the ramp offset error and use a single integrator.

The bottom plot of Fig. 6 shows the temperatures of the loads. Some loads are more flexible than others and allow a wider temperature interval, i.e. $b\pm a$ with a large a_i, indicated by the various dashed lines at different levels. Consequently, a more flexible load will have a more varying temperature. However, the temperature is still ensured to lie within the predefined interval, $b\pm a$, due to the constrained control price. The temperature interval can be adjusted for each load by the scaling a_i and can even be time varying. Naturally, the temperature does not depend exclusively on the control price; it also depends on the dynamics, i.e. the time constant, of the load and its controller tuning. The power consumption of each load is shown in the upper plot of the figure. As intended, power consumption mainly occurs when the price is low, as becomes evident when comparing to the price in Fig. 5. The stationary power consumption, when $p = 0$ and $d = 0$, varies from load to load as observed in Fig. 6 because of the different initial levels of u. In our example the combined stationary power consumption of all the loads when disregarding the disturbance is

$$z_a^0 = \sum_{i=1}^{L} \frac{b_i}{c_i} \tag{16}$$

In Fig. 5 power consumption was plotted around zero as the deviation from this stationary consumption z_a^0. From (16) it can be seen that the stationary power consumption depends on the number of loads L, their temperature settings (b,a), their efficiency c, and disturbance d. The methods accounts for local disturbances by forecasting a global disturbance $\hat{d}$ that acts on all loads. Any remaining sources of error will be eliminated by the MPC. A disturbance has also been used in the simulation shown in Fig. 5. After thirty time steps the disturbance kicks in, e.g. a change in outdoor temperature

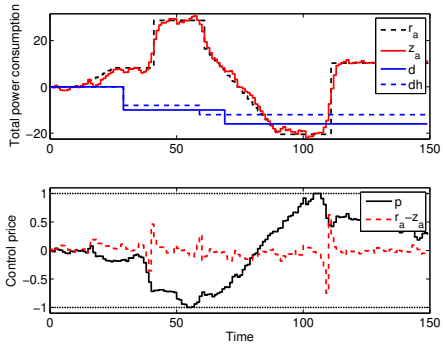

Fig. 5. Simulation of the aggregator tracking a power consumption r_a by controlling an aggregation of thermal loads. Total power consumption z_a is plotted around zero as the deviation from the stationary consumption z_a^0. The normalized residual is plotted below along with the control price p. As intended, load consumption is highest when the price is low. The disturbance is forecast dh and eliminated by the MPC. The disturbance shown here is scaled and does not match the units of the y-axis.

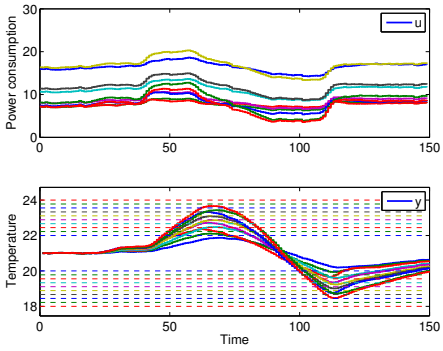

Fig. 6. Load output temperatures y_i (lower) and their temperature intervals $b_i \pm a_i$ (dashed lines). Also their power consumptions u_i are plotted (upper).

which changes the power consumption. By forecasting the disturbance, the tracking error can be greatly improved. A forecast that is close to the real disturbance is implemented and this is why almost no deviations are seen at the disturbance transitions after 30 and 70 time steps. A single disturbance acting on all loads can be justified when the loads are geographically close to each other and the disturbance considered is the outdoor temperature. Solar radiation has a more local impact on buildings but can also be forecast for a larger area [18].

V. Discussion

The control price used in this method should *not* be interpreted as the final billing price for each load. The control price helps the aggregator meet its balancing objective, but does not create an incentive for the loads to choose high temperature intervals, a_i. High temperature intervals increase the flexibility and thereby also the regulating power. Moreover, it lowers temperature variations for all aggregated loads. Consequently, all loads are forced to help the aggregator reach its tracking goals regardless of their own optimal strategy. This method is not optimal for every load in terms of energy savings, but will ensure that total aggregated power consumption follows production, e.g. from wind, to the benefit of the overall energy system.

A negative control price should not be considered a subsidy. However, the sign on p merely says whether the aggregator needs up or down regulation. It is evident from the simulations that if the price is negative a majority of the time, often the loads with the largest temperature interval will be at very low temperatures, thus saving a lot of power. If the price is mostly positive, the loads with low temperature intervals will save power. The opposite is true if we consider cooling rather than heating. In this case, the final electricity cost for each load should not depend exclusively on the control price. There must be a clear incentive to provide a large temperature interval, since this will enable more power at the aggregator level and less discomfort for all loads. Final billing could be calculated on the basis of consumption $u_{i,k}$, and temperature interval $2a_i$, defining how much load i allows the temperature to vary. Also the heat capacity of the load, e.g. the time constant τ_i, could play a role if it was measured. Instead of billing for power consumption using the control price, we suggest putting a price on flexibility, i.e. the temperature interval a_i which, in practice, could be time varying.

As a consequence of using linear unconstrained controllers for the loads, no actuator saturation was considered. If actuator constraints are involved, the price response will not be linear, and clipping of the power will be observed. As a result the response in Fig. 2 might look more sigmoidal and bend at the price limits ± 1. One way to prevent this problem is to restrain loads from setting a_i too high compared to its capacity and the expected disturbances. Another way is to include an adaptive model of the price response. Note that time-varying linear models can be easily implemented in the MPC algorithm by changing the coefficients of the controller model (15).

VI. Conclusions

The method described in this paper enables a linear MPC, based on a low-order SISO ARX model, to balance power production with consumption of a considerable number of thermal loads in real-time. The method requires linear temperature set point controllers to control the loads as well as model estimation of the price response at the aggregator level. The aggregator MPC controls total power consumption of all loads indirectly through a broadcast real-time price, i.e. one-way communication. It also handles the load temperature constraints through price constraints. The MPC incorporates forecasts of disturbances and power production, e.g. time-varying wind power forecasts, in order to react ahead of time. Added integral control eliminates model and forecast errors, while feedback is provided by measuring total load power consumption. Individual loads can set their own desired upper and lower temperature bounds. The method was demonstrated through simulation and allows for integration of flexible thermal loads a smart energy system in which consumption follows a changing production.

References

[1] R. Halvgaard, N. K. Poulsen, H. Madsen, and J. B. Jørgensen, "Economic Model Predictive Control for Building Climate Control in a Smart Grid," in *Proceedings of IEEE PES Innovative Smart Grid Technologies (ISGT)*, 2012.

[2] R. Halvgaard, P. Bacher, B. Perers, E. Andersen, S. Furbo, J. B. Jørgensen, N. K. Poulsen, and H. Madsen, "Model Predictive Control for a Smart Solar Tank based on Weather and Consumption Forecasts," in *Proceedings of 2012 International Conference on Solar Heating and Cooling for Buildings and Industry (SHC)*, 2012.

[3] T. G. Hovgaard, L. F. S. Larsen, K. Edlund, and J. B. Jørgensen, "Model predictive control technologies for efficient and flexible power consumption in refrigeration systems," *Energy*, vol. 44, no. 1, pp. 105–116, 2012.

[4] F. Oldewurtel, A. Ulbig, A. Parisio, G. Anderssonand, and M. Morari, "Reducing peak electricity demand in building climate control using real-time pricing and model predictive control," in *49th IEEE Conference on Decision and Control (CDC)*, dec 2010, pp. 1927–1932.

[5] M. Braun and P. Strauss, "A review on aggregation approaches of controllable distributed energy units in electrical power systems," *International Journal of Distributed Enery Resources*, vol. 4, pp. 297–319, 2008.

[6] A. Subramanian, M. Garcia, A. Dominguez-Garcia, D. Callaway, K. Poolla, and P. Varaiya, "Real-time Scheduling of Deferrable Electric Loads," in *2012 American Control Conference (ACC), Montreal, Canada, June 27-29*, 2012.

[7] R. Scattolini, "Architectures for distributed and hierarchical Model Predictive Control – A review," *Journal of Process Control*, vol. 19, pp. 723–731, 2009.

[8] O. Corradi and H. Ochsenfeld, "Integration of fluctuating energy by electricity price control," Master's thesis, Tech. Univ. Denmark, 2011.

[9] P. Nyeng, J. Østergaard, M. Togeby, and J. Hethey, "Design and Implementation of Frequency-responsive Thermostat Control," in *45th International Universities Power Engineering Conference (UPEC)*, 2010, pp. 1–6.

[10] M. Zugno, J. M. Morales, P. Pinson, and H. Madsen, "Modeling Demand Response in Electricity Retail Markets as a Stackelberg Game," in *Proceedings of IAEE conference*, 2012.

[11] T. G. Hovgaard, K. Edlund, and J. B. Jørgensen, "The Potential of Economic MPC for Power Management," in *49th IEEE Conference on Decision and Control (CDC)*, 2010, pp. 7533–7538.

[12] M. Kraning, E. Chu, J. Lavaei, and S. Boyd, "Message Passing for Dynamic Network Energy Management," *[To appear in] Foundations and Trends in Optimization*, 2013.

[13] J. B. Jørgensen and S. B. Jørgensen, "MPC-relevant prediction-error identification," in *Proceedings of ACC*, 2007, pp. 128–133.

[14] P. Bacher and H. Madsen, "Identifying suitable models for the heat dynamics of buildings," *Energy and Buildings*, vol. 43, no. 7, pp. 1511–1522, 2011.

[15] J. K. Huusom, N. K. Poulsen, S. B. Jørgensen, and J. B. Jørgensen, "Tuning SISO offset-free Model Predictive Control based on ARX models," *J. Process Control*, 2012.

[16] J. B. Jørgensen, J. K. Huusom, and J. B. Rawlings, "Finite Horizon MPC for Systems in Innovation Form," in *Proceedings of CDC*, 2011, pp. 1896–1903.

[17] J. K. Huusom, N. K. Poulsen, S. B. Jørgensen, and J. B. Jørgensen, "ARX-Model based Model and Predictive Control and with Offset-Free and Tracking," in *Proceedings of the 20th European Symposium on Computer Aided Process Engineering (ESCAPE)*, 2010.

[18] P. Bacher, H. Madsen, and B. Perers, "Short-term solar collector power forecasting," in *In proceedings of ISES Solar World Conference*, 2011.

Paper E

Distributed Model Predictive Control for Smart Energy Systems

---

Published in *Submitted to IEEE Transactions on Smart Grid, 2014.*

JOURNAL OF LATEX CLASS FILES, VOL. 11, NO. 4, DECEMBER 2014 1

Distributed Model Predictive Control for Smart Energy Systems

Rasmus Halvgaard, Lieven Vandenberghe, Niels K. Poulsen, Henrik Madsen, and John B. Jørgensen

***Abstract*—Integration of a large number of flexible consumers in a Smart Grid requires a scalable power balancing strategy. We formulate the control problem as an optimization problem to be solved repeatedly by the aggregator in a Model Predictive Control (MPC) framework. To solve the large-scale control problem in real-time requires decomposition methods. We propose a decomposition method based on Douglas-Rachford splitting to solve this large-scale control problem. The method decomposes the problem into smaller subproblems that can be solved in parallel, e.g. locally by each unit connected to an aggregator. The total power consumption is controlled through a negotiation procedure between all cooperating units and an aggregator that coordinates the overall objective. For large-scale systems this method is faster than solving the original problem and can be distributed to include an arbitrary number of units. We show how different aggregator objectives are implemented and provide simulations of the controller including the computational performance.**

***Index Terms*—Smart Grid, Model Predictive Control, Douglas-Rachford splitting**

I. Introduction

A large number of units with flexible power consumption are expected to be part of the future power system. In Denmark, examples of these units are electrical heat pumps for heating in buildings [1], commercial refrigeration [2], and Electric Vehicles (EVs) with batteries that can be charged and discharged [3]. If pooled together in a large-scale aggregated system these smaller consumption units could potentially offer flexibility to the power system. If the units are controlled and coordinated well, they can help to partially balance the fluctuating power production caused by renewable energy sources such as wind and solar. In real-time electricity markets the aggregated units can help to minimize the imbalances caused by forecast errors and in general provide ancillary services. Controlling a large number of units in real-time requires fast evaluation of the control algorithm that coordinates the power consumption. Thus methods for solving this large-scale optimization problem in real-time must be developed.

In this paper we consider the problem of real-time large-scale power balancing. We apply Douglas-Rachford splitting [4] to decompose the general problem into smaller dynamically decoupled subproblems. The subproblems can be distributed and solved in parallel either by a large central computer or locally by each unit. The latter case requires fast and very reliable two-way communication between the controller and the units since the subproblems must be solved many times at each time step. Each unit has its own model, constraints, and variables, and can even make decisions based on its own local control objective. All units must communicate their predicted consumption plan to an aggregator that coordinates the need for system level flexibility and minimizes imbalances. The aggregator continuously communicates control signals and synchronizes the global negotiation. This negotiation procedure is required to converge in every time step and thus requires fast evaluation of the unit subproblems that can be cast as convex optimal control problems. Convergence is achieved by coordinating all units' consumption through a negotiation procedure that is updated in the coordinating system level referred to as an aggregator.

With a least-squares tracking objective, the aggregator is able to control and deliver the requested combined power consumption of all units in real-time and continuously updates forecasts of the consumption by applying a receding horizon control principle. This principle, referred to as Model Predictive Control (MPC), repeatedly solves the control problem online for the predicted development of the system [5]. The first part of the obtained control action is implemented. At the next sample time, the procedure is repeated by using new measurements and by moving the prediction window one step. The sampling time in real-time markets could be lower than five minutes [6]. The precise sampling time is dictated by the settlement requirements of the regulating power market. This short sampling time motivates computational efficient optimization algorithms for the MPC that balances the power. For large-scale systems such as power balancing problems, decomposition methods are one computationally attractive option. The computation time for MPC problems grows polynomially in standard solvers as the number of units increase. By decomposing the problem and solving smaller subproblems in parallel, we can handle a much larger amount of units. Fig. 1 shows one month of produced wind power and the consumption pattern in Denmark. The fluctuating wind power could be the power reference to be tracked by the aggregator. However, in practice the consumption plan comes from the power market. We use the Nordic power market framework, where the goal of the power balancing aggregator would be to minimize the deviation from a consumption plan already negotiated in advance at the day-ahead market. Any deviations from this day-ahead plan cause power imbalances that must be settled in the regulating power market. These imbalances can be minimized by the aggregator by tracking

R. Halvgaard, N. K. Poulsen, H. Madsen, and J. B. Jørgensen are with the Department of Applied Mathematics and Computer Science, Technical University of Denmark, 2800 Kgs. Lyngby, Denmark, e-mail: {rhal,nkpo,hmad,jbjo}@dtu.dk (see www.compute.dtu.dk/~rhal).

L. Vandenberghe is with University of California Los Angeles, CA 90095-1594, USA, e-mail: {vandenbe@ucla.edu}.

Manuscript received February, 2014

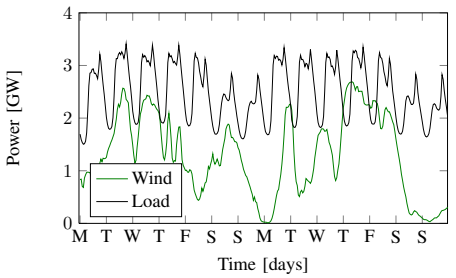

Fig. 1. Wind power and consumption in West Denmark January 2012.

the day-ahead plan as accurately as possible, while trying to eliminate forecast errors and unforeseen disturbances along the way. If the regulating power prices are predicted, the aggregator objective can reflect the actual imbalance costs. Many studies do not consider the imbalances they introduce when only optimizing over the day-ahead market prices [1], [2]. We therefore provide an example of taking regulating power prices into account. Grid capacity constraints on the total active power can also be applied as an aggregator constraint.

Compared to dual decomposition that uses the subgradient projection method with rather slow convergence [7], the Douglas-Rachford splitting used in this paper is often faster. Another advantage of the presented method is that it easily evaluates complicated and even non-linear expressions. Compared to a column generation method like Dantzig-Wolfe decomposition [8], which only handles linear programming problems, while the method considered in this paper handles continuous non-linear convex functions, and converges under very mild conditions. In our case, the subproblems even reduce to quadratic optimal control problems that can be solved very efficiently using the Riccati recursions [9]–[11]. A special case of Douglas-Rachford splitting is ADMM [12]. [13] use ADMM for Electric Vehicle charging coordination. [14] describe a general approach to Distributed MPC problems, while [15] provides convergence results for the splitting algorithm.

In this paper we illustrate the advantages of the Douglas-Rachford splitting method and show how an aggregator can use the method for power balancing flexible consumption units, exemplified by thermal storage units e.g. heat pumps in buildings. The method can be completely decentralized down to communication with neighbors only [16].

This paper is organized as follows. In Section II we formulate the general large-scale optimization problem for an aggregator with a large number of units in its portfolio. In Section III we introduce operator splitting and its convex optimization terminology. This leads to the Douglas Splitting algorithm explained and applied to the aggregator problem in Section III-A. Different aggregator objectives are introduced in Section IV. Finally, the method is demonstrated through simulations and its convergence and scalability is discussed in Section VI. Section VII provides conclusions.

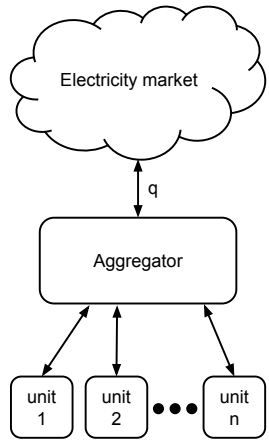

Fig. 2. *Aggregator role and portfolio of units. The aggregator gets a consumption plan q to follow from the market.*

II. The Aggregator Problem

We wish to control the power consumption of a large number of flexible and controllable units. The motivation for controlling the units is to continuously adapt their consumption to the changing stochastic power production from wind and solar. In the future this power balancing might be done by solving large-scale control problems. Instead of tracking the wind power directly, it is currently much more realistic to interface and bid into electricity markets. We assume that an *aggregator* controls a large number of flexible consumption units as shown in Fig. 2. Based on predictions of the aggregated unit behavior, the aggregator bids into the day-ahead power market and buys a certain amount of energy for the coming day. The plan could be a result of solving a unit commitment problem [17], where stochastics and integer variables are taken into account. The resulting consumption plan must be followed to avoid imbalances and in turn economic penalties. So a real-time controller must regulate the power to minimize any imbalances caused by prediction errors.

The power consumption profile is a vector denoted $q \in \mathbb{R}^N$ and denotes the amount of power to be consumed at each time step k for the entire prediction horizon $k = 1, ..., N$. This profile must be followed by the aggregator, such that the combined power consumption from all units sum to this at every time instant. The centralized large-scale problem that includes all units and their variables (p, x_j, y_j, u_j) and

constraints is

$$\underset{p_k, u_{j,k}}{\text{minimize}} \quad \sum_{k=0}^{N-1} g(p_k) + \sum_{j=1}^{n} \phi_j(u_{j,k}) \tag{1a}$$

$$\text{subject to} \quad p_k = \sum_{j=1}^{n} u_{j,k} \tag{1b}$$

$$x_{j,k+1} = A_j x_{j,k} + B_j u_{j,k} + E_j d_{j,k} \tag{1c}$$

$$y_{j,k} = C_j x_{j,k} \tag{1d}$$

$$y_{j,k}^{\min} \leq y_{j,k} \leq y_{j,k}^{\max} \tag{1e}$$

$$\Delta u_{j,k}^{\min} \leq \Delta u_{j,k} \leq \Delta u_{j,k}^{\max} \tag{1f}$$

$$u_{j,k}^{\min} \leq u_{j,k} \leq u_{j,k}^{\max} \tag{1g}$$

We model the $j = 1, 2, ..., n$ units with linear discrete-time state-space systems and define $\mathcal{U}_j$ as a closed convex set containing the model and constraints of the jth unit (1c)-(1g). $x_j \in \mathbb{R}^N$ is the time varying state vector in the discrete-time state-space system defined by the matrices (A_j, B_j, E_j, C_j) [1]. y_j is the output, of a linear system with controllable input u_j. d_j is the modeled and predictable disturbances (e.g. outdoor temperature). The time-varying input and output constraints are superscripted with max and min, and account for the available flexibility for each unit. For thermal storage units this is the power available and the accepted temperature interval, respectively. $\Delta u_{j,k} = u_{j,k} - u_{j,k-1}$ is the rate of movement, where k is the time step in the time varying input vector $u_j \in \mathbb{R}^N$. The total consumption $p \in \mathbb{R}^N$ is a sum of the predicted consumption profiles u_j. p can also be constrained to reflect capacity constraints in the power grid. g is the aggregator objective function. We investigate various choices of aggregator objectives in Section IV. However, the simulations in this paper are weighted least squares objective. This objective contains local control objectives and costs associated with operating the unit. Examples of local objective functions are

$$\phi_j^{\text{eco}}(u_j) = c_j u_j \tag{2a}$$

$$\phi_j^{\text{soft}}(\nu_j) = \gamma_j \nu_j \tag{2b}$$

$$\phi_j^{reg}(u_j) = ||\Delta u_j|| \tag{2c}$$

$$\phi_j^{\text{ref},y}(y_j) = ||y_j - y_j^{\text{ref}}|| \tag{2d}$$

$$\phi_j^{\text{ref},u}(u_j) = ||u_j - u_j^{\text{ref}}|| \tag{2e}$$

(2a) is an economic cost, c, of the power consumption; (2b) is a slack variable, ν_j, acting as a soft output constraint with penalty γ_j. This soft constraint prevents infeasible problems when the system is subject to noise; (2c) is a regularization term on the rate of input change; (2d) is a output (temperature) reference tracking objective; (2e) is an input reference. The slack variable should be heavily penalized in the the local objective function ϕ_j when added. We leave it out for a lighter notation in the remaining part of the paper. The functions ϕ_j and g may be indicator functions that represent constraints on the variables u_j or their sum. We exploit this later when decomposing the problem.

In this paper we consider three different aggregator objectives, g, sketched in Fig. 3. All objectives track the given power consumption profile q by minimizing $e = p - q$. First, the traditional tracking MPC with quadratic penalty on the residual e. Second, we also set up a linear economic MPC that includes the actual costs for imbalances. Third, the same economic objective but with asymmetric costs. All objectives are easily implemented in the decomposition algorithm described later in Section V where they are evaluated as simple analytic expressions in all three cases.

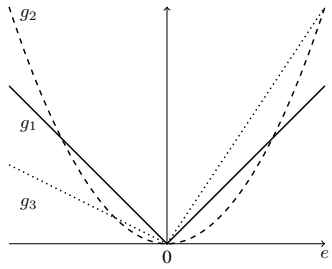

Fig. 3. Aggregator objective functions: g_1 (25), g_2 (20), and g_3 (23). $e = p - q$ is the power imbalance.

A. Decomposing the aggregator problem

With the use of indicator functions (4) the original problem (1) can be written as

$$\underset{u_j}{\text{minimize}} \quad \sum_{j=1}^{n} f_j(u_j) + g\left(\sum_{j=1}^{n} u_j\right). \tag{3}$$

Here the constraints in $\mathcal{U}_j$ are hidden in an indicator function f_j

$$f_j(u_j) = \begin{cases} \phi_j(u_j) & \text{if } u_j \in \mathcal{U}_j \\ +\infty & \text{otherwise.} \end{cases} \tag{4}$$

In decomposition literature [12], [18] a common and general formulation of the problem is on the form

$$\begin{aligned} \underset{u,p}{\text{minimize}} \quad & g(p) + f(u) \\ \text{subject to} \quad & p = Su. \end{aligned} \tag{5}$$

The functions $f_j : \mathbb{R}^N \to \mathbb{R}$ and $g : \mathbb{R}^N \to \mathbb{R}$ are assumed to be closed and convex. We define $u = [u_1^T, u_2^T, \ldots, u_n^T]^T$ as a stacked vector of individual unit consumption profiles and $f(u)$ as a sum of the unit indicator functions from (4)

$$f(u) = \sum_{j=1}^{n} f_j(u_j).$$

$S \in \mathbb{R}^{N \times Nn}$ simply sums all contributions to the total power consumption

$$S = \begin{bmatrix} I & I & \cdots & I \end{bmatrix}, \tag{6}$$

where I is the identity matrix. S remains constant even if we also add power production units by defining production as negative consumption. We limit S to this simple structure

that speeds up computation time in Section III-A. This optimization problem must be solved at every time instant in a Receding Horizon manner [19], [20]. We apply Douglas-Rachford splitting to solve this large-scale control problem in real-time. This splitting method is explained in the following section.

III. Operator splitting

We show how operator splitting can be done on a problem on the form

$$\underset{u}{\text{minimize}} \quad f(u) + g(Su). \tag{7}$$

This is equivalent to the control problem (1) on the form (5). The objective (7) can be split in separate functions with variable $u \in \mathbb{R}^N$ and where $f : \mathbb{R}^N \to \mathbb{R}$ and $g : \mathbb{R}^N \to \mathbb{R}$ are closed convex functions with nonempty domains. It captures a large class of constrained and unconstrained optimization problems. For example, if we let g be the indicator function of a convex set $\mathcal{U}$

$$g(Su) = \begin{cases} 0 & \text{if } Su \in \mathcal{U} \\ +\infty & \text{otherwise} \end{cases} \tag{8}$$

the problem (7) is equivalent to the following constrained optimization problem

$$\begin{aligned} \underset{u}{\text{minimize}} \quad & f(u) \\ \text{subject to} \quad & Su \in \mathcal{U}. \end{aligned}$$

In order to solve the problem we derive the optimality conditions associated with (7). The first-order optimality condition are expressed in inclusion form as

$$0 \in \partial f(u) + S^T \partial g(Su), \tag{9}$$

where $\partial f(u)$ denotes the subdifferential of f at u. The dual optimality condition of (7) is found by first introducing an extra variable p and a consensus constraint, such that

$$\begin{aligned} \underset{u,p}{\text{minimize}} \quad & f(u) + g(p) \\ \text{subject to} \quad & Su = p. \end{aligned} \tag{10}$$

The Lagrangian of (10) is

$$L = f(u) + g(p) + z^T(Su - p)$$

where z is the dual variable associated with the equality constraint. The dual problem is

$$\inf_{u,p,z} L = \inf_{u} \left(z^T Su + f(u)\right) + \inf_{p} \left(-z^T p + g(p)\right)$$

Two conjugate functions are readily identified in this expression. Since the conjugate function is defined as [21]

$$f^*(p) = \sup_u (p^T u - f(u))$$

the dual of (7) reduces to

$$\underset{z}{\text{maximize}} \quad -f^*(-S^T z) - g^*(z), \tag{11}$$

where f^* and g^* denote the conjugate functions of f and g. The first-order dual optimality condition associated with (11) can now be expressed as

$$0 \in -S\partial f^*(-S^T z) + \partial g^*(z). \tag{12}$$

The subdifferential of a closed convex function f satisfies $(\partial f)^{-1} = \partial f^*$ [22], i.e.

$$y \in \partial f(x) \;\Leftrightarrow\; \partial f^*(y) \in x$$

Hence if we let $u = \partial f^*(-S^T z)$ in (12) then

$$0 \in \begin{bmatrix} 0 & S^T \\ -S & 0 \end{bmatrix} \begin{bmatrix} u \\ z \end{bmatrix} + \begin{bmatrix} \partial f(u) \\ \partial g^*(z) \end{bmatrix}. \tag{13}$$

This is the primal dual optimality conditions that can be solved to find a solution of (7). Because we deal with subgradients we use the inclusion sign instead of equality in (13). It simply means that zero must be included in the set. The subdifferentials are monotone operators and (13) is a monotone inclusion problem. The solution to this problem has zero included in the sum of the two maximal monotone operators A and B

$$0 \in A(u, z) + B(u, z). \tag{14}$$

A. Douglas-Rachford splitting

We apply Douglas-Rachford splitting [4] to solve the problem and identify two splitting operators in (13) as

$$A(u, z) = \begin{bmatrix} 0 & S^T \\ -S & 0 \end{bmatrix} \begin{bmatrix} u \\ z \end{bmatrix} \tag{15}$$

$$B(u, z) = \begin{bmatrix} \partial f(u) \\ \partial g^*(z) \end{bmatrix}. \tag{16}$$

The primal-dual Douglas-Rachford splitting algorithm is a special case of the proximal point algorithm [23] and works by starting at any v and repeating the following iterations:

$$x^+ = (I + tB)^{-1}(v) \tag{17a}$$

$$y^+ = (I + tA)^{-1}(2x^+ - v) \tag{17b}$$

$$v^+ = v + \rho(y^+ - x^+). \tag{17c}$$

The superscript $^+$ indicates the next iterate, e.g. $x^+ = x_{i+1}$ if i is the iteration number. Note that this general algorithm fits our problem (15) when $x = [u^T \; z^T]^T$. The algorithm steps are: 1) optimize over x 2) keep x fixed and optimize over y 3) sum the error with gain $\rho \in]0; 2]$. Thus the algorithm requires the resolvents of A and B, but not their sum. The inverse function of the operators A and B is called a resolvent. The resolvent of an operator F is the operator $(I+tF)^{-1}$ with scaling $t > 0$. In our case we require the resolvents of the functions ∂f and ∂g^* from (13). The resolvent of ∂f is the proximal mapping

$$(I + t\partial f)^{-1}(x) = \text{prox}_{tf}(x). \tag{18}$$

This proximal mapping is defined as the prox-operator of f, if f is convex

$$\text{prox}_{tf}(x) = \underset{u}{\text{argmin}} \left(f(u) + \frac{1}{2t}\|u - x\|^2 \right).$$

If f is an indicator function similar to (8) the prox-operator is equivalent to solving the problem

$$\begin{aligned} \underset{u}{\text{minimize}} \quad & \tfrac{1}{2t}\|u - x\|^2 \\ \text{subject to} \quad & u \in \mathcal{U}. \end{aligned}$$

This can be even more simplified to a projection on the convex set $\mathcal{U}$.

The prox-operator of the conjugate g^* is related to the prox-operator of g via

$$\text{prox}_{tg^*}(s) = s - t\text{prox}_{g/t}(s/t)\,. \tag{19}$$

The algorithm can now be compactly written with prox-operators.

IV. Aggregator objectives

A. Tracking objective

If q represents a desired total power consumption profile to be followed by the aggregated units, we can choose the differentiable quadratic aggregator objective

$$g_2(p) = \frac{1}{2}||p-q||_2^2, \tag{20}$$

that is easily evaluated by the prox-operator required in the Douglas-Rachford z^+ update (28b). The conjugate of $g_2(p)$ is

$$g_2^*(y) = \sup_p(y^T p - g_2(p)) = \frac{1}{2}||y||_2^2 + q^T y, \tag{21}$$

and the prox-operator simplifies to the analytic expression

$$\text{prox}_{tg_2^*}(s) = \frac{1}{t+1}s - \frac{t}{t+1}q, \tag{22}$$

to be substituted for (28b).

B. Economic objectives

When the aggregated power consumption p deviates from the reference plan q, this power imbalance, denoted $e = p-q$, has a penalty cost c equal to the regulating power price. However, the price might depend on the sign of the imbalance and the overall system imbalance. These regulating power prices are difficult to forecast, but in the Nordic power market they have a lower or upper bound depending on imbalance direction, i.e. the sign of e. When the up and down-regulating power market prices, c^+ and c^- respectively, are forecasted individually, we get the following piecewise linear objective function to be minimized

$$g_3(e) = \sum_{k=0}^{N} \max\left(-c_k^+ e_k, c_k^- e_k\right). \tag{23}$$

This aggregator objective is non-differentiable, but is easily handled by the prox-operator required in the algorithm (28). In this case the conjugate function $g_3^*(e)$ is more difficult to find analytically, and we exploit the relation (19). The objective (23) is both separable in time and units, so the prox-operator of (23) becomes

$$\text{prox}_{g_3/t}(s/t) = \underset{\tilde{s}_k}{\text{argmin}} \sum_{k=0}^{N} \left(g_{3,k}(\tilde{s}_k) + \frac{t}{2}||\tilde{s}_k - s_k/t||_2^2 \right).$$

The prox-operator evaluation can be divided into several cases for the unconstrained minimum to be found, since it is a sum of a piecewise linear function $g_3(e)$ and a quadratic function. Analytically, this leaves the minimum to be found in the following three cases

$$\left[\text{prox}_{g_3/t}(s_k/t)\right]_k = \begin{cases} (s_k - c_k^-)/t & \text{if } s_k \le tq_k - c_k^- \\ (s_k + c_k^+)/t & \text{if } s_k \ge tq_k + c_k^+ \\ q_k & \text{otherwise} \end{cases}$$

Inserted into (19) yields the final analytical expression for (28b) when using the asymmetric economic objective (23)

$$\left[\text{prox}_{tg_3^*}(s_k)\right]_k = \begin{cases} c_k^- & \text{if } s_k \le tq_k - c_k^- \\ -c_k^+ & \text{if } s_k \ge tq_k + ci_k^+ \\ s_k - tq_k & \text{otherwise} \end{cases} \tag{24}$$

The case with a symmetric price is included as well when $c^- = c^+$ and

$$g_1(e) = c||e||_1. \tag{25}$$

C. Grid constraints

A constraint on p, a limit on power capacity, can also be added to (1). When $g(p) = 0$ we get the problem

$$\begin{aligned} &\text{minimize} && \frac{t}{2}\|p - s/t\|_2^2 \\ &\text{subject to} && p \ge h \end{aligned} \tag{26}$$

The prox-operator reduces to a simple projection

$$\text{prox}_{tg^*}(s) = (0, s-th)_- = \min(0, s-th) \tag{27}$$

where $h = -p_{\max}$. A zero lower bound on the total power is already ensured through (1g), i.e. negative consumption is not allowed as this is production.

V. Douglas-Rachford splitting algorithm

When the specific operators (15) from our problem (13) are inserted into the general Douglas-Rachford splitting algorithm (17) we get

$$u^+ = \text{prox}_{tf}(v) \tag{28a}$$

$$z^+ = \text{prox}_{tg^*}(s) \tag{28b}$$

$$\begin{bmatrix} w^+ \\ m^+ \end{bmatrix} = \begin{bmatrix} I & tS^T \\ -tS & I \end{bmatrix}^{-1} \begin{bmatrix} 2u^+ - v \\ 2z^+ - s \end{bmatrix} \tag{28c}$$

$$v^+ = v + \rho(w^+ - u^+) \tag{28d}$$

$$s^+ = s + \rho(m^+ - z^+). \tag{28e}$$

The A-operator from (15) is linear. The resolvent in (28c) is the matrix inverse.

In our case the algorithm has the following interpretation:

1) The aggregator sends suggested consumption profiles v_j to the units
2) The units evaluate their subproblems, i.e. the prox-operator in (28a), by solving a QP with their local unit model, costs, constraints, and variables
3) The units respond in parallel with their updated consumption profiles u_j^+
4) The remaining steps (28b)-(28e) simply updates the other variables and are computed by the aggregator alone

It is important to note that the prox-operators don't have to be evaluated by the units. If the units upload their objective

and constraints to the aggregator a large parallel computer could solve all the subproblems. This significantly reduces convergence speed and communication requirements in a practical system.

A. *Step* (28a)

The prox-operator evaluation in the first step (28a) is defined as

$$\text{prox}_{tf}(v) = \underset{\tilde{v}}{\text{argmin}} \left(f(\tilde{v}) + \frac{1}{2t}\|\tilde{v} - v\|_2^2 \right).$$

In our case we must solve this subproblem for all units and stack their solutions in u^+ . Since all units are decoupled, separability of $f(u) = \sum_j f_j(u_j)$ implies that

$$\text{prox}_{tf}(v) = \left(\text{prox}_{tf_1}(v_1), \ldots, \text{prox}_{tf_n}(v_n)\right).$$

Here $v = [v_1^T, v_2^T, \ldots, v_n^T]^T$ and each of these prox-operators involve only one unit. We thus have the jth unit subproblem

$$\text{prox}_{tf_j}(v_j) = \underset{u_j}{\text{argmin}} \left(f_j(u_j) + \frac{1}{2t}\|u_j - v_j\|_2^2 \right).$$

with the standard QP formulation

$$\begin{array}{ll} \underset{u_j}{\text{minimize}} & \frac{1}{2}\frac{1}{t}u_j^T u_j - \frac{1}{t}v_j^T u_j + \phi_j(u_j) \\ \text{subject to} & u_j \in \mathcal{U}_j \,. \end{array} \tag{29}$$

Note that ϕ_j contains slack variables and regularization (2c). v_j can be interpreted as a tracking reference trajectory or an individual linear coefficient for each unit. In our case, all of these quadratic subproblems reduce to finite horizon constrained LQR problems that can be solved efficiently by methods based on the Riccati recursion [11], [24].

B. *Step* (28c)

The (w, m)-update in (28c) gathers the unit consumption profiles and involves only multiplications with S and S^T. Due to the simple structure of S, defined in (6), we can simplify this update with a matrix inversion lemma to

$$\begin{bmatrix} I & tS^T \\ -tS & I \end{bmatrix}^{-1} = \begin{bmatrix} I & 0 \\ 0 & 0 \end{bmatrix} + \frac{1}{\tilde{n}} \begin{bmatrix} -tS^T \\ I \end{bmatrix} \begin{bmatrix} tS & I \end{bmatrix},$$

where $\tilde{n} = 1 + nt^2$. Due to the simple structure of S this update reduces to

$$\begin{aligned} w_j &= \tilde{v}_j - \frac{1}{\tilde{n}} \left(t\tilde{s} + t^2 \sum_{j=1}^{n} \tilde{v}_j \right) \\ w^+ &= [w_1^T, w_2^T, \ldots, w_n^T]^T \\ m^+ &= \frac{1}{\tilde{n}} \left(\tilde{s} + t \sum_{j=1}^{n} \tilde{v}_j \right), \end{aligned}$$

where $\tilde{v}_j = 2u_j^+ - v_j$ and $\tilde{s} = 2z^+ - s$. For a large-scale system with $nt^2 \gg 1$ we get expressions involving the mean consumption plan $\hat{v} = \frac{1}{n}\sum_{j=1}^{n} \tilde{v}_j$

$$w_j \simeq \tilde{v}_j - \hat{v} \qquad\qquad m^+ \simeq \frac{1}{t}\hat{v}$$

w_j is the difference between the unit consumption plan and the average $\hat{v}$.

C. *Convergence*

The primal and dual optimality conditions from (13) provide a measure of convergence, i.e.

$$r_p = \frac{v - u^+}{t} + S^T z^+ \qquad r_d = \frac{s - z^+}{t} - Su^+. \tag{30}$$

These expressions are obtained from the prox-operators (28a) and (28b) that defines the subgradients $\partial f(u)$ and $\partial g^*(z)$ in (13), respectively. The algorithm is converged when the norm of these residuals are below some user-defined tolerance. See [15] for more general convergence results.

From theory, it is known that the step size t in the algorithm must remain constant. However, various heuristics provide adaptive strategies, see for instance the references in [12]. In the numerical example provided in this paper, t was found experimentally, based on the observed convergence behavior. Also the scaling gain $\rho \in]0; 2]$ must be selected and usually $\rho = 1.5$ is good choice.

VI. Numerical Example

To illustrate the method we provide a two simulations. One with only $n = 2$ different thermal storage systems, and one with $n = 100$. We model a portfolio of different thermal storage systems as second order systems on the form

$$G_j(s) = \frac{Y_j(s)}{U_j(s)} = \frac{K}{(\tau_j^a s + 1)(\tau_j^b s + 1)}.$$

u_j is the consumption and y_j is the output temperature. One time constant is usually much bigger than the other. Realistic values for the dominating time constant in buildings with heat pumps or refrigeration systems is $\tau^a \in \{10; 120\}$ h [1], [2]. In our simulations we also set $\tau^b = \tau^a/5$ and pick τ^a randomly. The same model works for disturbances d_j, e.g. ambiant temperature, and is easily converted to the state space form (1c)-(1d). The constraints were selected equal for both units: $(y^{\min}, y^{\max}) = (15, 25)\ ^\circ C$, $(u^{\min}, u^{\max}) = (0, 50)\ W$, $(\Delta u^{\min}, \Delta u^{\max}) = (-50, 50)\ W$, and output slack variable penalty $\gamma = 10^4$.

We scale the gain K with $1/n$ such that the maximum possible power consumption automatically adds to $p_{\max} = 1$. The reference q is also scaled to always lie between 0 and 1. Better numerical performance and sensitivity to the step size t is obtained in this way.

A. *Case study* ($n = 2$)

Fig. 4 shows the simulation results with $t = 0.5$ using 25 iterations for every open loop problem. Full state information was used to produce these closed profiles. Both the temperatures and the consumption are kept within their operating intervals. Their combined consumption p is seen to match the reference q very well. The plot illustrates two cases where it is not always possible to follow the plan q. Obviously in periods where q is larger than the maximum total power. And in periods where q is close to zero and the outputs are near the constraints, e.g. around 20 h. It is simply not possible to follow the plan in that situation without violating the output constraints. However, around 45 h there is enough capacity

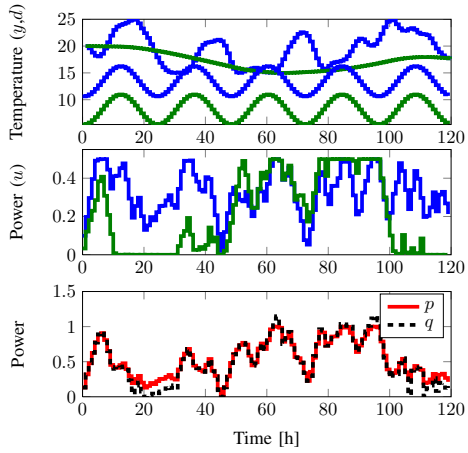

Fig. 4. *Closed loop simulation of power balancing with $n = 2$ thermal storage units. Prediction horizon was $N = 24$ and we used a quadratic objective function. The first plot shows the output temperatures of the two units in blue and green respectively. The two sinusoids below are the disturbances. The second plot shows the input power consumption. Right below is the resulting total power p and tracking profile q. All powers are scaled, such that the total maximum power of p is equal to 1. Consequently for $n = 2$ units their maximum power is $1/n = 0.5$.*

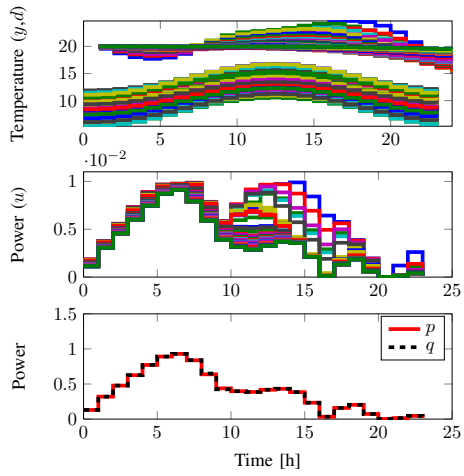

Fig. 5. *Open loop simulation of power balancing with $n = 100$ thermal storage units. Otherwise shows the same as Fig. 4.*

to turn the units completely off for a short period of time. q could be any profile but was selected here as a scaled version of the difference between the wind power and the load from Fig. 1.

B. Case study ($n = 100$)

To demonstrate that the algorithm works for a larger number of units, we chose $n = 100$ units with uniform randomly generated parameters as before. In Fig. 5 the same consumption profile q from the previous case study is tracked, but we only plotted the first open-loop profile.

C. Convergence

Fig. 6 shows how the Douglas-Rachford splitting algorithm converges during the iterations of one open-loop simulation. The optimality conditions (30) both reach a threshold below 10^{-2} after 25 iterations. The step size t was tuned to $t = 0.8$. This was done for different number of units in Fig. 7. For the simulation with $n = 100$ units, the algorithm is seen to converge within 50 iterations. As the number of units increases the computation time also increases. This is shown in Fig. 8. We measured the computation of all the subproblems and took the average (labeled DR parallel) to illustrate the unit scaling behavior. The total computation time for the serial implementation is labeled DR. For a large number of units the Douglas-Rachford splitting algorithm is faster than just solving the original problem, even the serial implementation.

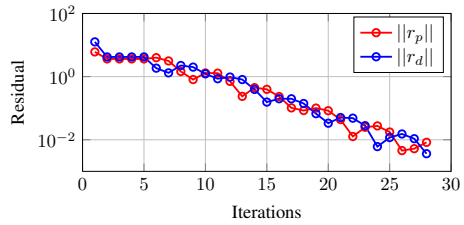

Fig. 6. Convergence for open-loop problem $n = 3$ and $t = 0.8$

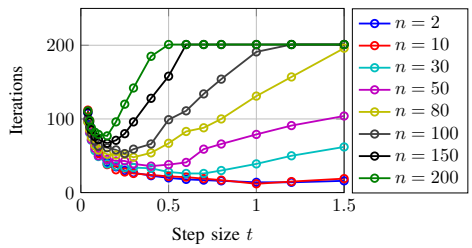

Fig. 7. Tuning of step size t as a function of the number of units n. Maximum number of iterations was limited to 200.

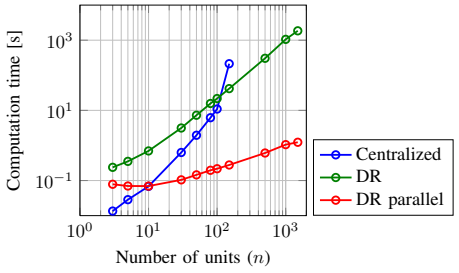

Fig. 8. Convergence for open-loop problem with tuned step sizes t from

We solved all QPs including the large scale problem using MOSEK in MATLAB running on an Intel Core i7 2.67 GHz laptop. It should be noted that MOSEK computes a much more accurate solution than the splitting algorithm. For most MPC applications a low accuracy is tolerated with a fast sampling closed-loop feedback [19].

VII. Conclusion

We solved the power balancing problem using a constrained model predictive controller with a least squares tracking error criterion. This is an example of a large-scale optimization problem that must be solved reliably and in real-time. We demonstrated how Douglas-Rachford splitting can be applied in solving this problem. By decomposing the original optimization problem thousands of units can be controlled in real-time by computing the problem in a distributed (parallel) manner. We considered a large-scale power balancing problem with flexible thermal storage units. A given power consumption profile can be followed by controlling the total power consumption of all flexible units through a negotiation procedure with the dual variables introduced in the method. An economic aggregator objective that takes the regulating power prices into account was derived. The obtained solution converges towards the original problem solution and requires two-way communication between units and the coordinating level. The resulting power balancing performance runs in closed loop while the local constraints and objectives for each unit are satisfied and aggregator operation costs are reduced. We showed that the decomposition algorithm scales well with the number of units compared to a standard solver, even when solving the subproblems serially.

Acknowledgment

This work was partly supported by the DSF iPower (Strategic Platform for Innovation and Research in Intelligent Power) project.

References

[1] R. Halvgaard, N. K. Poulsen, H. Madsen, and J. B. Jørgensen, "Economic Model Predictive Control for Building Climate Control in a Smart Grid," in *Proceedings of 2012 IEEE PES Innovative Smart Grid Technologies (ISGT)*, 2012. [Online]. Available: http://ieee-isgt.org/

[2] T. G. Hovgaard, L. F. S. Larsen, K. Edlund, and J. B. Jørgensen, "Model Predictive Control technologies for efficient and flexible power consumption in refrigeration systems," *Energy*, vol. 44, no. 1, pp. 105–116, Aug. 2012.

[3] R. Halvgaard, F. Marra, D. E. M. Bondy, N. K. Poulsen, H. Madsen, and J. B. Jørgensen, "Electric Vehicle Charge Planning using Economic Model Predictive Control," in *2012 IEEE International Electric Vehicle Conference (IEVC)*. Greenville, South Carolina, USA: IEEE, 2012, pp. 1–6. [Online]. Available: http://ieeexplore.ieee.org/lpdocs/epic03/wrapper.htm?arnumber=6183173

[4] J. Eckstein and D. P. Bertsekas, "On the Douglas-Rachford splitting method and the proximal point algorithm for maximal monotone operators," *Mathematical Programming*, vol. 55, no. 1-3, pp. 293–318, Apr. 1992.

[5] J. B. Rawlings and D. Q. Mayne, *Model Predictive Control*. Nob Hill Publishing, 2008.

[6] Y. Ding, S. Pineda, P. Nyeng, J. Østergaard, E. M. Larsen, and Q. Wu, "Real-Time Market Concept Architecture for EcoGrid EU - A Prototype for European Smart Grids," *IEEE Transactions on Smart Grid*, vol. 99, pp. 1–11, 2013.

[7] G. K. H. Larsen, N. D. van Foreest, and J. M. A. Scherpen, "Distributed Control of the Power Supply-Demand Balance," *IEEE Transactions on Smart Grid*, vol. 4, no. 2, pp. 828–836, Jun. 2013. [Online]. Available: http://ieeexplore.ieee.org/lpdocs/epic03/wrapper.htm?arnumber=6484218

[8] K. Edlund, J. D. Bendtsen, and J. B. Jørgensen, "Hierarchical model-based predictive control of a power plant portfolio," *Control Engineering Practice*, vol. 19, no. 10, pp. 1126–1136, 2011. [Online]. Available: http://www.sciencedirect.com/science/article/pii/S0967066111001171http://linkinghub.elsevier.com/retrieve/pii/S0967066111001171

[9] G. Frison and J. B. Jørgensen, "Efficient Implementation of the Riccati Recursion for Solving Linear-Quadratic Control Problems," in *2013 IEEE Multi-conference on Systems and Control (MSC)*, 2013, pp. pp. 1117–1122.

[10] J. B. Jørgensen, G. Frison, N. F. Gade-Nielsen, and B. Damman, "Numerical Methods for Solution of the Extended Linear Quadratic Control Problem," in *Proceedings of 4th IFAC Nonlinear Model Predictive Control Conference International Federation of Automatic Control Noordwijkerhout, NL. August 23-27, 2012*, 2012.

[11] C. V. Rao, S. J. Wright, and J. B. Rawlings, "Application of Interior-Point Methods to Model Predictive Control," *Journal of Optimization Theory*, vol. 99, no. 3, pp. 723–757, Dec. 1998.

[12] S. Boyd, N. Parikh, E. Chu, B. Peleato, and J. Eckstein, "Distributed Optimization and Statistical Learning via the Alternating Direction Method of Multipliers," *Foundations and Trends in Machine Learning*, vol. 3, no. 1, pp. 1–122, 2011.

[13] A. Mercurio, A. Di Giorgio, and F. Purificato, "Optimal Fully Electric Vehicle load balancing with an ADMM algorithm in Smartgrids," May 2013. [Online]. Available: http://arxiv.org/abs/1305.1044

[14] T. H. Summers and J. Lygeros, "Distributed Model Predictive Consensus via the Alternating Direction Method of Multipliers," Dec. 2012. [Online]. Available: http://arxiv.org/abs/1212.1296

[15] E. Ghadimi, A. Teixeira, I. Shames, and M. Johansson, "Optimal parameter selection for the alternating direction method of multipliers (ADMM): quadratic problems," Jun. 2013. [Online]. Available: http://arxiv.org/abs/1306.2454

[16] M. Kraning, E. Chu, J. Lavaei, and S. Boyd, "Message Passing for Dynamic Network Energy Management," *[To appear in] Foundations and Trends in Optimization*, 2013. [Online]. Available: C:\Users\rhal.AD\Desktop\Literature\Kraning-MessagePassingforDynamicNetworkEnergyManagement.pdf

[17] T. Shiina and J. R. Birge, "Stochastic unit commitment problem," *International Transactions in Operational Research*, vol. 11, no. 1, pp. 19–32, Jan. 2004. [Online]. Available: http://doi.wiley.com/10.1111/j.1475-3995.2004.00437.x

[18] N. Parikh and S. Boyd, "Proximal Algorithms," *Foundations and Trends in Optimization*, vol. 1, no. 3, pp. 123–231, 2013.

[19] Y. Wang and S. Boyd, "Fast Model Predictive Control Using Online Optimization," *IEEE Transactions on Control Systems Technology*, vol. 18, no. 2, pp. 267–278, 2010.

[20] A. N. Venkat, I. A. Hiskens, J. B. Rawlings, and S. J. Wright, "Distributed MPC Strategies With Application to Power System Automatic Generation Control," *IEEE Transactions on Control Systems Technology*, vol. 16, no. 6, pp. 1192—-1206, 2008.

[21] S. Boyd and L. Vandenberghe, *Convex Optimization*. Cambridge University Press, 2004.

[22] R. T. Rockafellar, *Convex Analysis*, 1997. [Online]. Available: http://books.google.dk/books/about/Convex_Analysis.html?id=1TiOka9bx3sC&pgis=1
[23] B. Djafari Rouhani and H. Khatibzadeh, "On the Proximal Point Algorithm," *Journal of Optimization Theory and Applications*, vol. 137, no. 2, pp. 411–417, Dec. 2008.
[24] J. B. Jørgensen, "Moving Horizon Estimation and Control," Ph.D. dissertation, Technical University of Denmark, 2005.

Paper F

Dual Decomposition for Large-Scale Power Balancing

Published in *Proceedings of 18th Nordic Process Control Workshop (NPCW), 2013.*

Dual Decomposition for Large-Scale Power Balancing

Rasmus Halvgaard * **John B. Jørgensen** *
Lieven Vandenberghe **

* *Technical University of Denmark, Kgs. Lyngby, Denmark (e-mail: {rhal,jbjo}@dtu.dk).*
** *UCLA, Los Angeles, CA 90095 USA (e-mail: lieven.vandenberghe@ucla.edu)*

Abstract: Dual decomposition is applied to power balancing of flexible thermal storage units. The centralized large-scale problem is decomposed into smaller subproblems and solved locally by each unit in the Smart Grid. Convergence is achieved by coordinating the units consumption through a negotiation procedure with the dual variables.

Keywords: Decomposition methods, Decentralized Control, Model Predictive Control, Smart Grid, Smart power applications

1. INTRODUCTION

A large number of flexible thermal storage units, e.g. electrical heating in buildings or cooling in refrigeration systems, will soon part of the Danish power system. These units could potentially provide a large flexible consumption by aggregating or pooling them together. This will enable them to be coordinated and help follow the fluctuating energy production from renewables such as wind power. We formulate an optimization problem of tracking a power reference. To solve this large-scale control problem in real-time, we decompose the original problem into smaller subproblems to be solved locally by each unit. Each unit has its own model and variables and can make decisions based on its own local control strategy. The need for system level flexibility is communicated to the units from an aggregator that broadcasts dual variables to the units and coordinates the negotiation until global convergence is reached. This negotiation procedure is required in every time step and requires fast evaluation of the subproblems that can be cast as linear quadratic optimal control problems. The subgradient method is used to minimize the system level power imbalance. The cost function of this imbalance can be non-differentiable, which is the case in power balancing, due to the nonlinear penalties on imbalances. A simple example with models of thermal storage systems is used to show how an aggregator can apply dual decomposition for power balancing in a smart energy system. Power capacity constraints in the distribution system can also be accounted for by the aggregator.

2. PROBLEM FORMULATION

The centralized large-scale problem to be solved at every time instant t is

$$\begin{aligned} \text{minimize} \quad & g(p(t), q(t)) \\ \text{subject to} \quad & p(t) = \sum_{k=1}^{n} u_k(t) \\ & x_k(t+1) = A_k x_k(t) + B_k u_k(t) \\ & y_k(t) = C_k x_k(t) \\ & y_k^{\min} \le y_k(t) \le y_k^{\max} \\ & u_k^{\min} \le u_k(t) \le u_k^{\max}. \end{aligned} \tag{1}$$

$q(t), t = 1, ..., N$ represents a desired power consumption profile over a period of length N.$p(t)$ is the actual power demand and is a sum of the power demands $p_k(t), k = 1, ..., n$ for each of the n units. A power capacity limitation can also be included by adding the inequality constraint $p(t) \le p^{\max}(t)$. $y_k(t)$ is the output of a linear system with input $u_k(t)$. The variables are $p(t)$, $p_k(t)$, $x_k(t)$, and $u_k(t)$.

We define the set F_k as a bounded polyhedron containing the linear state space system and its constraints in (1). To lighten notation further the time argument will be omitted from here on. The unit constraints in F_k can be moved to the objective by expressing them as an indicator function

$$f_k(u_k) = \begin{cases} 0 & \text{if } u_k \in F_k \\ +\infty & \text{otherwise} \end{cases}$$

Finally, the optimization problem to be solved by the receding horizon controller at every time instant is

$$\begin{aligned} \text{minimize} \quad & g(p) + \sum_k f_k(u_k) \\ \text{subject to} \quad & p = \sum_k u_k \end{aligned} \tag{2}$$

3. DUAL DECOMPOSITION

We solve the problem (2) by solving its unconstrained dual problem with the subgradient descent method Vandenberghe (2011); Bertsekas (1999). The dual is obtained via the Lagrangian L

$$L = \frac{1}{2}||p-q||^2 + \sum f_k(u_k) + z^T\left(p - \sum_k u_k\right)$$

where z is the dual variable. The dual function is

$$\begin{aligned}\inf_p L &= \frac{1}{2}||z||^2 + q^T z - ||z||^2 + \sum_k \inf_{u_k}\left(f_k(u_k) - z^T u_k\right)\\ &= -\frac{1}{2}||z||^2 + q^T z - \sum_k \sup_{u_k}\left(z^T u_k - f_k(u_k)\right)\end{aligned}$$

Finally, the dual problem is

$$\text{maximize} \quad -\frac{1}{2}||z||^2 + q^T z - \sum_k S_k(z) \tag{3}$$

with

$$S_k(z) = \sup_{u_k \in F_k} z^T u_k\,.$$

$S_k(z)$ is the support function of F_k. If F_k is a bounded polyhedron, we can evaluate S_k by solving an LP subproblem

$$u_k^+ = \operatorname*{argmin}_{u_k \in F_k}\left(z^T u_k\right) \tag{4}$$

and the optimal u_k gives us a subgradient of S_k at z. Solving (3) with the subgradient projection method gives us the updates

$$z^+ = z + t^+\left(\sum_k u_k^+ - (z+q)\right)\,. \tag{5}$$

The step size t^+ must be decreasing at each iteration j, i.e. $t^+ = \frac{t}{j} \to 0$, for $j \to \infty$. If t doesn't decrease the subgradient method will not converge to the minimum.

With the chosen LP subproblems the dual gradient method converges but the primal solution is not easily recoverable from the dual. An extra strictly convex term can be added to the subproblems, e.g. a temperature reference on the output

$$\begin{aligned}&\text{minimize} \quad \frac{1}{2}||\sum_k u_k - q||^2 + \frac{1}{2}\sum_k ||y_k - r_k||^2\\ &\text{subject to} \quad u_k \in F_k\,.\end{aligned}$$

The LP subproblems from (4) are now QPs on the form

$$u_k^+ = \operatorname*{argmin}_{u_k \in F_k}\left(\frac{1}{2}||y_k - r_k||^2 + z^T u_k\right)\,.$$

This problem formulation is equivalent to the ordinary optimal control problem with an added linear term, that can be solved efficiently by methods based on the Riccati recursion Jørgensen et al. (2004, 2012).

If an upper bound on the power p is added, the dual variable z can be clipped in (5) by keeping $0 \le p \le p^{\max}$.

4. NUMERICAL EXAMPLE

An example with two different first order thermal storage systems is was simulated. The models have unity gain, time constants 5 and 10, and both a temperature reference equal to $r_k = y_k^{\min}$. The results for step size $t = 0.3$ after 100 iterations is shown in Fig. 1. The power tracking profile is seen match most of the time, but it is not possible to control the consumption amplitude of each unit very accurate through the dual variables, since each unit has its own objective leaving the tracking at some compromise.

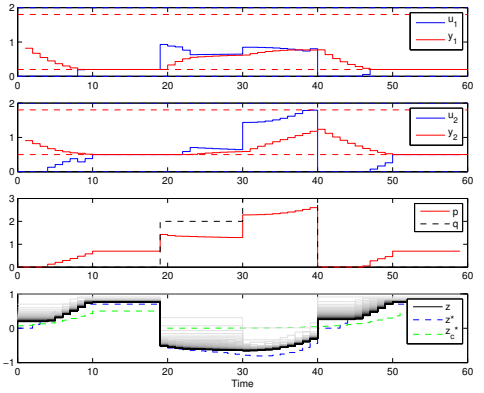

Fig. 1. *Simulation of power balancing with two first order systems. The two input/output pairs (blue/red) with constraints (dotted) are shown above the resulting power tracking profile. The lower plot shows the converged dual variable (black), its iterations (gray), and the optimal dual variable of the original problem (dotted blue). Also the optimal dual variable when using* (4) *as the subproblem is shown (dotted green).*

However, shifting the load in time is quite accurate, since the sharp variations in the dual variables, that can be interpreted as prices, causes the consumption to be placed in this cheap period.

5. CONCLUSION

Controlling the consumption of a large number of flexible thermal storage units in a Smart Grid was achieved by distributing the optimization problem to be solved and coordinating the total consumption through dual variables. The resulting power balancing performance is a compromise between system level balancing needs and the state and objectives of each unit.

REFERENCES

Bertsekas, D.P. (1999). *Nonlinear programming*. Athena Scientific.

Jørgensen, J.B., Frison, G., Gade-Nielsen, N.F., and Damman, B. (2012). Numerical Methods for Solution of the Extended Linear Quadratic Control Problem.

Jørgensen, J.B., Rawlings, J., and Jørgensen, S.B. (2004). Numerical Methods for Large Scale Moving Horizon Estimation and Control. In *7th International Symposium on Dynamics and Control of Process Systems (DYCOPS), Boston, USA*.

Vandenberghe, L. (2011). Lecture notes on Dual Decomposition. URL `www.ee.ucla.edu/~vandenbe/ee236c.html`.

[This page intentionally left blank]

[This page intentionally left blank]